97p.

N 62 14720

NASA TN D-1115

NASA TN D-1115

A

TECHNICAL NOTE

D-1115

NUCLEAR RADIATION TRANSFER AND HEAT DEPOSITION RATES IN LIQUID HYDROGEN

By M. O. Burrell

George C. Marshall Space Flight Center
Huntsville, Alabama

NATIONAL AERONAUTICS AND SPACE ADMINISTRATION

WASHINGTON August 1962

NATIONAL AERONAUTICS AND SPACE ADMINISTRATION

TECHNICAL NOTE D-1115

NUCLEAR RADIATION TRANSFER AND HEAT DEPOSITION RATES IN LIQUID HYDROGEN

By M. O. Burrell

SUMMARY

Stochastic methods are used to calculate the radiation transport and energy deposition of neutrons and gamma rays in liquid hydrogen slabs and cylinders. The sources are treated as mono-energetic and either point isotropic for the cylinder or plane parallel rays for the slabs. A description of the methods used and a rather extensive compilation of results are given. The results include heat rate deposition as a function of depth, albedo factors, slow neutron spatial distributions, and transmitted angular distributions of gamma rays.

INTRODUCTION

One of the most pressing problems in the development of nuclear powered rockets is the accurate determination of the nuclear radiation heating in the rocket fuel and of the radiation transmitted to the payload region. Since liquid hydrogen is a likely fuel for propulsion, the accurate calculation of radiation heat deposition and radiation transfer in liquid hydrogen is mandatory. At the present stage of development, it is desirable to base calculations on simple geometries and discrete energies which are adaptable to future configurations and energy spectra. The calculations in this report are intended to fulfil this need.

The present calculations utilize Monte Carlo techniques and are for plane slab geometries and right circular cylinders with flat ends. The source (either neutrons or gamma rays) is always mono-energetic. The source for the cylinder is point isotropic and on the axis of the cylinder, while the slab source is plane parallel rays incident at any specified angle. The calculation provides statistical estimates of the transmitted and reflected number current, flux, and energy as well as

the heat deposition rate as a function of depth in the hydrogen. The angular and energy distributions of the gamma ray transmissions are also calculated.

The neutron histories are terminated when their energy is reduced below 1 ev. The location of these terminations is tabulated and averaged over a volume element, thus giving the spatial distribution of the slow neutrons. The average energy of these neutrons is 0.5 ev. This volume distribution of slow neutrons may be representative of the source distribution for the 2.23 Mev gamma rays produced by the hydrogen capture of a neutron. However, the para-hydrogen scattering cross section will decrease below 0.1 ev [1] and this may result in considerable migration of the neutrons. There is no obvious reason to assume that the para-hydrogen absorption cross section will be different than for ortho-hydrogen. A practical justification for using the 0.5 ev neutron spatial distribtuion as capture gamma sources is that the mean free path of 2.23-Mev gammas in liquid hydrogen is about 68 inches, and an error as great as 2 inches in the capture gamma source position corresponds to an error of only 3% in one mean free path.

Neutrons lose a large fraction of their energy in a few collisions with protons and scatter only into the forward hemisphere. The neutron energy deposition in a cylinder of liquid hydrogen is a large fraction of the total neutron energy incident on the cylinder. This is expected since the mean free path of a 2-Mev neutron, in liquid hydrogen (ρ = .07 gm/cm^3), is about 3.2 inches. Since the neutrons scatter only into the forward hemisphere, and because the energy is reduced considerably after a few collisions (on the order of one-half at each scatter), the neutron energy which escapes the cylinder by reflection or transmission is a very small fraction of the incident energy. This is substantiated in the calculations presented in this report. The foregoing is not true of the gamma rays which have a mean free path about 20 times that of neutrons in hydrogen. Compton scattering is the only mechanism for energy deposition in the gamma ray energy range of interest. In hydrogen, photoelectric absorption is of no consequence until the gamma's energy is below 10^{-2} Mev and pair production is negligible below 20 Mev. Because of the low Compton energy absorption cross section below 0.1 Mev, the photon must scatter a very large number of times in order to degrade the energy to 0.01 Mev. From the foregoing, it is expected that an appreciable fraction of the incident gamma ray energy will escape a hydrogen cylinder of feasible dimensions. For example, the energy deposition in a 30-foot diameter hydrogen cylinder of 50-foot length was calculated for a point isotropic source of 2-Mev neutrons and gamma rays on the center line 20 feet from the cylinder. In this case, 97% of the incident neutron energy and 65% of the incident gamma ray energy were transferred to the liquid hydrogen. Thus, 35% of the gamma ray energy and only 3% of the neutron energy escaped the cylinder. The fraction of the gamma energy transmitted to the far end of the cylinder was negligible; hence, most of the escaping gamma energy was transmitted through the sides or reflected to the rear.

SECTION I. PLANE GEOMETRY METHODS

A. PLANE GEOMETRY MONTE CARLO METHODS

This section presents the method used to calculate the transport and energy deposition of neutrons or photons in hydrogen slabs of infinite expanse, but finite thickness. Figure 1 depicts the geometry of the calculation.

The radiation is assumed to have a number current density of 1 particle/cm^2 -sec, which is incident as a plane parallel beam at energy E_o and angle θ_o to the slab normal. Thus, if J_o is used to indicate the incident number current density, then the incident number flux is given by

$$F_o = J_o \sec \theta_o .$$

Likewise, the incident energy current and energy flux are simply

$$J_{Eo} = E_o J_o$$

and

$$F_{Eo} = E_o F_o .$$

First, the uncollided component of transmitted radiation is calculated, as follows:

$$U_J = J_o \exp(-\Sigma(E_o) Z_T \sec \theta_o),$$

where Z_T = total thickness of slab.

Also, for the unscattered flux and energy,

$$U_F = U_J \sec \theta_o,$$

$$U_{JE} = E_o U_J,$$

and

$$U_{FE} = E_o U_F.$$

The distance to the first point of scatter is sampled from the probability density function

$$f^*(r)dr = \frac{\Sigma^*(E_o)\exp[-\Sigma^*(E_o)r]dr}{1 - P_o}$$

$$0 < r \leq Z_T \sec \theta$$

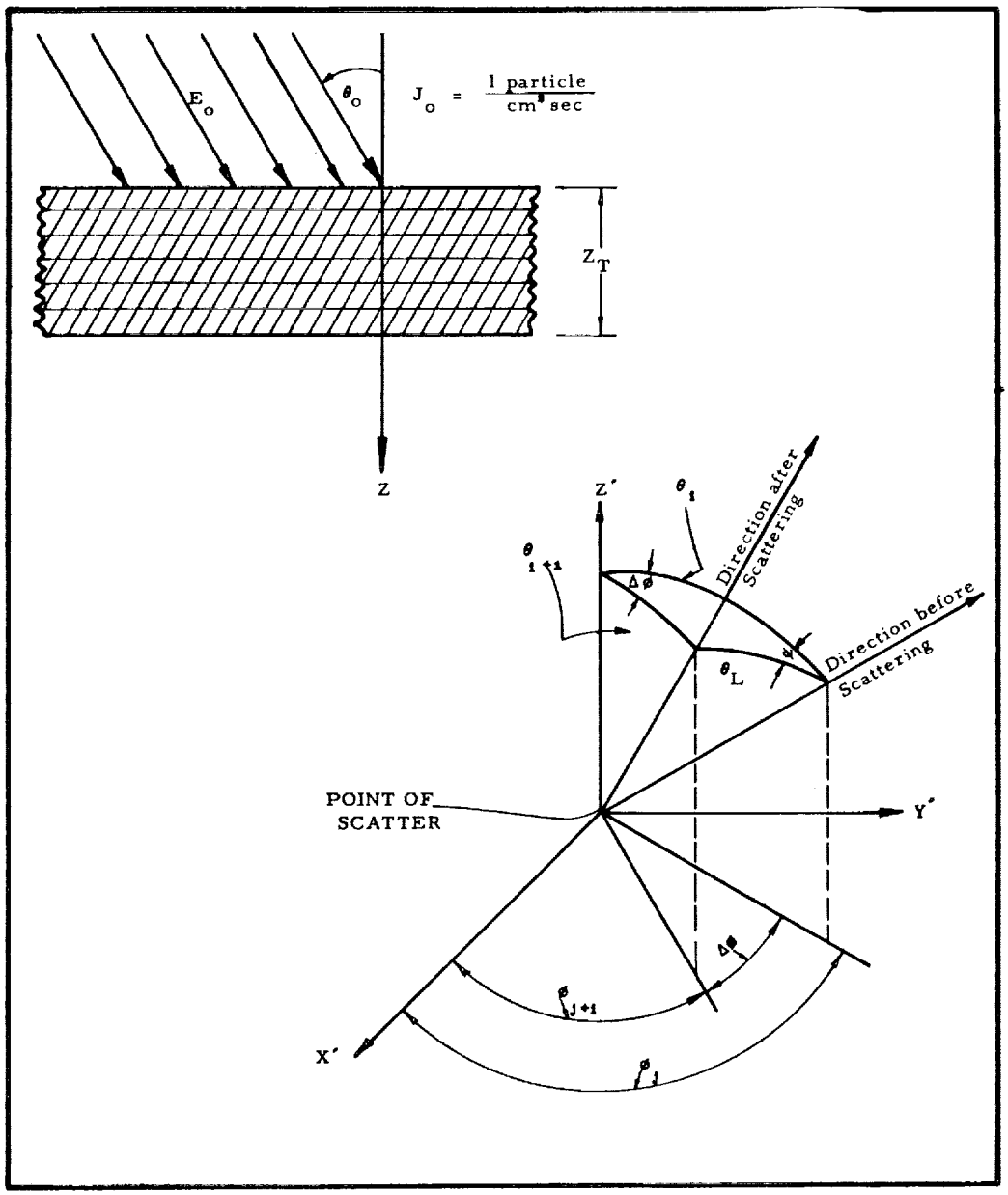

FIGURE 1. SLAB GEOMETRY AND SCATTERING ANGLE RELATIONSHIPS

where $r = Z \sec \theta_o$,

and $P_o = \exp\left[-\Sigma^*(E_o) Z_T \sec \theta_o\right]$.

The $\Sigma^*(E_o) = (1 - M_o \cos \theta_o)\, \Sigma(E_o)$, where $\Sigma(E_o)$ is the macroscopic cross section. The M_o (usually taken as 0.9) is a biasing parameter between 0 and 1 which is used to increase the first path length; if $M_o = 0$ there is no biasing. Also, the probability density function, $f^*(r)\,dr$, produces a truncated path length (i.e., the particle stays within the slab boundaries).

Because of the above biasing, a weight must be given to the particle. The weight of the particle at the first collision point is

$$W_1 = \frac{1 - P_o}{(1 - M_o \cos \theta_o)} \exp\left[-\Sigma(E_o)\, r_1\, M_o \cos \theta_o\right] ,$$

where r_1 is the length of the first path. The value of r_1 is found by solving the following equation:

$$\int_0^{r_1} f^*(r)\,dr = \xi ,$$

where ξ is a pseudo-random number generated in the computer 2 ; $0<\xi<1$. From this equation,

$$r_1 = \frac{-1}{\Sigma_T^*(E_o)} \ln\left[1 - (1 - P_o)\xi\right] .$$

If ξ is replaced by $(2k-1/2N)$ where k refers to the kth history and N is the total sample size, the values of r_1 are systematically taken from the density function $f^*(r)$. This procedure eliminates statistical fluctuation on the first path length. On higher order scatters, the particle is allowed to escape the slab and no biasing is used. The probability density function of path lengths then becomes:

$$f(r)\,dr = \Sigma(E_i) \exp\left[-\Sigma(E_i) r\right] ,$$

and

$$r_i = -\frac{1}{\Sigma_i} (\ln \xi).$$

For very deep penetrations ($\Sigma_o Z_T > 10$m.f.p.), it may be necessary to incorporate the same biasing as used on the first scatter in order to obtain sufficient statistics to accurately estimate the transmission. However, for reliable energy deposition estimates in the hydrogen, such biasing is not desired.

After each collision, the scattered direction of the particle is found, as follows:

Neutrons: Scattering is assumed to be isotropic in the center of mass coordinate system. This assumption is valid in the range $10^{-6} \leq E \leq 14$ Mev. Let $\mu_c = \cos\theta_c$ and $\mu_L = \cos\theta_L$ represent the cosines of the scattering angle in the center of mass and the laboratory system, respectively. Then it follows from the scattering mechanics of neutron-proton collisions that

$$\mu_L = \frac{1 + \mu_c}{2}$$

Now the probability density function for isotropic scattering can be written:

$$f(\mu_c)\, d\mu_c = \frac{1}{2}\, d\mu_c; \quad -1 \leq \mu_c \leq 1.$$

Making a change in variables to the laboratory system,

$$\mu_c = 2\mu_L^2 - 1; \quad d\mu_c = 4\mu_L d\mu_L .$$

Therefore,

$$g(\mu_L)\, d\mu_L = 2\mu_L\, d\mu_L, \quad 0 \leq \mu_L \leq 1$$

becomes the probability density function for scattering in the laboratory system. One obvious method of sampling from this density function is to solve the following equation for μ_L:

$$\int_0^{\mu_L} 2\mu\, d\mu = \xi,$$

where ξ is a random number between 0 and 1. The solution yields

$$\mu_L = \sqrt{\xi} .$$

However, a rejection sampling technique leads to the following method: Choose two random numbers ξ_1 and ξ_2, then

$$\cos\theta_L = \mu_L = \text{Max}\left[\xi_1, \xi_2\right] ;$$

or simply select μ_L to be the larger of the two random numbers, ξ_1 and ξ_2 .

Gamma Rays: In order to choose a direction for the scattered photon, recourse is made to rejection sampling from the Klein-Nishina differential scattering formula,

$$f(\mu, \alpha) = \frac{1}{r_o^2} \frac{d\sigma}{d\Omega} = \frac{1}{2A^2} \left\{ 1 + \mu^2 + \frac{[\alpha_i (1 - \mu)]^2}{A} \right\} ,$$

where $\mu = \cos \theta_s$ gives the angle the scattered photon makes with the incident direction; r_o is the classical electron radius; $\alpha_i = E_i/0.511$ is the energy of the photon in M_oc^2 units; and $A = 1 + \alpha_i (1 - \mu)$. The rejection sampling is accomplished by choosing two random numbers, ξ_1 and ξ_2, and conditionally assuming $\mu = 1 - 2\xi_1$. A test is then made to determine if the above value of μ is acceptable. If $f(\mu,\alpha) \geq \xi_2$ the above value of μ is used; otherwise, two other random numbers are chosen and the process repeated until a μ is selected.

The azimuthal angle of scattering, ψ, is considered to be random from 0 to 2π for both neutrons and photons. A proper choice of ψ would be $\psi = 2\pi\xi$, where $0<\xi<1$. However, in terms of computing efficiency, the following rejection technique is commonly used. Two random numbers ξ_1 and ξ_2 are chosen in the range (0, 1) and then

$$a = 1 - 2\xi_1,$$

$$b = 1 - 2\xi_2,$$

and

$$c = a^2 + b^2.$$

If $c \leq 1$, then the choice becomes

$$\cos\psi = \frac{a^2 - b^2}{c}$$

and

$$\sin\psi = \frac{2ab}{c} .$$

If $c > 1$, two other random numbers are chosen and the routine repeated until $c \leq 1$.

Having found the cosine of the polar angle, μ, and the azimuthal angle, ψ, for the scattered direction of the particle, it is necessary to determine the cosine of the angle the particle has with the Z-axis. Thus,

$$\cos \theta_{i+1} = \cos \theta_i \mu + \sin \theta_i \sqrt{1 - \mu^2} \cos \psi,$$

where $\sin\theta_i = \sqrt{1 - \cos^2\theta_i}$, μ corresponds to μ_L for neutrons and $i = 0, 1, 2, \ldots$ represents the sequence of scattering. When a detailed description of the particle's direction is needed, the following terms are found (Fig. 1):

$$\cos\Delta\phi = \frac{\mu - \cos\theta_i \cos\theta_{i+1}}{\sin\theta_i \sin\theta_{i+1}}$$

$$\sin\Delta\phi = \frac{\sin\psi\sqrt{1 - \mu^2}}{\sin\theta_{i+1}}$$

Then $\cos\phi_{j+1} = \cos\phi_j \cdot \cos\Delta\phi - \sin\phi_j \sin\Delta\phi$ and

$$\sin\phi_{j+1} = \sin\phi_j \cdot \cos\Delta\phi + \cos\phi_j \sin\Delta\phi \quad ,$$

where the angle ϕj refers to the spherical coordinate measured from the X-axis in the XY-plane. Thus, the coordinates (θ_i, ϕ_j) give the spherical coordinates of the direction vector of the particle and tie it to a fixed coordinate system, the Z-axis and the X-axis. In slab geometry of infinite expanse, the angle ϕ is not necessary to describe the location of the particle and is found only if an angular distribution[1] of the transmitted particles is needed in the spherical coordinates (θ,ϕ).

After each scatter the probability of the particle escaping the slab is found. Thus, for the ith scatter of the kth history

$$P_{ik} = \exp\left[-\Sigma(E_i)t_i\right] ,$$

where $t_i = (Z_T - Z_i) \sec\theta_i$, if $0 \leq \theta_i < 90°$ (a transmission), and $t_i = Z_i \left|\sec\theta_i\right|$, if $\theta_i > 90°$ (a reflection). From this quantity (P_{ik}), the scattered transmitted and reflected current, flux, energy current, and energy flux are calculated as follows. On the ith scatter of the kth history,

$$J_{ik} = J_o \cdot W_{ik} \cdot P_{ik} ;$$

$$F_{ik} = J_{ik} (\sec\theta_{ik}) ;$$

$$(J_E)_{ik} = E_{ik} \cdot J_{ik} ;$$

and

$$(F_E)_{ik} = E_{ik} \cdot F_{ik} ,$$

[1] If $\theta_o = 0°$, the angular distribution has no ϕ dependence.

where W_{ik} is the appropriate weight of the particle. If $0 \leq \theta < 90°$ the value is recorded as a transmitted quantity, and if $\theta > 90°$ the value is tabulated as a reflected quantity. For the kth history the above quantities are summed in the reflected or transmitted tables; thus

$$J_k = \sum_i J_{ik} ,$$

$$F_k = \sum_i F_{ik}, \text{ etc,}$$

After N histories the final estimate for the scattered transmission or reflection is obtained:

$$\langle J \rangle_s = \frac{1}{N} \sum_{k=1}^{N} J_k$$

$$\langle F \rangle_s = \frac{1}{N} \sum_{k=1}^{N} N_k$$

$$\langle J_E \rangle_s = \frac{1}{N} \sum_{k=1}^{N} E_k \, J_k$$

$$\langle F_E \rangle_s = \frac{1}{N} \sum_{k=1}^{N} E_k \cdot F_k$$

The transmitted quantities are tabulated in one table and the reflected quantities in another. Also, for gamma rays the transmitted and reflected dose rate factor (r/hr) are found by multiplying the differential energy flux by the energy flux to dose rate conversion factor taken from p.17 of [3] .

The standard error for the scattered component is calculated and is given by the relation

$$\sigma_s = \frac{1}{N} \sqrt{\sum_{k=1}^{N} \Sigma_i \; s_{ik}^2 \; - N\bar{s}^2}$$

where $$\bar{s} = \frac{1}{N} \sum_{k=1}^{N} \sum_i s_{ik} .$$

The s is a generic term representing either scattered current, flux, energy current, or energy flux.

The energy deposition rate at a specified depth in the slab is estimated by recording the energy loss at each scatter in a pre-chosen set of layers. Thus, the energy deposition rate in the nth layer is given by:

$$Q_n = \frac{1}{N} \sum_k \sum_i \frac{q_{ikn}}{\Delta Z} \left[\frac{\text{MEV}}{\text{cm}^3\text{-sec}} \right],$$

where ΔZ is the layer width, N is the sample size, and q_{ikn} is the energy loss from the ith scatter of the kth history in the nth layer. The value q_{ikn} is zero when i and k are not for the appropriate layer n . The quantity q_{ikn} is calculated from the relation

$$q_{ikn} = W_{ik} \cdot \Delta E_{ikn} \cdot J_o$$

where W_{ik} is the appropriate weight of the particle and ΔE_{ikn} is the energy loss from the ith scatter of the kth history when it scatters in the nth layer of the slab.

The methods of calculating the energy losses due to the scattering of neutrons on protons and gamma rays on electrons follow.

<u>Neutrons</u>: The energy of the neutron after scattering through an angle in the center of mass coordinates, given by $\cos\theta_c = \mu_c$, is

$$E_{i+1} = E_i \left(\frac{1 + \mu_c}{2} \right) = E_i \quad \mu_L^2 ,$$

where μ_L is in the laboratory system. Therefore,

$$\Delta E_{i+1} = E_i - E_{i+1} = E_i \ (1 - \mu_L^2)$$

is the energy loss due to the $(i + 1)^{th}$ scatter of a neutron on a proton.

<u>Gamma Rays:</u> The energy of a photon after scattering through an angle given by $\cos\theta_s = \mu$ is

$$E_{i+1} = \frac{E_i}{1 + \frac{E_i}{.511} (1-\mu)}$$

Therefore,

$$\Delta E_{i+1} = E_i - E_{i+1} = \frac{E_i^2 \ (1 - \mu)}{E_i \ (1 - \mu) + 0.511}$$

is the energy loss due to the $(i+1)^{th}$ scatter of a photon on an electron.

The Monte Carlo histories are terminated either by the particle escaping the slab or by the particle's energy falling below an energy cutoff, E_n . For neutrons, E_n is chosen to be 10^{-6} Mev (unless otherwise stated), and when the energy of a neutron is degraded below 10^{-6} Mev the weight of the neutron is tabulated in the appropriate layer n, of thickness ΔZ, as a function of depth. The quantity

$$T_n = \frac{1}{N} \sum_{i,k} \frac{W_{ikn} \cdot J_o}{\Delta Z} \left(\frac{\text{neutrons}}{\text{cm}^3 - \text{sec}} \right)$$

defines the spatial distribution for the neutrons degraded below 10^{-6} Mev. The average energy of these neutrons is approximately 0.5×10^{-6} Mev. In the case of gamma rays, the energy cutoff, E_n is chosen as follows (unless otherwise specified):

$$E_n = 0.1 \text{ Mev if } E_o \geq 4 \text{ Mev};$$

$$E_n = 0.025\ E_o \text{ Mev if } 1 \leq E_o < 4 \text{ Mev};$$

$$E_n = 0.025 \text{ Mev if } E_o < 1 \text{ Mev}.$$

The total cross sections for neutrons in hydrogen are taken from the following empirical formulas:*

$$\Sigma(E) = \left(\frac{6.47}{E + 1.66}\right) \rho \quad (\text{cm}^{-1}) \text{ for } E > 1.2 \text{ Mev},$$

$$\Sigma(E) = \left(\sqrt{\frac{6.57}{E}}\right) \rho \quad (\text{cm}^{-1}) \text{ for } 0.16 \leq E \leq 1.2 \text{ Mev},$$

$$\Sigma(E) = \frac{2.01\rho}{E + 0.166} \quad (\text{cm}^{-1}) \text{ for } 10^{-4} \leq E < 0.16 \text{ Mev},$$

$$\Sigma(E) = 12.37\rho \quad (\text{cm}^{-1}) \text{ for } 10^{-6} \leq E < 10^{-4} \text{ Mev},$$

where ρ is the density of hydrogen in gm/cm^3 . The value of ρ is chosen as 0.07 gm/cm^3 in all the present calculations. The absorption cross section is not treated separately, since it is not of major importance until E is below 10^{-6} Mev. At 10^{-6} Mev, σ_a is about 0.05 barns and would result in approximately 25 neutron captures out of 10,000 collisions.

*From data in BNL 325.

For gamma rays in hydrogen the Klein-Nishina total cross section formula is used. Photoelectric absorption and pair production are ignored, as explained in the Introduction. The Klein-Nishina total cross section formula in (cm^{-1}) units is given by

$$\Sigma(\alpha) = 0.3006\left\{\left(\frac{1+\alpha}{\alpha^2}\right)\left[\frac{2(1+\alpha)}{1+2\alpha} - \frac{1}{\alpha}\ln(1+2\alpha)\right] + \frac{1}{2\alpha}\ln(1+2\alpha) - \frac{1+3\alpha}{(1+2\alpha)^2}\right\}\rho,$$

where $\alpha = E/.511$

The computer code for the slab geometry calculations is written for the IBM 7090. The running time is about one minute for 1,000 histories (varying with E_n). All results presented are based on a sample size of at least 5,000 histories. The results of the Monte Carlo slab geometry calculations are discussed in parts B and C.

B. RESULTS OF NEUTRON TRANSPORT

1. Albedo Factors The results given in Table I and Figures 2 through 7 are albedo or reflection factors of neutrons incident on a hydrogen slab at the indicated energy and angle. The albedo factor is defined in general as

$$\beta = \frac{I_R}{I_o},$$

where I_R is the reflected quantity (current, energy current, or flux) and I_o is the corresponding incident quantity at the slab surface. Thus, the statistical estimate of the number flux albedo in slab geometry is given by

$$\left\langle \beta_E \right\rangle = \left\langle \frac{J^-}{|\cos\theta|} \right\rangle \Big/ J_o \sec\theta_o ,$$

where J_o = incident number current (1 n/cm^2 -sec), and θ_o is the angle of incidence; the J^- connotes the differential number current in the reflected or negative direction, and the angle θ is the associated angle of reflection. In a similar manner, the statistical estimate of the energy current albedo is given by

$$\left\langle \beta_{JE} \right\rangle = \left\langle E \cdot J^- \right\rangle \Big/ E_o J_o .$$

The albedo factors are based on neutron energies above 10^{-6} Mev. Hence, the statistical estimates are low for number current and flux albedo since additional neutrons would escape in going from 1 ev to the low energies (.001 ev) that may exist before capture. However, the energy current albedo is quite sufficient since the remaining energy of the neutrons is a negligible fraction of the incident neutron energy.

2. Buildup Factors The results presented in Tables II and III and Figure 8 are for neutron buildup factors in liquid hydrogen. Only the calculations which preserved a reasonable degree of accuracy are presented here. In many cases the heat deposition calculations were for such great depth that the transmission data was unreliable. The data in Table II were generated specifically to obtain transmission data of normal incident 8-Mev neutrons. Figure 8 compares the present results of the 8-Mev neutron's penetrations in liquid hydrogen (ρ = .07 gm/cm^3) to calculations that are reported in NDA-15C-39 [4]. The discrepancies between the results are attributed to different geometries, slightly different hydrogen cross section data, and the minimum neutron energy considered. The buildup factors calculated in plane geometry have the following properties: Let

U = uncollided component of transmitted radiation;

S = scattered component of transmitted radiation determined by Monte Carlo calculations;

I_o= incident quantity (current, flux, energy, etc.);

B = slab buildup factor for incident quantity and slab thickness (i.e., $B = B(\theta_o, E_o, Z_T)$);

and T = slab transmission factor (ratio of transmitted quantity to incident quantity).

Then, $U = I_o \exp(-\Sigma(E_o) Z_T \sec \theta_o)$,

$$B = \frac{U + S}{U},$$

and $$T = \frac{U + S}{I_o}.$$

From the last three relationships, a useful connection between slab transmission factors and slab buildup factors is:

$$T = \frac{BU}{I_o} = B \exp(-\Sigma(E_o) Z_T \sec \theta_o).$$

3. Heat Rates Figure 9 and Tables IV through VIII present the results for the neutron energy deposition rate as a function of depth in the liquid hydrogen. The results are presented for eight incident energies and five incident angles on the slab surface. The results are given in BTU/in^3 -sec for an incident number current of 1 neutron/cm^2 -sec at the indicated initial energy E_o and angle θ_o . For convenience of conversion between different units, the following relationships are given:

$$\rho = 0.07 \text{ gm/cm}^3 = 0.00253 \text{ lb/in}^3 ,$$

$$1 \left[\frac{\text{MEV}}{\text{cm}^3}\right] = 2.486 \times 10^{-15} \text{ BTU/in}^3$$

$$1 \left[\frac{\text{BTU}}{\text{Lb.Liq.H}}\right] = 395.4 \text{ BTU/in}^3$$

4. Slow Neutrons Figures 10 and 11 and Tables IX through XIII present the calculations for the spatial distribution of slow neutrons which have an average energy of about 0.5 ev. The units are neutrons/cm^3 -sec per incident neutron/cm^2 -sec on the slab surface. The tables give the results for eight incident energies and five incident angles. There is some justification for assuming that this spatial distribution can be used to represent point isotropic sources for the 2.23 Mev capture gammas associated with the neutron absorption in hydrogen.

C. RESULTS OF GAMMA RAY TRANSPORT

1. Albedo Factors Table XIV and Figure 12 present the calculated gamma ray albedo factors for hydrogen slabs. It is interesting to note that the energy current albedos for gamma rays are usually higher than for the neutrons (Figs. 2 - 6) except at the more oblique angles of incidence. For a more detailed discussion of albedo factors, see part B.

2. Buildup Factors Table XV and Figure 13 present calculated gamma ray buildup factors for six incident energies and four thicknesses of hydrogen slabs. Figure 13 gives a comparison of the present calculations to NDA [5] moment method calculations for water. The differences are explainable in terms of geometry (NDA uses a semi-infinite medium) and the photoelectric absorption of oxygen. Note that all the Monte Carlo buildup factors given in Table XV are for gamma rays reduced to 0.025 Mev where the photoelectric cross section of oxygen is fairly large. The reason that the absorption cross section of oxygen is important is that photons degraded in energy are readily absorbed, thus reducing the number of low-energy photons escaping the

slab. However, for pure hydrogen, the low-energy photon is much more likely to escape the slab - noticeably reducing the magnitude of the average transmitted energy flux if E_o is not too large ($E_o < 3$ Mev). This effect is shown dramatically by comparing the energy flux buildup of 6-Mev photons and 1-Mev photons in hydrogen to those in water. For a more detailed discussion of buildup factors, see part B.

3. Heat Rates Figure 14 and Tables XVI - XX give the results for the gamma ray energy deposition rates as a function of depth. The results are given for seven initial energies and five incident angles. The units are in BTU/in^3 -sec for an incident number current density of 1 photon/cm^2 -sec. Part B provides a more detailed discussion.

4. Angular Distributions Figure 15 and Tables XXI - XXIV present the transmitted scattered angular distribution and associated energies for gamma rays (1 photon/cm^2 -sec) normally incident on hydrogen slabs of 1, 2, 4, and 7 mean free path's thickness. The quantities presented have the units of Mev/cm^2 -sec-ster. The quantity represents the energy current/steradian in each of ten equal solid angles ($\Delta\Omega = 2\pi\,\Delta\cos\theta = \pi/5$). Thus,

$$\frac{\Delta\Omega}{U_{J_E}} \sum_{i=1}^{10} \left(\frac{\Delta J_E}{\Delta\Omega}\right)_i = B_{J_E} - 1; \text{ where } \left(\frac{J_E}{\Delta\Omega}\right)_i \text{ is the}$$

quantity tabulated; B_{J_E} is the total energy current buildup factor for the slab (Table XV), and $U_{J_E} = E_o \exp(-\Sigma(E_o)Z_T)$. The average energy associated with each solid angle is given in the tables and calculated as follows: $E_i = (\Delta J_E)_i / (\Delta J)_i$, where i denotes the solid angle.

SECTION II. CYLINDRICAL GEOMETRY METHODS

A. CYLINDRICAL GEOMETRY MONTE CARLO METHODS

The basic scattering phenomena for neutrons and photons as well as the general methods of treating radiation transfer and energy deposition rates are essentially unchanged in the cylindrical geometry. Hence, only those differences which are a consequence of the change in geometry and source will be developed in this section.

A point isotropic monoenergetic source of 1 particle/second is taken on the axis of a right circular cylinder, as shown in Figure 16. Thus, if θ_o is half the angle subtended by the cylinder at the source*,

* Continued on page 54.

TABLE I

Neutron Albedo Factors for Monoenergetic Parallel Beams Incident on Hydrogen Slabs at Indicated Angle and Energy

Number Current Albedo

θ_o \ E_o	7 (Mev)	5 (Mev)	3 (Mev)	2 (Mev)	1 (Mev)	0.3 (Mev)	0.04 (Mev)
0°	0.036 ±.003*	0.044 ±.004	0.060 ±.004	.075 ±.004	.105 ±0.005	.174 ±.006	.242 ±.007
25°		0.062 ±.004	.086 ±.004	.101 ±.005	.129 ±.006	.199 ±.008	
45°		0.119 ±.006	0.149 ±.005	.181 ±.006	.202 ±.007	.288 ±.009	
60°		0.202 ±.006	.244 ±.007	.259 ±.007	.307 ±.008	.379 ±.009	
75°		0.374 ±.008	.410 ±.008	.447 ±.009	.483 ±.009	.511 ±.009	

Energy Current Albedo

0°	0.00056 ±.00008	.00057 ±.00008	.00060 ±.00008	.00064 ±.00007	.00085 ±.00009	.0015 ±.0001	.0027 ±.00015
25°		0.0017 ±.0002	.0018 ±.0002	.0017 ±.0002	.0019 ±.0002	.0032 ±.0003	
45°		.0085 ±.0007	.0084 ±.0005	.0098 ±.0006	.0085 ±.0005	.0112 ±.0017	
60°		.026 ±.001	.029 ±.001	.028 ±.001	.029 ±.001	.034 ±.002	
75°		.080 ±.002	.084 ±.002	.087 ±.002	.094 ±.003	.0895 ±.0024	

Number Flux Albedo

0°	0.065 ±.006	0.074 ±.006	0.105 ±.007	0.131 ±.008	.186 ±.010	.323 ±.013	.453 ±.015
25°		.111 ±.009	.154 ±.013	.180 ±.010	.239 ±.025	.344 ±.016	
45°		0.194 ±.012	.230 ±.014	.280 ±.012	.317 ±.016	.439 ±.022	
60°		0.255 ±.012	.292 ±.013	.295 ±.012	.346 ±.013	.428 ±.014	
75°		0.256 ±.008	.278 ±.008	.293 ±.009	.332 ±.009	.348 ±.012	

* The (±) quantity is the standard error in the statistical estimate of the albedo (σ_β).

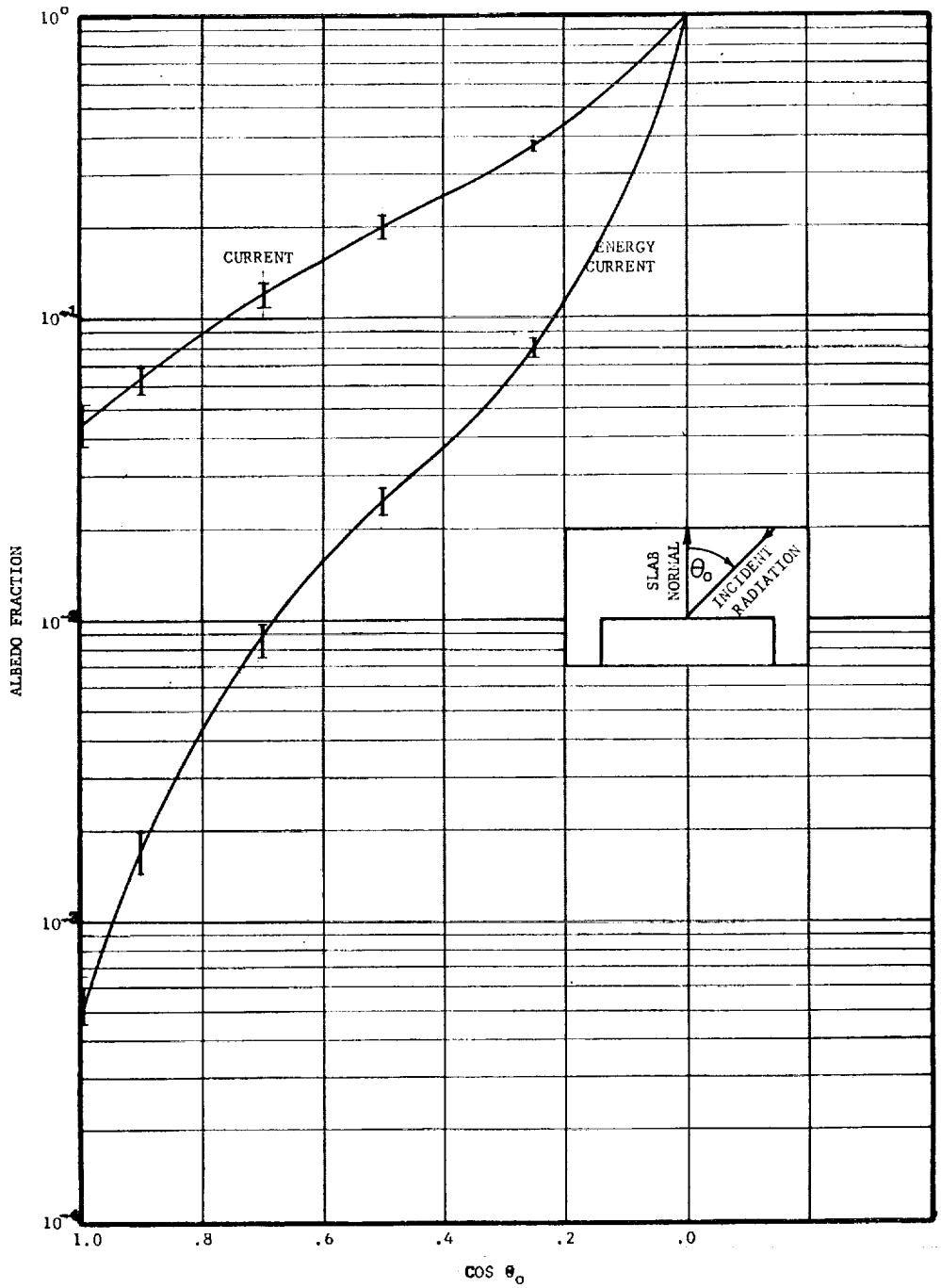

FIGURE 2. NEUTRON ALBEDO VERSUS COS θ_o FOR E_o = MEV, $E_N = 10^{-6}$ MEV

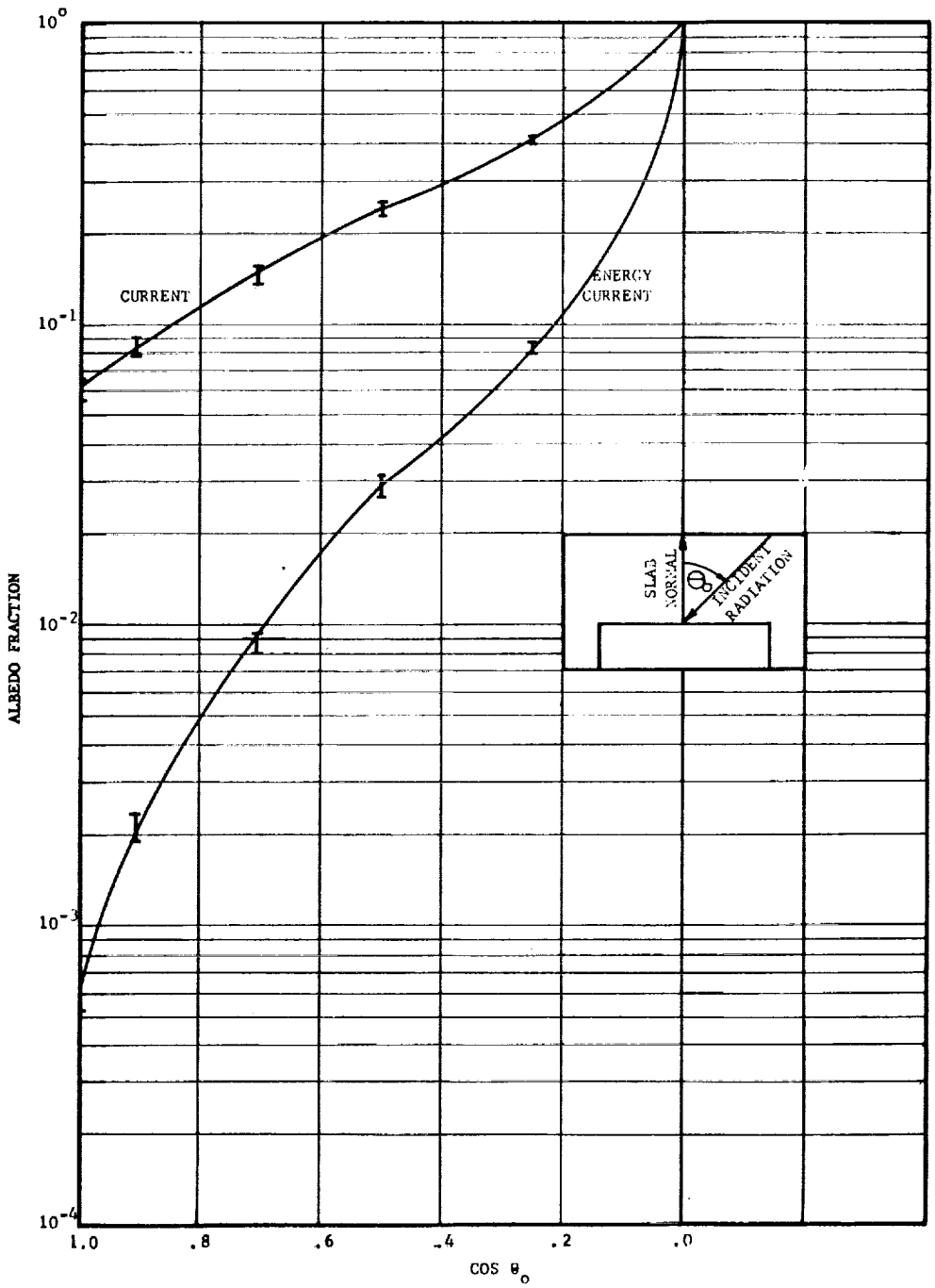

FIGURE 3. NEUTRON ALBEDO VERSUS COS θ_o FOR E_o = 3 MEV, $E_N = 10^{-6}$ MEV

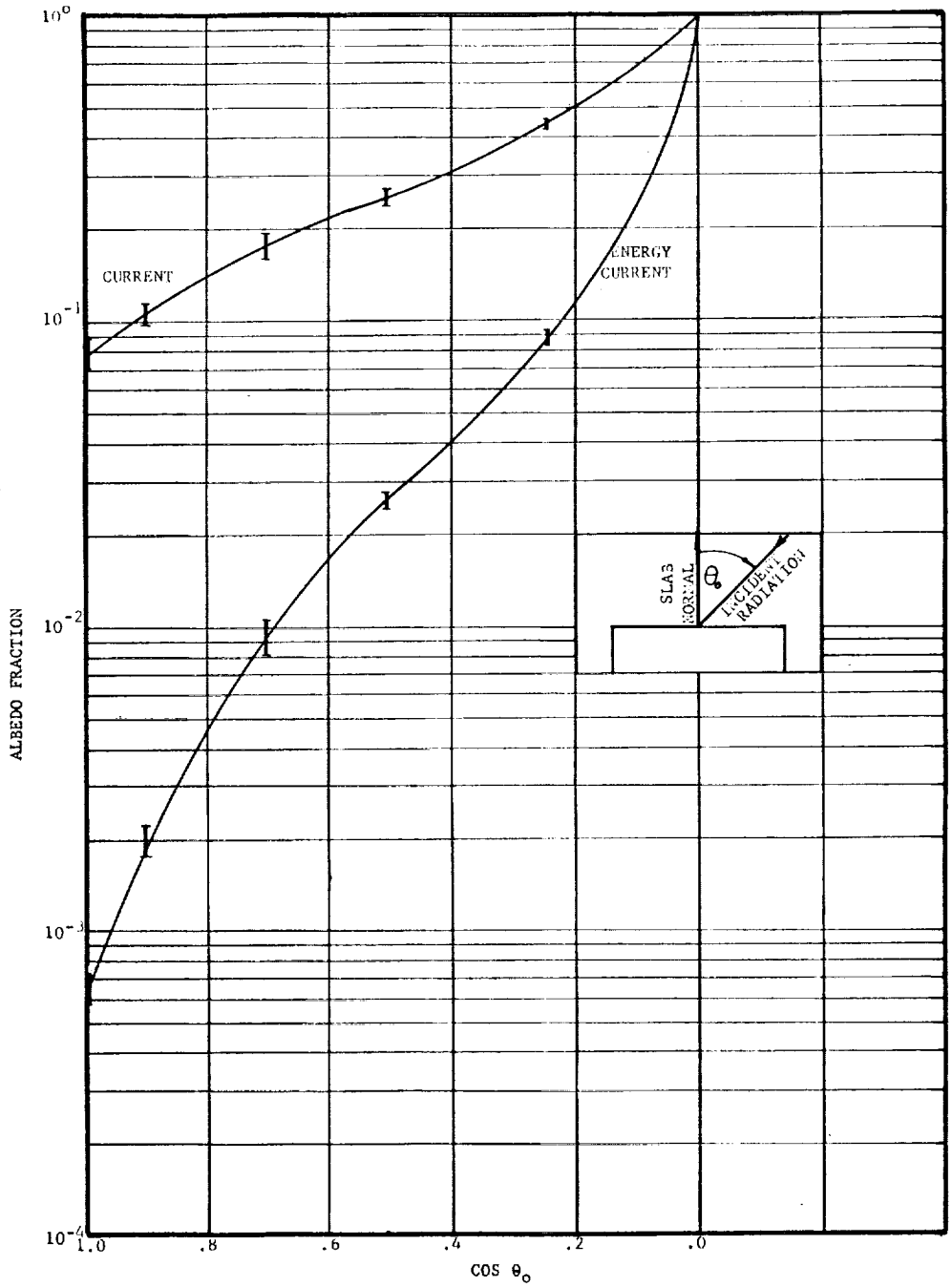

FIGURE 4. NEUTRON ALBEDO VERSUS COS θ_o FOR E_o = 2 MEV, $E_N = 10^{-6}$ MEV

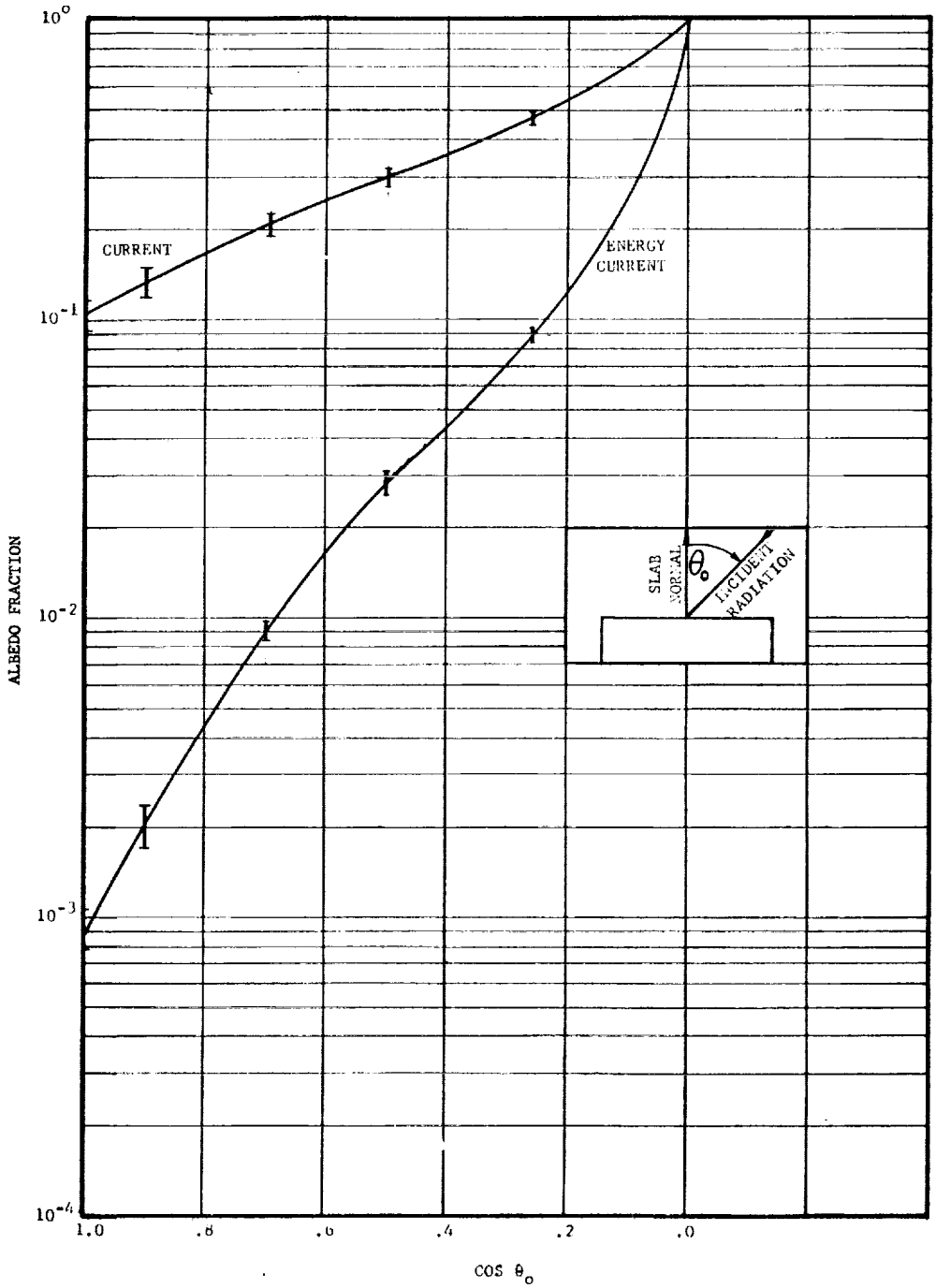

FIGURE 5. NEUTRON ALBEDO VERSUS COS θ_o FOR E_o = 1 MEV, E_N + 10^{-6} MEV

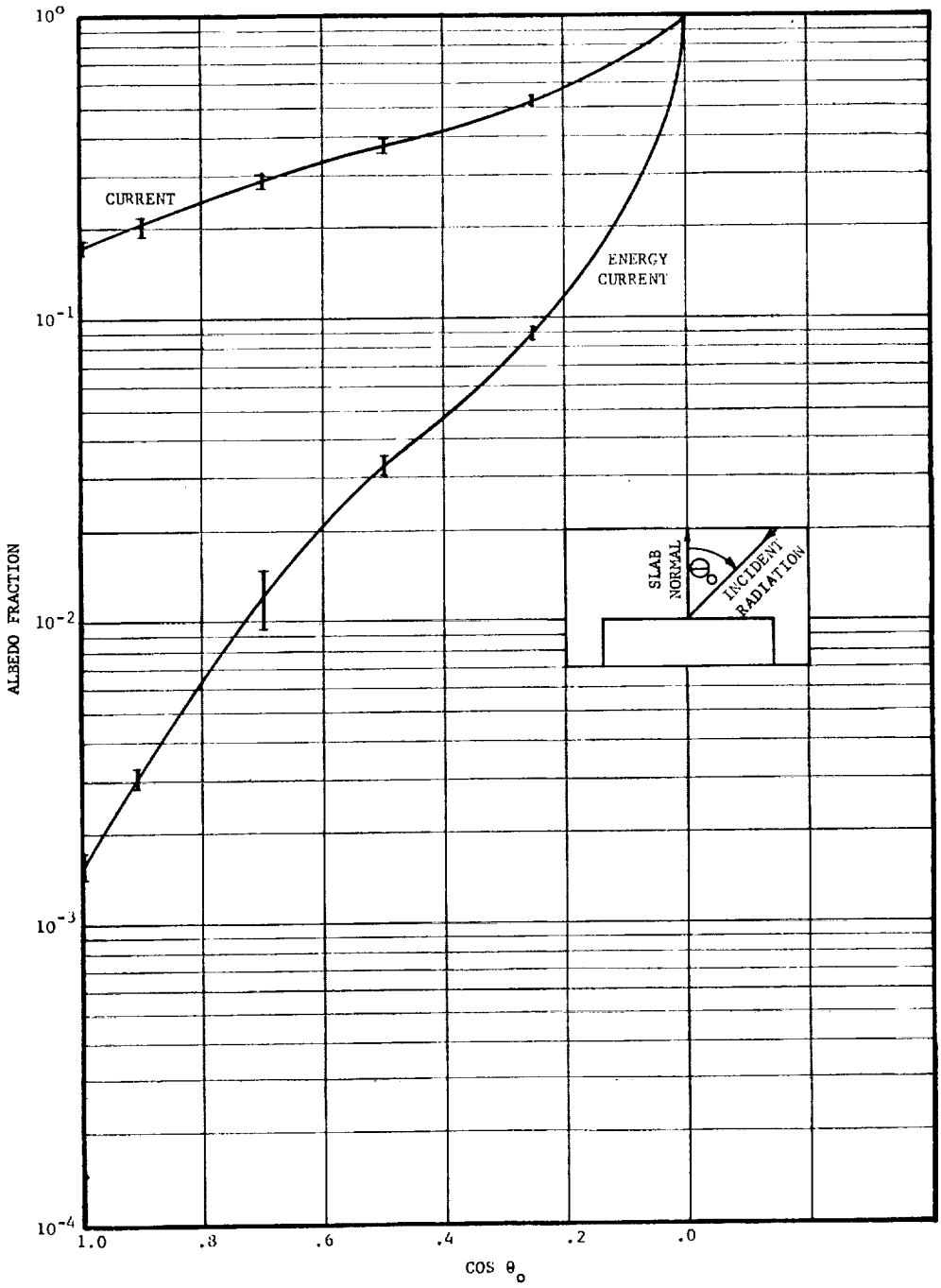

FIGURE 6. NEUTRON ALBEDO VERSUS θ_o FOR E_o = 0.3 MEV, $E_N = 10^{-6}$ MEV

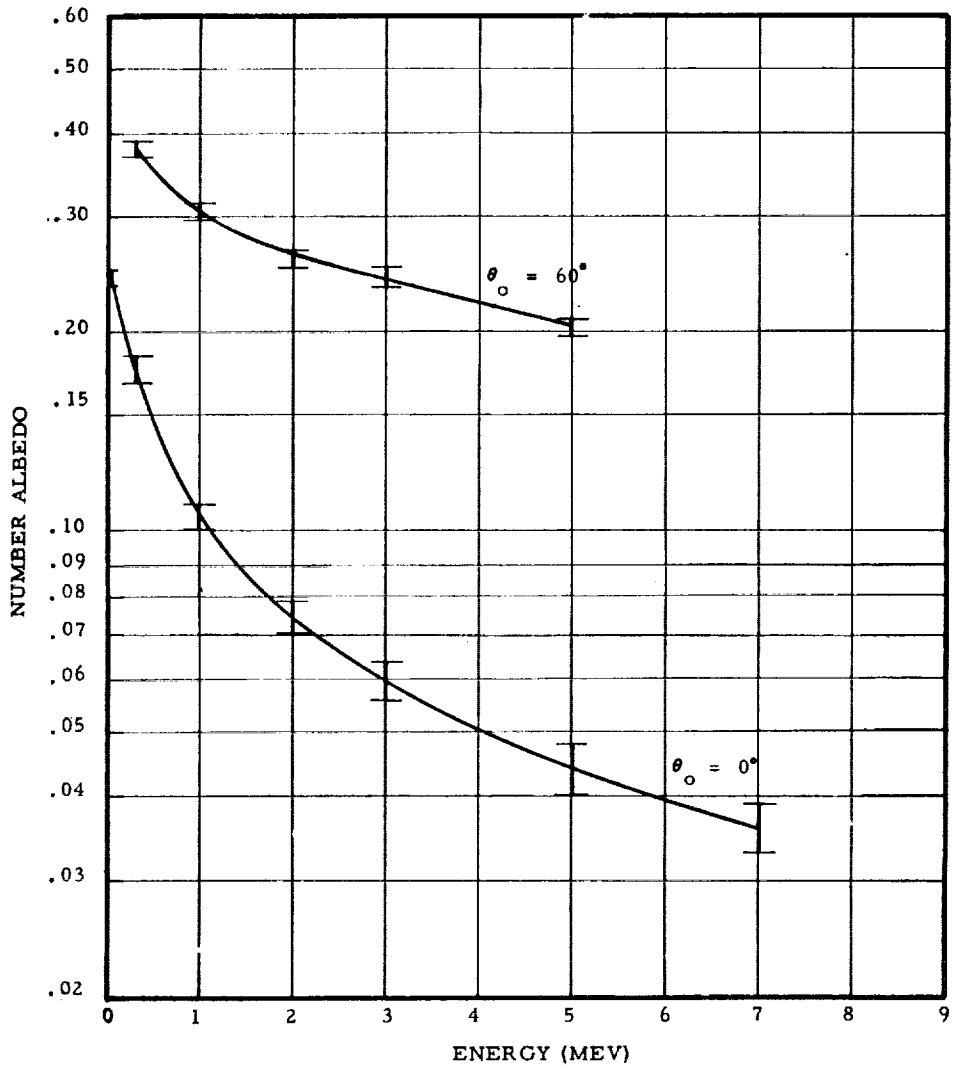

FIGURE 7. NEUTRON NUMBER CURRENT ALBEDO AS A FUNCTION OF INCIDENT ENERGY FOR $\theta_o = 0^\circ$ AND $\theta_o = 60^\circ$

TABLE II

Neutron Buildup Factors for 8 Mev Neutrons Incident Normally on Hydrogen Slabs; Cutoff Energy is 0.01 Mev

Buildup Factors

Mean Free Paths $\Sigma_o X$	Thickness (Inches)	Energy Current	Number Current	Number Flux	Exp(- $\Sigma_o X$)
2	16.8	1.894 ±.014*	2.83 ±.03	3.64 ±.05	1.353(-1)**
4	33.6	2.63 ±.05	4.4 ±.1	5.7 ±.2	1.831(-2)
6	50.4	3.6 ±.2	6.0 ±.4	7.5 ±.6	2.476(-3)
8	67.2	3.9 ±.5	6.6 ±1.1	8.5 ±1.6	3.360(-4)
16	134.4	5.6 ±.3	10.3 ±1.3	13.7 ±1.8	1.124(-7)
24	201.5	7.8 ±.8	13.2 ±1.8	17.8 ± 2.7	3.775(-11)

* The standard error in the quantity calculated.
** The integer in parenthesis is the power of ten by which the number is multiplied.

TABLE III

Neutron Buildup Factors for Indicated Initial Energies and Hydrogen Slab Thicknesses. Neutrons are Normally Incident with Cut-off Energy of 10^{-6} Mev.

E_o (Mev)	Mean Free Paths $\Sigma_o X$	Thickness (in)	Energy Current	Number Current	Number Flux
7	2.66	20	2.14 ±.03*	3.68 ±.08	4.80 ±.12
7	5.31	40	3.00 ±.16	5.8 ±.4	7.7 ±.7
7	10.63	80	4.3 ±.4	7.6 ±.9	9.8 ±1.2
5	3.46	20	2.56 ±.06	4.92 ±.15	6.8 ±.3
5	6.91	40	3.9 ±.2	8.5 ±.6	11.8 ±.9
5	13.82	80	5.3 ±.6	12.3 ±1.8	16.7 ±2.5
3	4.94	20	3.47 ±.15	7.6 ±.4	10.5 ±.7
3	9.87	40	5.7 ±.9	16.2 ±4.2	20.3 ±4.9
2	6.29	20	4.6 ±.3	12.4 ±1.1	17.5 ±1.8
2	12.6	40	6.9 ±.9	16.6 ±2.8	21.9 ±3.9
1	9.12	20	5.2 ±1.0	28.2 ±7.6	42.4 ±12.7

* The standard error in quantity calculated.

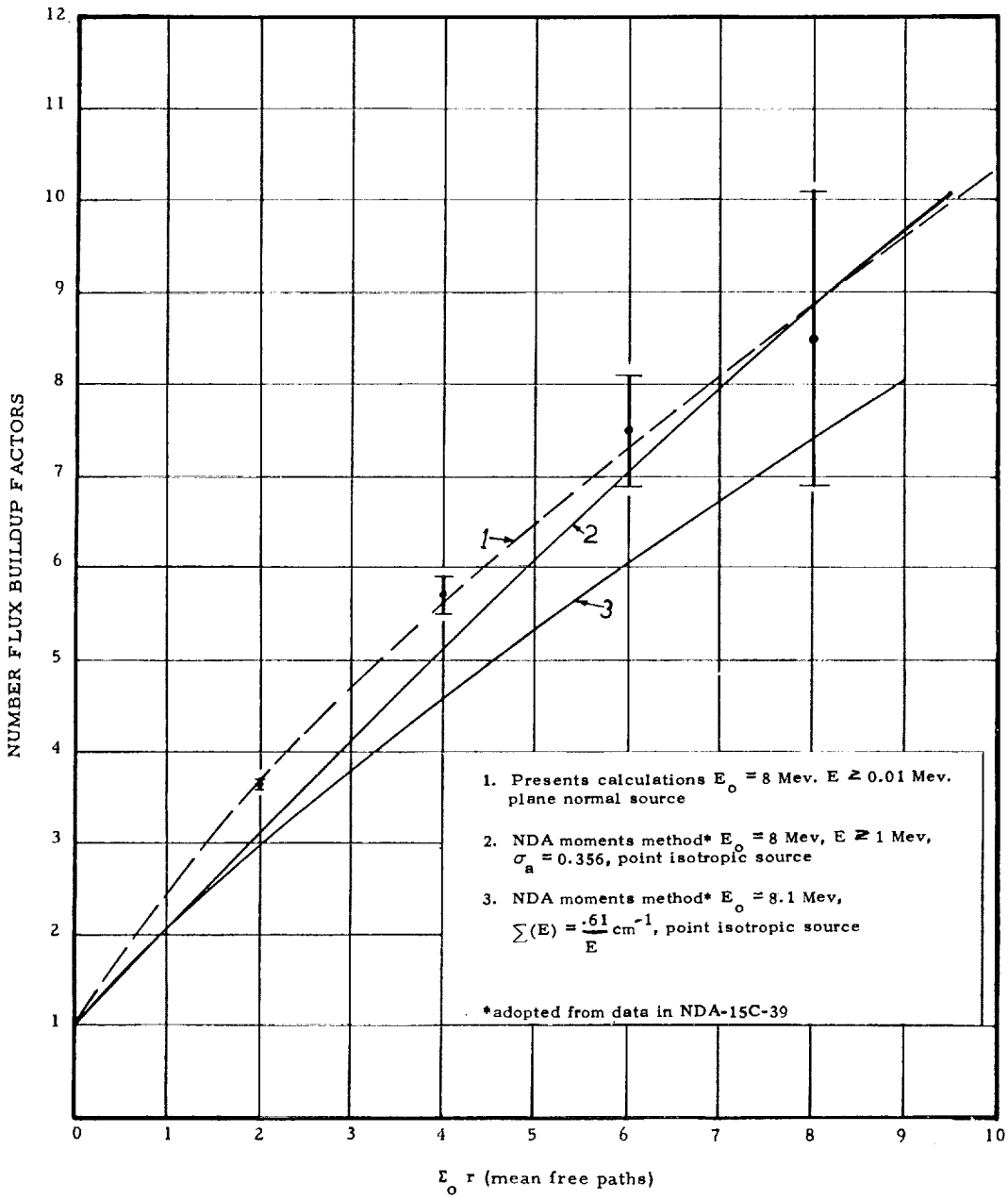

FIGURE 8. FLUX BUILDUP FACTORS VERSUS MEAN FREE PATHS FOR 8 MEV NEUTRONS IN HYDROGEN

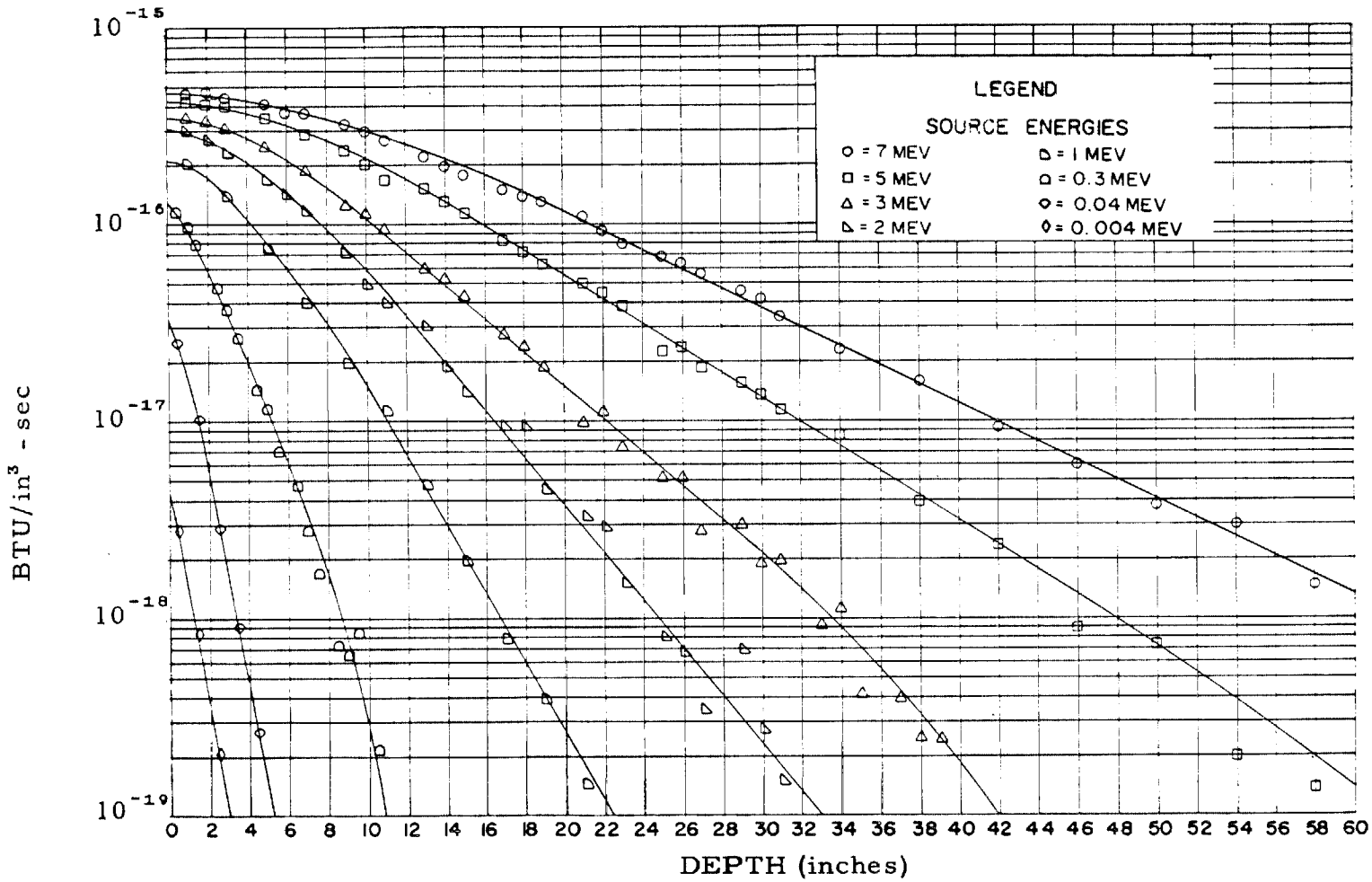

FIGURE 9. HEAT DEPOSITION VERSUS DEPTH IN LIQUID HYDROGEN SLABS FOR MONOENERGETIC NEUTRONS (1 NEUTRON/CM^2- SEC) INCIDENT NORMAL TO THE SURFACE

TABLE IV

Neutron Energy Deposition, BTU/in^3-sec of One Incident Neutron/cm^2-sec

With Neutrons Incident at $\theta_o = 0^\circ$ and Initial Energies E_o

Depth Inches	E_o=0.004Mev 10^{-18}*	E_o=0.04 Mev 10^{-17}	E_o=0.3 Mev 10^{-16}	E_o=1.0 Mev 10^{-16}	E_o=2.0 Mev 10^{-16}	E_o=3.0 Mev 10^{-16}	E_o=5.0 Mev 10^{-16}	E_o=7.0 Mev 10^{-16}
0.5	2.795	2.489	1.108	2.182	3.070	3.599	4.284	4.740
1.5	0.838	1.008	0.768	1.908	2.848	3.383	4.160	4.446
2.5	0.207	0.283	0.491	1.536	2.428	3.213	4.106	4.494
3.5	0.049	0.090	0.274	1.166	2.166	2.896	3.798	4.462
4.5	0.011	0.026	0.141	0.837	1.806	2.581	3.564	4.051
5.5	0.003	0.005	0.077	0.635	1.479	2.147	3.148	4.077
6.5		0.002	0.041	0.439	1.243	1.906	2.939	3.691
7.5			0.016	0.316	0.959	1.610	2.607	3.197
8.5			0.009	0.223	0.746	1.408	2.381	3.066
9.5			0.004	0.185	0.648	1.108	2.042	2.862
10.5			0.002	0.106	0.504	0.972	1.952	2.760
11.5				0.075	0.354	0.847	1.689	2.488
12.5				0.052	0.268	0.654	1.536	2.334
13.5				0.038	0.228	0.540	1.373	2.075
14.5				0.021	0.163	0.470	1.217	1.803
15.5				0.019	0.131	0.380	1.071	1.747
17.0				0.008	0.093	0.272	0.827	1.486
19.0				0.004	0.045	0.186	0.625	1.289
21.0				0.001	0.033	0.097	0.498	1.083
23.0				0.001	0.015	0.073	0.380	0.800
25.0					0.008	0.052	0.223	0.675
27.0					0.005	0.035	0.188	0.544
29.0					0.003	0.025	0.158	0.457
31.0					0.001	0.020	0.113	0.332
34.0						0.008	0.080	0.245
38.0						0.003	0.044	0.158
42.0						0.001	0.024	0.098
46.0							0.012	0.062
50.0							0.006	0.038

* Powers of ten by which number in table should be multiplied.

TABLE V

Neutron Energy Deposition, BTU/in³-sec of One Incident Neutron/cm²-sec

With Neutrons Incident at $\theta_o = 25^\circ$ and Initial Energies E_o

Depth Inches	E_o=0.3 Mev 10^{-16}*	E_o=1.0 Mev 10^{-16}	E_o=2.0 Mev 10^{-16}	E_o=3.0 Mev 10^{-16}	E_o=5.0 Mev 10^{-16}
0.5	1.238	2.367	3.403	4.106	4.869
1.5	0.785	2.015	3.155	3.804	4.778
2.5	0.447	1.538	2.607	3.356	4.683
3.5	0.236	1.166	2.154	2.986	4.039
4.5	0.111	0.836	1.765	2.527	3.809
5.5	0.055	0.596	1.438	2.259	3.212
6.5	0.028	0.406	1.115	1.961	2.821
7.5	0.016	0.286	0.901	1.570	2.604
8.5	0.005	0.183	0.720	1.287	2.373
9.5	0.002	0.128	0.535	1.036	2.045
10.5	0.001	0.078	0.456	0.799	1.884
11.5	0.001	0.060	0.330	0.723	1.719
12.5		0.036	0.224	0.591	1.342
13.5		0.028	0.162	0.430	1.226
14.5		0.014	0.138	0.336	1.061
15.5		0.010	0.113	0.286	0.853
16.5		0.009	0.080	0.227	0.767
17.5		0.003	0.067	0.191	0.656
18.5		0.002	0.045	0.177	0.624
19.5		0.001	0.034	0.126	0.531
21.0			0.017	0.098	0.413
23.0			0.012	0.059	0.324
25.0			0.009	0.037	0.191
27.0			0.007	0.025	0.144
29.0			0.003	0.013	0.111
31.0			0.002	0.008	0.088
33.0				0.006	0.060
35.0				0.005	0.045
37.0				0.002	0.041
39.0					0.030

* Powers of ten by which number in table should be multiplied.

TABLE VI

Neutron Energy Deposition, BTU/in^3-sec of One Incident Neutron/cm^2-sec With Neutrons Incident at $\theta_o = 45^\circ$ and Initial Energies E_o

Depth Inches	E_o = 0.3 Mev 10^{-16}*	E_o=1.0 Mev 10^{-16}	E_o=2.0 Mev 10^{-16}	E_o=3.0 Mev 10^{-16}	E_o=5.0 Mev 10^{-16}
0.5	1.490	3.082	4.534	5.417	6.294
1.5	0.762	2.313	3.664	4.677	5.835
2.5	0.369	1.579	2.919	4.025	5.331
3.5	0.162	0.998	2.220	3.199	4.579
4.5	0.070	0.627	1.656	2.595	4.077
5.5	0.029	0.438	1.185	2.030	3.562
6.5	0.012	0.261	0.902	1.555	3.040
7.5	0.004	0.146	0.636	1.158	2.570
8.5	0.002	0.102	0.499	1.016	2.263
9.5	0.001	0.060	0.308	0.762	1.910
10.5		0.033	0.263	0.622	1.601
11.5		0.024	0.181	0.486	1.358
12.5		0.013	0.103	0.370	1.066
13.5		0.009	0.085	0.307	0.890
14.5		0.005	0.065	0.203	0.679
15.5		0.001	0.042	0.173	0.557
16.5		0.001	0.028	0.116	0.509
17.5			0.027	0.112	0.408
18.5			0.018	0.068	0.338
19.5			0.008	0.051	0.304
21.0			0.007	0.046	0.251
23.0			0.004	0.029	0.121
25.0				0.011	0.085
27.0				0.007	0.074
29.0				0.005	0.043
31.0				0.004	0.034
33.0				0.003	0.025
35.0					0.015
37.0					0.007
39.0					0.006

* Powers of ten by which number in table should be multiplied.

TABLE VII

Neutron Energy Deposition, BTU/in^3-sec of One Incident Neutron/cm^2-sec With Neutrons Incident at $\theta_o = 60^\circ$ and Initial Energies E_o

Depth Inches	E_o=0.3 Mev 10^{-16}*	E_o=1.0 Mev 10^{-16}	E_o=2.0 Mev 10^{-16}	E_o=3.0 Mev 10^{-16}	E_o=5.0 Mev 10^{-16}
0.5	1.842	4.151	6.032	7.406	8.998
1.5	0.649	2.351	4.253	5.847	7.655
2.5	0.223	1.357	3.013	4.244	6.293
3.5	0.078	0.714	1.931	3.143	5.242
4.5	0.027	0.407	1.268	2.310	4.058
5.5	0.008	0.226	0.806	1.549	3.284
6.5	0.003	0.136	0.523	1.095	2.601
7.5	0.002	0.066	0.395	0.786	1.893
8.5		0.040	0.229	0.634	1.590
9.5		0.026	0.164	0.409	1.294
10.5		0.014	0.129	0.315	0.895
11.5		0.009	0.095	0.205	0.813
12.5		0.005	0.055	0.144	0.640
13.5		0.002	0.038	0.111	0.550
14.5		0.002	0.020	0.082	0.385
15.5			0.012	0.062	0.311
16.5			0.010	0.042	0.227
17.5			0.006	0.032	0.184
18.5			0.005	0.035	0.133
19.5			0.003	0.020	0.118
21.0					0.066
23.0					0.046
25.0					0.039
27.0					0.020
29.0					0.014
31.0					0.010
33.0					0.010
35.0					0.003

* Powers of ten by which number in table should be multiplied.

TABLE VIII

Neutron Energy Deposition, BTU/in^3-sec of One Incident Neutron/cm^2-sec With Neutrons Incident at $\theta_o = 75^\circ$ and Initial Energies E_o

Depth Inches	E_o=0.3 Mev 10^{-16}*	E_o=1.0 Mev 10^{-16}	E_o=2.0 Mev 10^{-16}	E_o=3.0 Mev 10^{-15}	E_o=5.0 Mev 10^{-15}
0.5	2.226	5.860	9.529	1.225	1.559
1.5	0.330	1.808	4.183	0.622	0.976
2.5	0.080	0.649	1.878	0.348	0.636
3.5	0.026	0.278	1.006	0.183	0.415
4.5	0.007	0.132	0.525	0.115	0.262
5.5	0.003	0.066	0.271	0.067	0.197
6.5	0.001	0.031	0.187	0.043	0.126
7.5		0.021	0.120	0.030	0.078
8.5		0.007	0.079	0.018	0.066
9.5		0.006	0.050	0.011	0.041
10.5		0.006	0.030	0.010	0.034
11.5		0.003	0.012	0.006	0.023
12.5			0.009	0.006	0.015
13.5			0.007	0.003	0.012
14.5			0.006	0.003	0.011
15.5			0.004	0.001	0.009
16.5			0.001	0.001	0.006
17.5				0.001	0.005
18.5					0.004
19.5					0.004

* Powers of ten by which number in table should be multiplied.

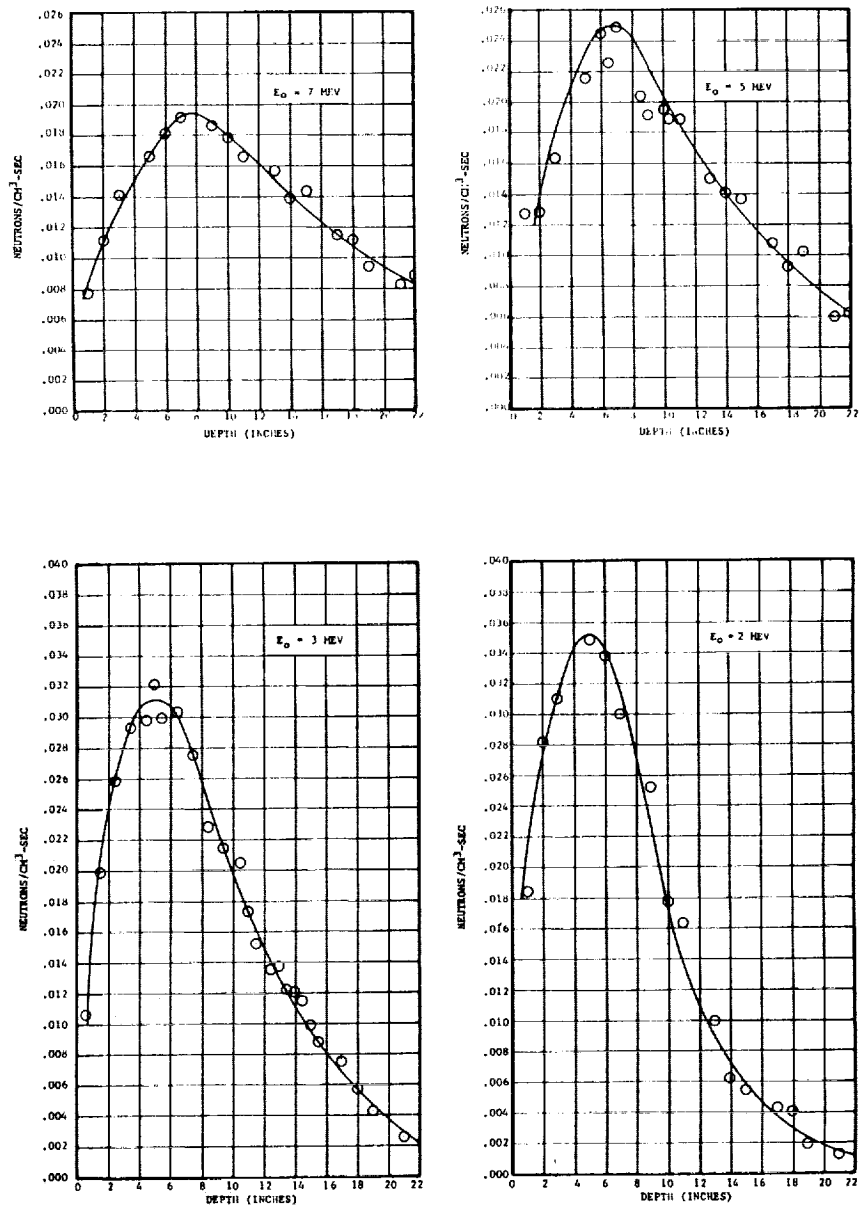

FIGURE 10. SPATIAL DISTRIBUTION OF 0.5 EV NEUTRONS IN LIQUID HYDROGEN DUE TO NORMAL INCIDENT, MONOENERGETIC NEUTRONS (1 NEUTRON/CM^2 - SEC) ON HYDROGEN SLABS. INCIDENT ENERGY IS GIVEN BY E_o ON GRAPH.

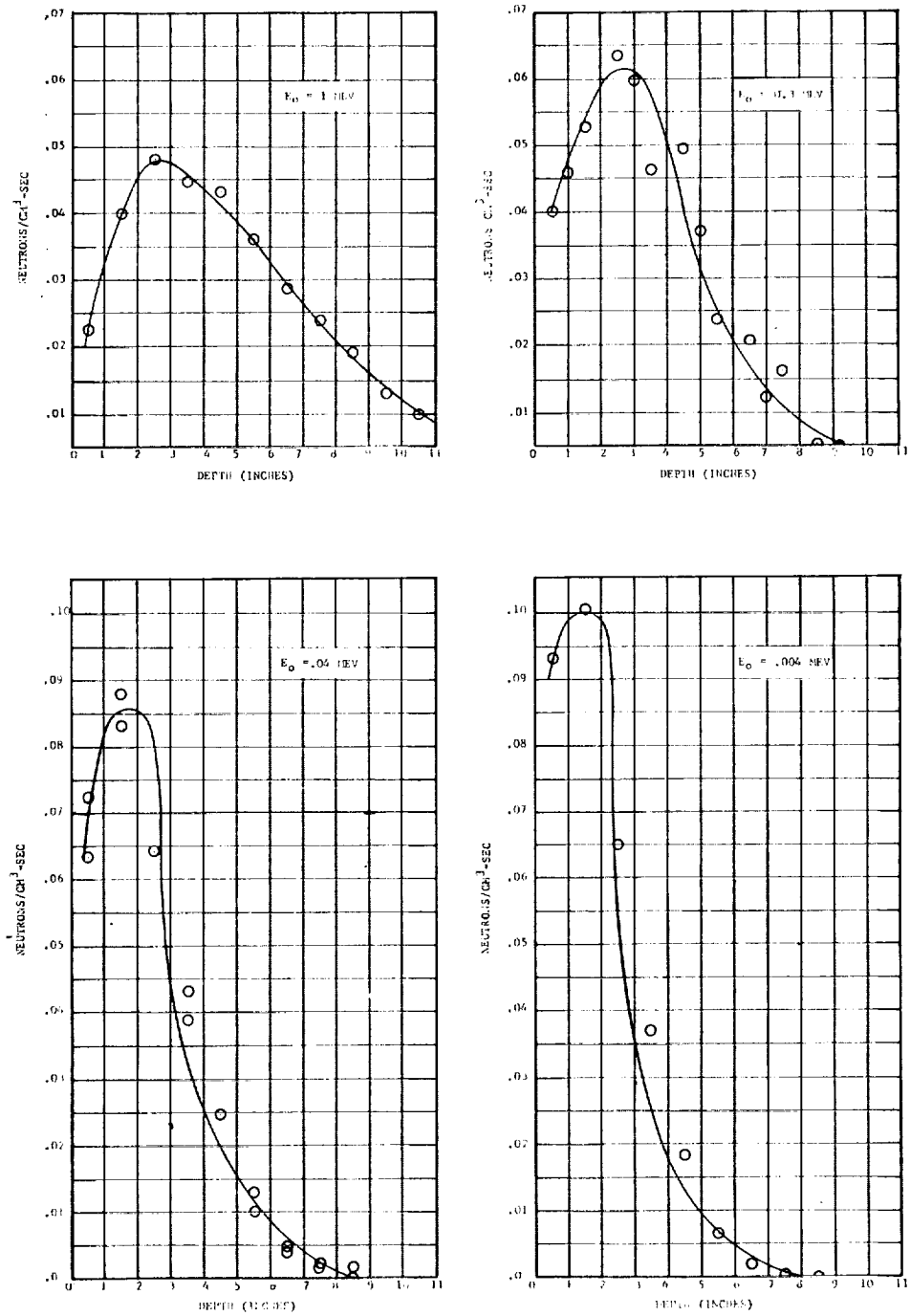

FIGURE 11. SPATIAL DISTRIBUTION OF 0.5 EV NEUTRONS IN LIQUID HYDROGEN DUE TO NORMAL INCIDENT, MONOENERGETIC NEUTRONS (1 NEUTRON/CM^2 - SEC) ON HYDROGEN SLABS. INCIDENT ENERGY IS GIVEN BY E_O ON GRAPH.

TABLE IX

Spatial Distribution of 0.5 ev Neutrons in Liquid Hydrogen Due to Monoenergetic Neutrons of Energy E_0 Incident on Hydrogen Slabs at an Angle $\theta_0 = 0^\circ$. The Incident Number Current is 1 Neutron/cm^2-sec.

Depth Inches	E_0=0.004Mev 10^{-1}*	E_0=0.04Mev 10^{-2}	E_0=0.3 Mev 10^{-2}	E_0=1.0 Mev 10^{-2}	E_0=2.0 Mev 10^{-2}	E_0=3.0 Mev 10^{-2}	E_0=5.0 Mev 10^{-2}	E_0=7.0 Mev 10^{-2}
0.5	0.930**	6.323	4.031	2.236	1.753	1.063	0.808	0.432
1.5	1.049	8.291	5.913	3.984	2.303	1.993	1.403	0.930
2.5	0.649	6.819	6.024	4.834	3.120	2.580	1.891	1.376
3.5	0.371	4.299	5.764	4.488	3.427	2.932	2.036	1.464
4.5	0.182	2.472	4.252	4.322	3.812	2.978	2.097	1.691
5.5	0.063	1.008	2.787	3.606	3.403	2.994	2.219	2.057
6.5	0.018	0.472	1.843	2.858	3.042	3.033	2.257	1.728
7.5	0.004	0.221	0.953	2.386	2.688	2.752	2.120	2.043
8.5		0.087	0.512	1.905	2.319	2.267	2.044	1.852
9.5		0.024	0.323	1.331	2.004	2.142	1.769	1.559
10.5		0.016	0.173	0.984	1.650	2.048	1.937	1.684
11.5			0.079	0.709	1.501	1.524	1.983	1.655
12.5			0.071	0.433	1.030	1.345	1.624	1.501
13.5			0.016	0.260	0.778	1.220	1.556	1.472
14.5			0.008	0.315	0.700	1.149	1.357	1.420
15.5			0.008	0.205	0.511	0.883	1.342	1.252
17.0				0.100	0.421	0.748	1.081	1.140
19.0				0.066	0.190	0.422	1.009	0.936
21.0				0.016	0.121	0.248	0.592	0.823
23.0				0.009	0.066	0.168	0.468	0.713
25.0				0.002	0.055	0.109	0.316	0.576
27.0				0.001	0.015	0.091	0.243	0.513
29.0					0.020	0.068	0.173	0.404
31.0					0.006	0.043	0.167	0.333
33.0					0.006	0.027	0.120	0.278
35.0					0.002	0.017	0.108	0.176
38.0					0.001	0.009	0.088	0.129
42.0						0.002	0.023	0.094
46.0						0.002	0.017	0.064
50.0							0.012	0.039

* Powers of ten by which number in table should be multiplied.

** Neutrons/cm^3-sec .

TABLE X

Spatial Distribution of 0.5 ev Neutrons in Liquid Hydrogen Due to Monoenergetic Neutrons of Energy E_0 Incident on Hydrogen Slabs at an Angle $\theta_0 = 25^\circ$. The Incident Number Current is 1 Neutron/cm^2-sec.

Depth Inches	E_0=0.3 Mev 10^{-2}*	E_0=1.0 Mev 10^{-2}	E_0=2.0 Mev 10^{-2}	E_0=3.0 Mev 10^{-2}	E_0=5.0 Mev 10^{-2}
0.5	4.442**	2.574	1.819	1.392	0.874
1.5	5.981	3.642	2.881	1.880	1.772
2.5	6.242	4.705	3.401	2.784	2.186
3.5	5.320	4.947	3.637	3.091	2.311
4.5	4.010	4.152	3.645	2.949	2.311
5.5	2.488	3.800	3.314	3.154	2.506
6.5	1.477	3.056	3.102	2.949	2.178
7.5	0.896	2.145	2.527	2.674	2.326
8.5	0.488	1.407	2.086	2.336	2.084
9.5	0.172	1.338	1.937	2.171	1.913
10.5	0.124	0.756	1.575	1.966	1.920
11.5	0.054	0.618	1.071	1.715	1.780
12.5	0.040	0.431	1.102	1.227	1.585
13.5	0.015	0.257	0.787	1.991	1.296
14.5	0.004	0.178	0.551	0.952	1.194
15.5	0.002	0.153	0.433	0.645	1.062
16.5	0.003	0.088	0.315	0.590	1.031
17.5	0.001	0.035	0.299	0.472	0.906
18.5		0.031	0.268	0.370	0.664
19.5		0.026	0.236	0.362	0.671
21.0			0.109	0.250	0.516
23.0			0.050	0.142	0.406
25.0			0.041	0.096	0.390
27.0			0.022	0.090	0.224
29.0			0.013	0.039	0.126
31.0			0.012	0.027	0.138
33.0			0.009	0.015	0.106
35.0			0.001	0.008	0.067
37.0				0.007	0.043
39.0				0.004	0.067

* Powers of ten by which number in table should be multiplied.

** Neutrons/cm^3-sec

TABLE XI

Spatial Distribution of 0.5 ev Neutrons in Liquid Hydrogen Due to Monoenergetic Neutrons of Energy E_0 Incident on Hydrogen Slabs at an Angle $\theta_p = 45^\circ$. The Incident Number Current is 1 Neutron/cm^2-sec.

Depth Inches	E_0=0.3 Mev 10^{-2} *	E_0=1.0 Mev 10^{-2}	E_0=2.0 Mev 10^{-2}	E_0=3.0 Mev 10^{-2}	E_0=5.0 Mev 10^{-2}
0.5	4.510**	3.098	2.126	1.787	1.155
1.5	5.678	4.517	3.433	2.590	1.815
2.5	5.877	4.952	3.756	3.055	2.475
3.5	4.640	4.440	3.961	3.511	2.451
4.5	3.169	3.637	3.842	3.464	2.781
5.5	2.213	3.140	2.921	3.000	2.679
6.5	1.095	2.432	2.732	2.842	2.750
7.5	0.588	1.734	2.252	2.291	2.200
8.5	0.302	1.281	1.898	2.149	2.208
9.5	0.208	0.692	1.370	1.614	2.035
10.5	0.034	0.474	1.008	1.299	1.886
11.5	0.013	0.292	0.953	1.307	1.571
12.5	0.006	0.206	0.614	0.976	1.296
13.5	0.013	0.175	0.386	0.842	1.281
14.5	0.001	0.078	0.260	0.593	0.935
15.5		0.057	0.307	0.528	0.786
16.5		0.046	0.213	0.457	0.825
17.5		0.017	0.118	0.346	0.613
18.5		0.018	0.071	0.197	0.503
19.5		0.006	0.118	0.173	0.385
21.0			0.068	0.145	0.385
23.0			0.020	0.078	0.252
25.0			0.002	0.053	0.128
27.0			0.007	0.027	0.089
29.0			0.001	0.018	0.071
31.0				0.022	0.058
33.0				0.008	0.044
35.0				0.001	0.024
37.0					0.035
39.0					0.020

* Powers of ten by which number in table should be multiplied.

** Neutrons/cm^3-sec

TABLE XII

Spatial Distribution of 0.5 ev Neutrons in Liquid Hydrogen Due to Monoenergetic Neutrons of Energy E_o Incident on Hydrogen Slabs at an Angle $\theta_0 = 60°$. The Incident Number Current is 1 Neutron/cm^2-sec.

Depth Inches	E_o=0.3 Mev 10^{-2} *	E_o=1.0 Mev 10^{-2}	E_o=2.0 Mev 10^{-2}	E_o=3.0 Mev 10^{-2}	E_o=5.0 Mev 10^{-2}
0.5	4.238**	3.146	2.377	1.939	1.480
1.5	5.859	4.845	3.647	2.917	2.181
2.5	5.049	4.860	4.001	3.239	2.944
3.5	3.928	3.841	3.744	3.934	2.842
4.5	2.610	3.254	3.449	3.358	2.889
5.5	1.352	2.606	2.835	2.837	2.755
6.5	0.714	1.724	2.395	2.269	2.559
7.5	0.286	1.178	1.545	2.046	2.126
8.5	0.194	0.741	1.406	1.534	1.866
9.5	0.025	0.408	0.985	1.472	1.614
10.5	0.006	0.300	0.641	1.024	1.543
11.5		0.138	0.623	0.824	1.016
12.5		0.104	0.362	0.632	1.055
13.5		0.062	0.348	0.428	0.819
14.5		0.029	0.132	0.328	0.630
15.5		0.022	0.105	0.192	0.535
16.5		0.006	0.073	0.156	0.464
17.5			0.052	0.138	0.307
18.5			0.036	0.103	0.260
19.5			0.022	0.113	0.315
21.0				0.045	0.135
23.0				0.041	0.131
25.0					0.066
27.0					0.070
29.0					0.030
31.0					0.016
33.0					0.011
35.0					0.006

* Powers of ten by which number in table should be multiplied.

** Neutrons/cm^3-sec

TABLE XIII

Spatial Distribution of 0.5 ev Neutrons in Liquid Hydrogen Due to Monoenergetic Neutrons of Energy E_0 Incident on Hydrogen Slabs at an Angle $\theta_0 = 75°$. The Incident Number Current is 1 Neutron/cm^2-sec.

Depth Inches	E_0=0.3 Mev 10^{-2} *	E_0= 1.0 Mev 10^{-2}	E_0= 2.0 Mev 10^{-2}	E_0= 3.0 Mev 10^{-2}	E_0=5.0 Mev 10^{-2}
0.5	4.115**	3.293	2.650	2.150	1.787
1.5	5.062	4.103	3.333	3.172	2.733
2.5	4.152	3.977	3.733	3.305	2.974
3.5	2.667	3.315	3.156	3.166	2.930
4.5	1.531	2.194	2.431	2.431	2.672
5.5	0.925	1.422	1.858	2.192	2.428
6.5	0.351	1.033	1.534	1.683	1.807
7.5	0.154	0.440	1.044	1.529	1.417
8.5	0.045	0.306	0.833	0.982	1.117
9.5	0.026	0.240	0.474	0.673	1.161
10.5	0.029	0.069	0.330	0.424	0.813
11.5	0.024	0.085	0.156	0.413	0.647
12.5		0.046	0.158	0.280	0.489
13.5		0.018	0.087	0.220	0.326
14.5		0.007	0.064	0.100	0.244
15.5			0.023	0.093	0.244
16.5			0.030	0.055	0.178
17.5			0.011	0.083	0.110
18.5			0.010	0.008	0.101
19.5			0.018	0.035	0.094

* Powers of ten by which number in table should be multiplied.

** Neutrons/cm^3-sec

TABLE XIV

Gamma Ray Albedo Factors for Monoenergetic
Parallel Beams Incident on Hydrogen Slabs
at Indicated Angle and Energy

Number Current Albedo

θ_o \ E_o	8.0(Mev)	6.0(Mev)	4.0(Mev)	3.0(Mev)	2.0(Mev)	1.0 (Mev)	0.5 (Mev)
0°	.063 ±.003*	.070 ±.003	.099 ±.004	0.142 ±.005	0.217 ±.006	0.369 ±.008	0.450 ±.008
25°	.072 ±.003	.090 ±.004	0.113 ±.004	0.147 ±.005	0.239 ±.006	0.396 ±.008	0.469 ±.008
45°	.097 ±.004	0.119 ±.004	0.152 ±.005	0.196 ±.005	0.287 ±.006	0.459 ±.008	0.538 ±.008
60°	0.157 ±.005	0.182 ±.005	0.216 ±.005	0.279 ±.006	0.364 ±.007	0.536 ±.008	0.603 ±.008
75°	.027 ±.002	0.328 ±.006	0.359 ±.006	0.424 ±.007	0.513 ±.008	0.656 ±.008	0.698 ±.008

Energy Current Albedo

0°	.0019 ±.0001	.0028 ±.0001	.0058 ±.0002	.0096 ±.0003	.0192 ±.0006	.050 ±.001	0.102 ±.009
25°	.0024 ±.0001	.0037 ±.0002	.0071 ±.0003	.0109 ±.0004	.0223 ±.0006	.055 ±.001	0.114 ±.002
45°	.0036 ±.0002	.0061 ±.0003	.0112 ±.0004	.0166 ±.0005	.0320 ±.0008	.072 ±.001	0.144 ±.002
60°	.0079 ±.0003	.0114 ±.0004	.0202 ±.0006	.0303 ±.0008	.050 ±.001	0.103 ±.002	0.179 ±.003
75°	.0236 ±.0008	.035 ±.001	.049 ±.001	.068 ±.002	.096 ±.002	0.167 ±.003	0.254 ±.003

Energy Flux Albedo

0°	.0038 ±.0002	.0061 ±.0006	.0123 ±.0007	.020 ±.001	.041 ±.002	0.103 ±.004	0.211 ±.007
25°	.0047 ±.0003	.0069 ±.0005	.0142 ±.0009	.021 ±.001	.041 ±.002	0.106 ±.004	0.216 ±.006
45°	.0061 ±.0004	.0105 ±.0008	.021 ±.002	.027 ±.001	.055 ±.004	0.112 ±.004	0.215 ±.006
60°	.0116 ±.0009	.016 ±.001	.028 ±.002	.041 ±.002	.064 ±.003	0.139 ±.006	0.212 ±.006
75°	.027 ±.002	.037 ±.002	.045 ±.002	.065 ±.003	.086 ±.004	0.126 ±.004	0.186 ±.005

*The (±) quantity is the standard error in the statistical estimate of the albedo.

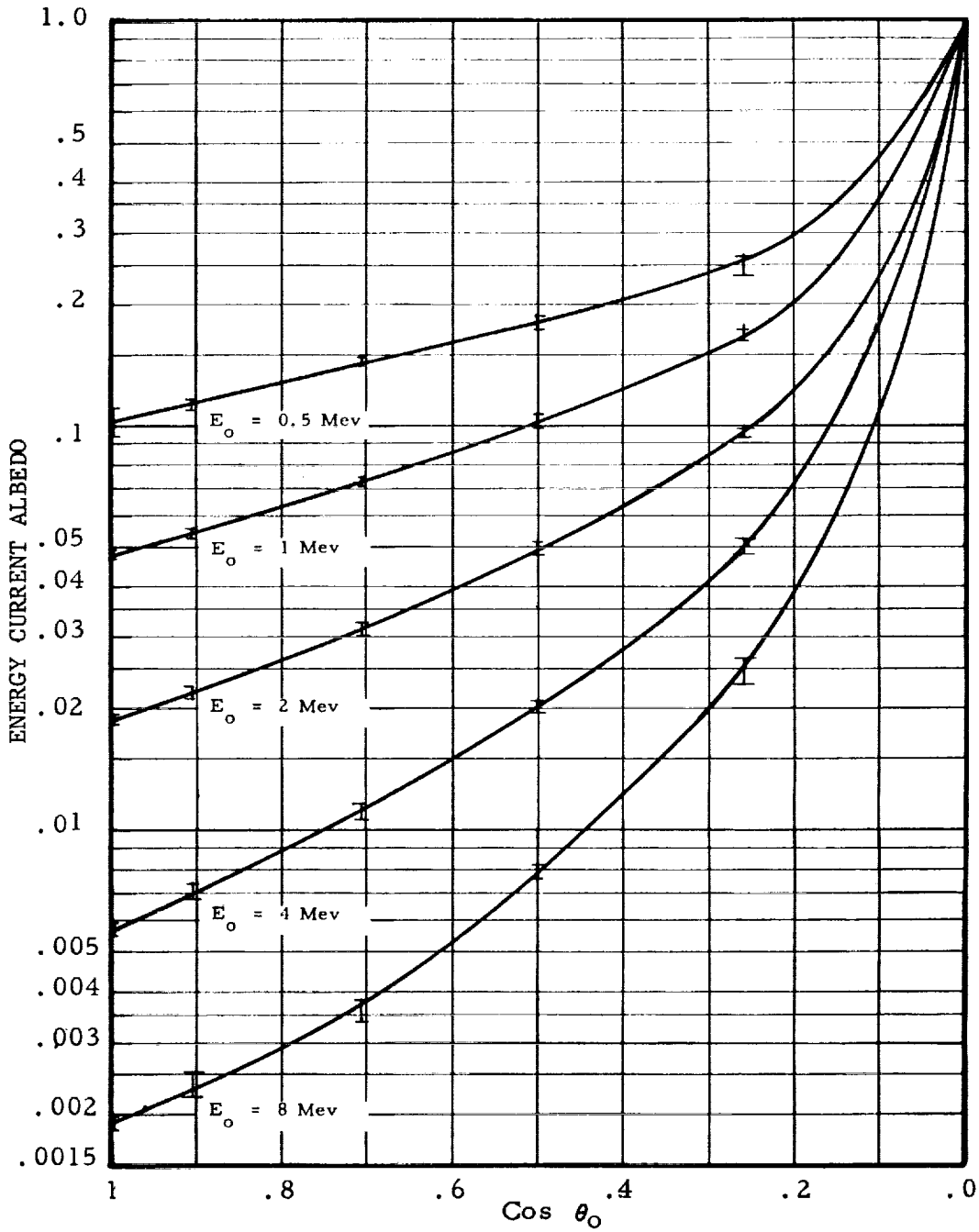

FIGURE 12. GAMMA RAY ENERGY CURRENT ALBEDO FACTORS VERSUS ANGLE OF INCIDENCE FOR MONOENERGETIC PARALLEL RAYS INCIDENT ON HYDROGEN SLABS

TABLE XV

Buildup Factors for Normal Incident Monoenergetic Gamma Rays in Hydrogen Slabs, $E_n = 0.025$ Mev

Energy Current Buildup Factors

$\mu_o x$ Mean Free Paths \ Energy E_o	6	4	3	2	1	0.5
7	3.00 ±.20*	3.18 ±.21	3.30 ±.18	4.14 ±.25	6.86 ±.38	9.22 ±.41
4	2.23 ±.06	2.44 ±.04	2.55 ±.07	2.96 ±.08	3.61 ±.10	4.49 ±.11
2	1.60 ±.01	1.69 ±.02	1.77 ±.02	1.91 ±.03	2.15 ±.05	2.39 ±.05
1	1.319 ±.003	1.35 ±.01	1.39 ±.01	1.45 ±.01	1.48 ±.02	1.61 ±.02

Energy Flux Buildup

7	3.30 ±.24	3.48 ±.24	3.76 ±.23	4.80 ±.30	8.95 ±.54	13.38 ±.67
4	2.36 ±.07	2.66 ±.04	2.89 ±.09	3.58 ±.11	4.60 ±.15	6.24 ±.19
2	1.68 ±.01	1.82 ±.02	1.94 ±.02	2.16 ±.04	2.62 ±.08	3.16 ±.10
1	1.364 ±.004	1.42 ±.01	1.50 ±.01	1.58 ±.01	1.70 ±.02	1.96 ±.03

Dose Buildup Factors

7	3.86 ±.32	4.03 ±.29	4.43 ±.29	5.70 ±.36	10.75 ±.60	19.33 ±.96
4	2.64 ±.08	3.02 ±.05	3.32 ±.11	4.07 ±.13	5.03 ±.16	7.16 ±.21
2	1.84 ±.01	2.01 ±.02	2.14 ±.02	2.35 ±.04	2.73 ±.08	3.24 ±.10
1	1.449 ±.004	1.52 ±.01	1.60 ±.01	1.66 ±.01	1.73 ±.02	1.94 ±.03

* The (±) quantity is the standard error in the statistical estimate of the buildup factor.

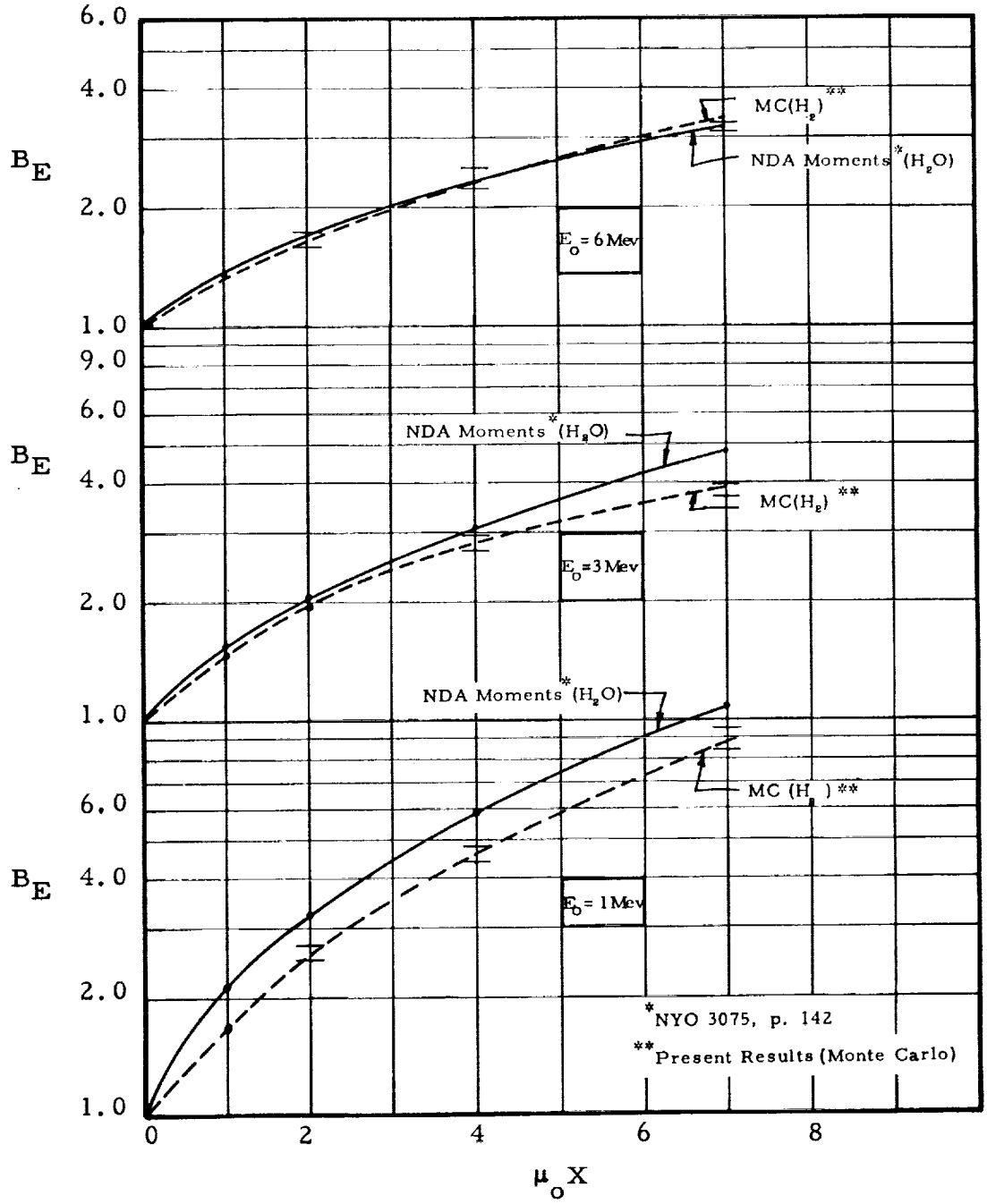

FIGURE 13. ENERGY FLUX BUILDUP FACTORS VERSUS MEAN FREE PATHS FOR NORMAL INCIDENT GAMMA RAYS IN H_2O AND H_2; PLANE MONOENERGETIC SOURCES. ENERGIES ARE ABOVE 0.025 MEV IN MONTE CARLO CALCULATIONS

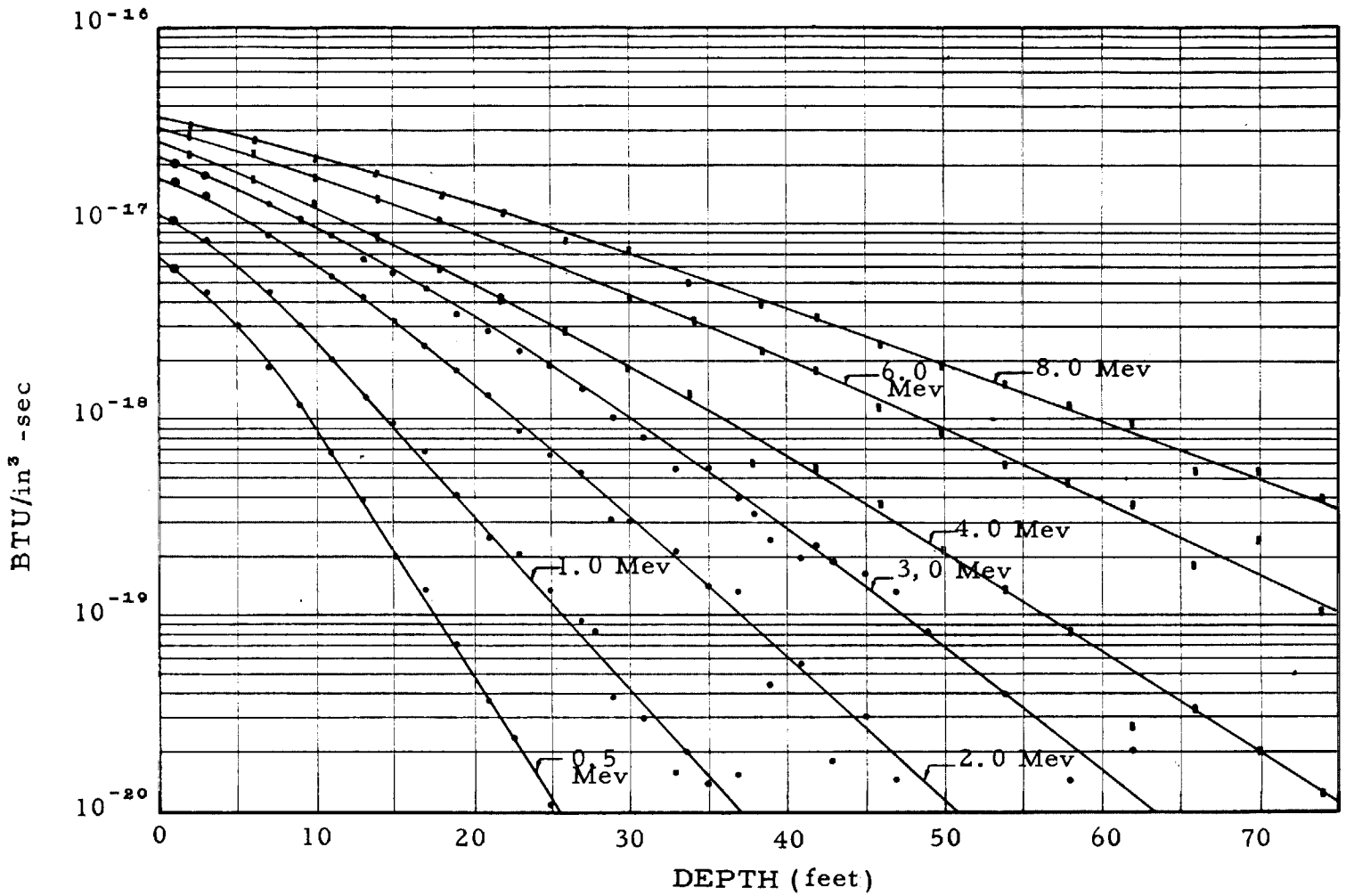

FIGURE 14. HEAT DEPOSITION VERSUS DEPTH IN LIQUID HYDROGEN SLABS FOR MONOENERGETIC GAMMA RAYS (1 PHOTON/CM^2-SEC) INCIDENT NORMAL TO THE SURFACE

TABLE XVI

Gamma Ray Energy Deposition, BTU/in^3-sec of One Incident Gamma/cm^2-sec

With Gamma Incident at $\theta_o = 0°$ and Initial Energies E_o

Depth Feet	0.5 Mev 10^{-18}*	1 Mev 10^{-18}	2 Mev 10^{-17}	3 Mev 10^{-17}	4 Mev 10^{-17}	6 Mev 10^{-17}	8 Mev 10^{-17}
2	5.099	9.150	1.499	1.918	2.264	2.753	3.195
6	2.417	5.565	1.013	1.394	1.697	2.312	2.650
10	0.933	2.529	0.630	0.937	1.284	1.706	2.134
14	0.297	1.172	0.348	0.645	0.881	1.330	1.805
18	0.103	0.554	0.196	0.410	0.595	1.038	1.390
22	0.029	0.228	0.110	0.228	0.411	0.750	1.110
26	0.009	0.114	0.061	0.162	0.284	0.566	0.809
30		0.034	0.031	0.098	0.182	0.424	0.735
34		0.015	0.018	0.057	0.135	0.324	0.496
38		0.010	0.013	0.034	0.060	0.222	0.381
42			0.005	0.024	0.055	0.179	0.325
46			0.002	0.016	0.037	0.118	0.248
50			0.001	0.008	0.021	0.086	0.187
54				0.004	0.014	0.059	0.154
58				0.002	0.073	0.048	0.121
62					0.044	0.037	0.098
66					0.031	0.018	0.055
70					0.017	0.024	0.055
74					0.019	0.011	0.040
78					0.012	0.008	0.024
82					0.005	0.004	0.028
86						0.002	0.011
90							0.017
94							0.007
98							0.007

*Powers of ten by which number in table should be multiplied.

TABLE XVII

Gamma Ray Energy Deposition, BTU/in^3-sec of One Incident Gamma/cm^2-sec

With Gamma Incident at $\theta_o = 25^\circ$ and Initial Energies E_o

Depth Feet	0.5 Mev 10^{-18}*	1 Mev 10^{-18}	2 Mev 10^{-17}	3 Mev 10^{-17}	4 Mev 10^{-17}	6 Mev 10^{-17}	8 Mev 10^{-17}
2	5.359	9.770	1.610	2.075	2.489	3.062	3.430
6	2.298	5.082	1.030	1.484	1.799	2.406	2.829
10	0.776	2.390	0.602	0.940	1.249	1.765	2.319
14	0.235	1.004	0.328	0.560	0.855	1.347	1.792
18	0.068	0.441	0.172	0.355	0.551	0.946	1.400
22	0.018	0.150	0.082	0.215	0.345	0.742	1.048
26	0.007	0.071	0.045	0.136	0.260	0.520	0.815
30	0.001	0.025	0.022	0.077	0.161	0.388	0.655
34		0.005	0.008	0.044	0.085	0.264	0.488
38			0.006	0.022	0.054	0.171	0.362
42			0.004	0.012	0.033	0.122	0.232
46			0.001	0.005	0.019	0.080	0.174
50				0.002	0.018	0.068	0.152
54					0.008	0.041	0.092
58					0.004	0.028	0.088
62					0.003	0.024	0.075
66					0.002	0.014	0.043
70						0.012	0.026
74						0.007	0.016
78						0.003	0.022
82							0.017
86							0.007
90							0.005
94							0.004
98							0.004

* Powers of ten by which number in table should be multiplied.

TABLE XVIII

Gamma Ray Energy Deposition, BTU/in^3-sec of One Incident Gamma/cm^2-sec

With Gamma Incident at $\theta_o = 45^\circ$ and Initial Energies E_o

Depth Feet	0.5 Mev 10^{-18}*	1 Mev 10^{-17}	2 Mev 10^{-17}	3 Mev 10^{-17}	4 Mev 10^{-17}	6 Mev 10^{-17}	8 Mev 10^{-17}
2	5.904	1.138	1.960	2.542	3.041	3.773	4.327
6	1.831	0.464	1.027	1.566	1.943	2.784	3.345
10	0.547	0.170	0.486	0.831	1.220	1.866	2.505
14	0.141	0.058	0.219	0.462	0.716	1.257	1.779
18	0.044	0.021	0.100	0.246	0.419	0.852	1.260
22	0.011	0.008	0.043	0.130	0.263	0.554	0.896
26	0.006	0.002	0.025	0.066	0.139	0.329	0.631
30		0.001	0.008	0.029	0.077	0.212	0.434
34			0.006	0.014	0.035	0.146	0.290
38			0.002	0.011	0.026	0.088	0.206
42				0.004	0.015	0.066	0.123
46				0.002	0.006	0.036	0.091
50				0.001	0.005	0.016	0.055
54					0.004	0.008	0.051
58						0.004	0.022
62						0.004	0.017
66						0.004	0.014
70						0.004	0.008
74						0.001	0.011
78							0.004
82							0.005
86							
90							
94							
98							

* Powers of ten by which number in table should be multiplied.

TABLE XIX

Gamma Ray Energy Deposition, BTU/in^3-sec of One Incident Gamma/cm^2-sec

With Gamma Incident at $\theta_o = 60^\circ$ and Initial Energies E_o

Depth Feet	0.5 Mev 10^{-18}*	1 Mev 10^{-17}	2 Mev 10^{-17}	3 Mev 10^{-17}	4 Mev 10^{-17}	6 Mev 10^{-17}	8 Mev 10^{-17}
2	6.440	1.309	2.407	3.276	3.950	5.090	5.907
6	1.372	0.361	0.890	1.442	2.039	3.021	3.880
10	0.293	0.099	0.327	0.646	0.972	1.734	2.403
14	0.082	0.025	0.114	0.269	0.478	0.964	1.484
18	0.021	0.010	0.044	0.113	0.212	0.516	0.918
22	0.004	0.002	0.017	0.050	0.097	0.312	0.593
26	0.002	0.001	0.005	0.021	0.049	0.144	0.347
30			0.002	0.009	0.023	0.077	0.191
34			0.002	0.004	0.008	0.038	0.108
38				0.001	0.009	0.019	0.078
42				0.002	0.001	0.014	0.054
46					0.001	0.004	0.032
50						0.004	0.013
54						0.005	0.009
58						0.002	0.007
62							0.003

*Powers of ten by which number in table should be multiplied.

TABLE XX

Gamma Ray Energy Deposition, BTU/in^3-sec of One Incident Gamma/cm^2-sec
With Gamma Incident at $\theta_o = 75^\circ$ and Initial Energies E_o

Depth Feet	0.5 Mev 10^{-18}*	1 Mev 10^{-17}	2 Mev 10^{-17}	3 Mev 10^{-17}	4 Mev 10^{-17}	6 Mev 10^{-17}	8 Mev 10^{-17}
2	6.562	1.452	3.034	4.422	5.666	7.746	9.412
6	0.654	0.164	0.455	0.872	1.414	2.589	3.827
10	0.158	0.041	0.109	0.215	0.378	0.858	1.539
14	0.041	0.011	0.033	0.064	0.116	0.296	0.599
18	0.011	0.003	0.013	0.023	0.035	0.127	0.255
22	0.002		0.004	0.007	0.014	0.042	0.113
26	0.001		0.001	0.005	0.008	0.016	0.039
30				0.001	0.002	0.009	0.019
34						0.004	0.005
38						0.001	0.004

* Powers of ten by which number in table should be multiplied.

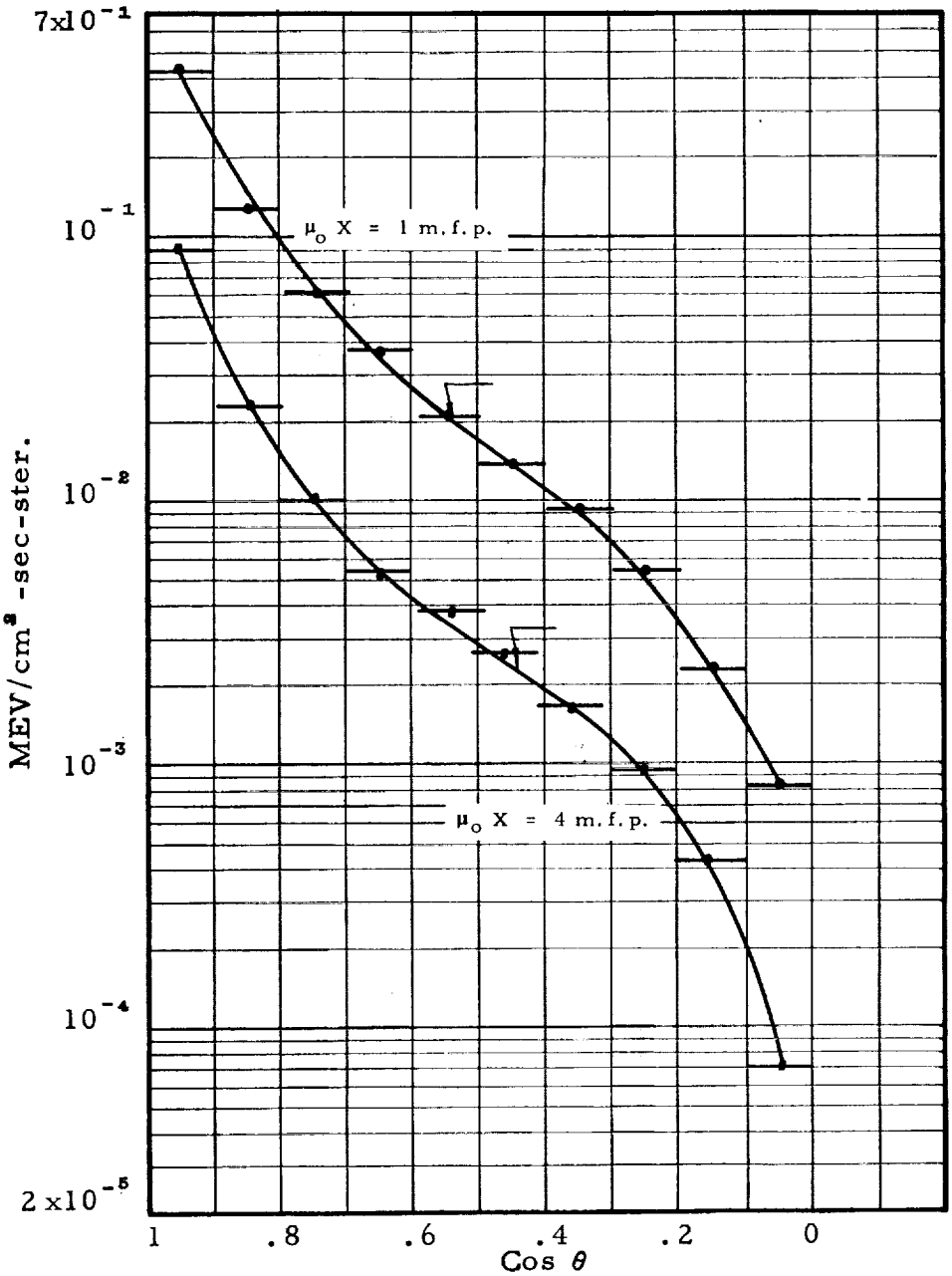

FIGURE 15. TRANSMITTED SCATTERED ANGULAR DISTRIBUTION FOR 3 MEV GAMMA RAYS INCIDENT NORMALLY ON HYDROGEN SLABS OF 1 AND 4 MEAN FREE PATHS; J_o=1 PHOTON/CM^2 - SEC

TABLE XXI

Angular Distribution and Associated Average Energies of Scattered Gamma Rays for Normal Incident Photons of Energy E_0, on Liquid Hydrogen Slabs of 1 Mean Free Path Thickness; In Units of (Photons-Mev/cm^2-sec-steradian)

Slab Thickness (Feet)	10.62	8.10	6.76	5.32	3.68	2.69
Initial Energy (Mev) / cos θ Interval	6	4	3	2	1	0.5
1-.9	8.33(-1)*	5.33(-1)	4.16(-1)	2.88(-1)	1.02(-1)	5.74(-2)
.9-.8	1.53(-1)	1.48(-1)	1.26(-1)	9.42(-1)	6.33(-2)	3.74(-2)
.8-.7	6.05(-2)	6.48(-2)	6.12(-2)	5.51(-2)	4.04(-2)	2.50(-2)
.7-.6	3.26(-2)	3.20(-2)	3.75(-2)	3.41(-2)	2.78(-2)	1.85(-2)
.6-.5	1.85(-2)	2.13(-2)	2.09(-2)	2.16(-2)	1.83(-2)	1.51(-2)
.5-.4	1.07(-2)	1.25(-2)	1.34(-2)	1.09(-2)	1.38(-2)	1.02(-2)
.4-.3	6.42(-3)	8.56(-3)	9.35(-3)	9.07(-3)	8.52(-3)	7.14(-3)
.3-.2	3.31(-3)	4.55(-3)	5.51(-3)	5.17(-3)	5.09(-3)	3.62(-3)
.2-.1	1.85(-3)	1.77(-3)	2.27(-3)	3.23(-3)	2.54(-3)	2.97(-3)
.1-0	4.99(-4)	3.22(-4)	8.15(-4)	6.91(-4)	5.51(-4)	6.95(-4)

Average Energy (Mev) of Scattered Transmitted Photons

1-.9	3.39	2.36	1.82	1.32	0.63	0.38
.9-.8	1.44	1.22	1.05	0.83	0.56	0.31
.8-.7	0.88	0.81	0.72	0.62	0.47	0.28
.7-.6	0.65	0.58	0.57	0.49	0.39	0.26
.6-.5	0.51	0.48	0.46	0.42	0.33	0.23
.5-.4	0.42	0.41	0.37	0.35	0.31	0.24
.4-.3	0.37	0.38	0.37	0.33	0.32	0.20
.3-.2	0.33	0.33	0.30	0.34	0.28	0.19
.2-.1	0.30	0.32	0.29	0.30	0.19	0.20
.1-0	0.26	0.20	0.33	0.39	0.24	0.15

* The number in parenthesis is the power of ten by which the number is multiplied.

TABLE XXII

Angular Distribution and Associated Average Energies of Scattered Gamma Rays for Normal Incident Photons, of Energy E_0, on Liquid Hydrogen Slabs of 2 Mean Free Path Thickness; In Units of (Photons-Mev/cm^2-sec-steradian)

Slab Thickness (Feet)	21.25	16.21	13.52	10.63	7.37	5.38
Initial Energy (Mev) / cos θ Interval	6	4	3	2	1	0.5
1-.9	5.99(-1)*	4.01(-1)	3.10(-1)	2.11(-1)	9.04(-2)	4.53(-2)
.9-.8	9.74(-2)	1.02(-1)	8.97(-2)	7.93(-2)	6.28(-2)	3.20(-2)
.8-.7	3.65(-2)	4.09(-2)	4.21(-2)	4.20(-2)	3.05(-2)	2.35(-2)
.7-.6	2.01(-2)	2.36(-2)	2.55(-2)	2.17(-2)	2.33(-2)	1.74(-2)
.6-.5	1.14(-2)	1.44(-2)	1.34(-2)	1.73(-2)	1.58(-2)	1.13(-2)
.5-.4	6.83(-3)	7.32(-3)	8.80(-3)	7.95(-3)	1.15(-2)	8.62(-3)
.4-.3	4.43(-3)	3.90(-3)	5.34(-3)	7.02(-3)	7.45(-3)	5.60(-3)
.3-.2	2.44(-3)	3.35(-3)	3.34(-3)	3.90(-3)	3.98(-3)	3.79(-3)
.2-.1	1.06(-3)	1.12(-3)	1.69(-3)	1.32(-3)	9.14(-4)	1.76(-3)
.1-0	3.13(-4)	5.16(-4)	2.55(-4)	2.85(-4)	4.70(-4)	3.66(-4)

Average Energy (Mev) of Scattered Transmitted Photons

1-.9	3.30	2.18	1.64	1.08	0.50	0.27
.9-.8	1.35	1.07	0.86	0.67	0.42	0.25
.8-.7	0.79	0.68	0.60	0.48	0.21	0.26
.7-.6	0.58	0.55	0.47	0.34	0.27	0.19
.6-.5	0.47	0.45	0.40	0.34	0.28	0.19
.5-.4	0.38	0.37	0.36	0.27	0.25	0.17
.4-.3	0.34	0.32	0.30	0.27	0.23	0.17
.3-.2	0.30	0.32	0.28	0.24	0.20	0.16
.2-.1	0.28	0.22	0.28	0.24	0.16	0.14
.1-0	0.22	0.30	0.23	0.12	0.18	0.16

* The number in parenthesis is the power of ten by which the number is multiplied.

TABLE XXIII

Angular Distribution and Associated Average Energies of Scattered Gamma Rays for Normal Incident Photons, of Energy E_o , on Liquid Hydrogen Slabs of 4 Mean Free Path Thickness; In Units of (Photon-Mev/cm^2-sec-steradian)

Slab Thickness (Feet)	42.49	37.41	27.04	21.26	14.74	10.76
Initial Energy (Mev) / cosθ Interval	6	4	3	2	1	0.5
1-.9	1.71(-1)*	1.21(-1)	8.80(-2)	6.23(-2)	3.34(-2)	1.75(-2)
.9-.8	2.37(-2)	2.44(-2)	2.29(-2)	2.15(-2)	1.65(-2)	1.09(-2)
.8-.7	9.31(-3)	1.07(-2)	1.01(-2)	1.16(-2)	9.24(-3)	7.96(-3)
.7-.6	4.81(-3)	4.61(-3)	5.40(-3)	7.36(-3)	6.43(-3)	5.19(-3)
.6-.5	3.02(-3)	2.62(-3)	3.81(-3)	3.92(-3)	4.48(-3)	3.08(-3)
.5-.4	1.71(-3)	2.10(-3)	2.59(-3)	2.78(-3)	2.29(-3)	2.64(-3)
.4-.3	7.28(-4)	1.16(-3)	1.65(-3)	1.92(-3)	1.71(-3)	1.75(-3)
.3-.2	5.09(-4)	6.24(-4)	9.38(-4)	1.58(-3)	1.27(-3)	1.01(-3)
.2-.1	1.74(-4)	2.98(-4)	4.32(-4)	9.05(-4)	4.88(-4)	7.01(-4)
.1-0	3.00(-6)	6.18(-5)	7.23(-5)	1.56(-4)	9.55(-5)	4.78(-5)

Average Energy (Mev) of Scattered Transmitted Photons

1-.9	3.40	2.16	1.57	0.97	0.45	0.21
.9-.8	1.45	1.05	0.77	0.56	0.32	0.17
.8-.7	0.82	0.64	0.50	0.42	0.26	0.16
.7-.6	0.54	0.46	0.35	0.37	0.22	0.14
.6-.5	0.44	0.34	0.28	0.27	0.24	0.11
.5-.4	0.46	0.32	0.27	0.24	0.15	0.13
.4-.3	0.36	0.27	0.26	0.21	0.15	0.11
.3-.2	0.43	0.28	0.24	0.29	0.18	0.10
.2-.1	0.20	0.32	0.26	0.28	0.15	0.13
.1-0	0.08	0.19	0.33	0.36	0.12	0.12

* The number in parenthesis is the power of ten by which the number is multiplied.

TABLE XXIV

Angular Distribution and Associated Average Energies of Scattered Gamma Rays for Normal Incident Photons of Energy E_o, on Liquid Hydrogen Slabs of 7 Mean Free Path Thickness; In Units of (Photon-Mev/cm^2-sec-steradian)

Slab Thickness (Feet)	74.37	56.72	47.31	37.20	25.79	18.83
Initial Energy (Mev) / cos θ Interval	6	4	3	2	1	0.5
1-.9	1.30(-2)*	9.70(-3)	6.52(-3)	5.68(-3)	3.71(-3)	1.84(-3)
.9-.8	2.22(-3)	1.26(-3)	1.84(-3)	1.69(-3)	1.88(-3)	1.35(-3)
.8-.7	9.75(-4)	7.80(-4)	7.14(-4)	6.66(-4)	1.03(-3)	9.37(-4)
.7-.6	6.75(-4)	3.72(-4)	3.07(-4)	3.59(-4)	6.92(-4)	6.71(-4)
.6-.5	2.72(-4)	1.39(-4)	2.73(-4)	2.85(-4)	5.01(-4)	3.75(-4)
.5-.4	6.67(-5)	2.16(-4)	1.74(-4)	2.43(-4)	3.38(-4)	3.43(-4)
.4-.3	4.96(-5)	2.10(-4)	5.40(-5)	1.75(-4)	1.07(-4)	2.56(-4)
.3-.2	2.74(-5)	1.42(-6)	1.07(-4)	1.70(-5)	1.56(-4)	1.30(-4)
.2-.1	7.14(-6)	8.92(-6)	1.60(-5)	1.10(-5)	6.11(-5)	5.25(-5)
.1-0.	5.47(-5)	1.05(-7)	3.64(-6)	3.46(-6)	5.12(-6)	1.02(-5)

Average Energy (Mev) of Scattered Transmitted Photons

1-.9	3.16	2.18	1.33	0.94	0.35	0.14
.9-.8	1.24	0.87	0.66	0.46	0.30	0.12
.8-.7	0.83	0.57	0.35	0.28	0.21	0.11
.7-.6	0.72	0.40	0.21	0.21	0.19	0.11
.6-.5	0.38	0.28	0.34	0.21	0.16	.08
.5-.4	0.25	0.40	0.28	0.21	0.14	.08
.4-.3	0.41	0.41	0.20	0.20	0.10	.08
.3-.2	0.20	0.06	0.19	0.08	0.18	.07
.2-.1	0.09	0.14	0.15	0.04	0.12	.05
.1-0	0.44	0.48	0.43	0.04	0.04	.05

* The number in parenthesis is the power of ten by which the number is multiplied.

there are $(1-\cos\theta_o)/2$ particles per second incident on the end of the cylinder. The particles are emitted isotropically and the fraction which intercepts the cylinder in a solid angle $\Delta\Omega = 2\pi \sin\theta\, d\theta$ is given by the probability density function

$$f(\upsilon)d\upsilon = \frac{d\upsilon}{1-\upsilon_o}, \quad \upsilon_o \leq \upsilon \leq 1,$$

where $\upsilon = \cos\theta$ and $\upsilon_o = \cos\theta_o$. A value υ_k can be chosen by solving the following equation for the upper limit:

$$\int_{\upsilon_o}^{\upsilon_k} \frac{d\upsilon}{1-\upsilon_o} = \xi$$

where ξ is a random number between 0 and 1.

Thus, $\upsilon_k = \upsilon_o + \xi\,(1-\upsilon_o)$. However, the value υ_k is more efficiently chosen by using the systematic relationship

$$\upsilon_k = \upsilon_o + \frac{k}{N}(1-\upsilon_o), \quad 1 \leq k \leq N,$$

where k denotes the kth history and N is the total sample size. Thus, one history is taken in each direction defined by υ_k. Because only one particle is taken in each direction, each particle has the same weight. Thus,

$$W_o = \frac{1-\upsilon_o}{2N} \cdot S_o \quad \text{(particle/sec)}$$

is the weight of each particle where N is the total number of sampled directions and S_o is the source strength (1 particle/sec).

In order to estimate the number of particles per cm^2 which escape the bounding surfaces of the cylinder, the cylinder's surface is divided in the following manner. Each end is divided into ten concentric circles so that the area between any two circles is 1/10 of the total cross-sectional area (Fig. 16). Thus $R_j = \sqrt{j/10}\,R$, where $j = 0, 1, 2, \ldots, 10$, R = radius of cylinder, and the area $\Delta A = \pi R^2/10 = \pi(R_j^2 - R_{j-1}^2)$. Next, the cylinder is divided into ten equal disks of radius R and bounded by planes $Z_i = (Z_T/10)i$, where $i=0,1,2,\ldots,10$. The curved surface area of each disk is given by $\Delta s = 2\pi R(Z_T/10)$, where Z_T is the total length of the cylinder. The differential volumes of the cylinder are formed by the intersections of the concentric cylinders of radius R_j and the disks bounded by Z_i. Thus, there are 100 equal differential volumes

$$\Delta v_{ij} = \frac{\pi R^2 Z_T}{100},$$

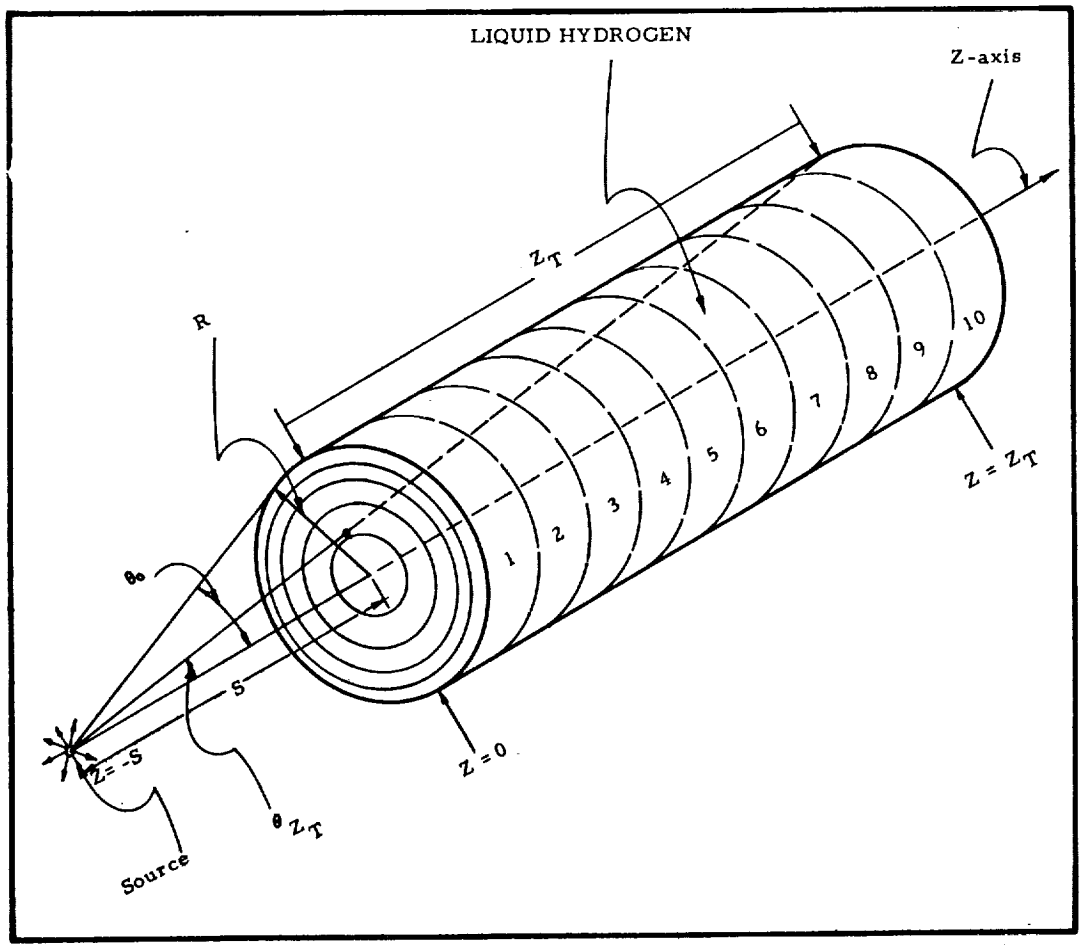

FIGURE 16. SOURCE AND GEOMETRY USED IN THE CYLINDRICAL MONTE CARLO CALCULATIONS

which are defined by the boundaries $(Z_i - Z_{i-1})$ and $(R_j - R_{j-1})$.

The particles are traced through the cylinder in the following manner. The kth particle of weight W_o has an initial direction specified by the unit vector $\vec{\Omega}(\upsilon_{ok}, \phi_{ok})$ where $\upsilon_{ok} = \cos\theta_{ok} = \upsilon_o + \frac{k}{N}(1 - \upsilon_o)$, and the azimuthal angle $\theta_{ok} = 0°$. The particle is assumed to start at the source (Z = -S) and intersects the cylinder at the coordinates,

$$X_{ok} = S \tan\theta_{ok}$$

$$Y_{ok} = 0$$

$$Z_{ok} = 0,$$

and at a radial distance from the Z-axis given by

$$r_{ok} = X_{ok}$$

First, the probability of the particle escaping the cylinder without a collision is calculated. This probability is determined in one of two ways, according to whether (1) the uncollided particle escapes the end at $Z = Z_T$, or (2) the uncollided particle escapes the side. In order to choose the correct case, the boundary relationship

$$\cos\theta_{Z_T} = \frac{S + Z}{\sqrt{R^2 + (S + Z)^2}}$$

is used (Fig.2). If $\nu_{ok} \geq \cos\theta Z_T$, the particle escapes as in case (1); otherwise, it escapes as in case (2). The treatment of the two cases follow

Case 1: The probability of the kth particle escaping the end without a collision is given by

$$P_{ok} = \exp\left[-\Sigma(E_o)\, Z_T \sec\theta_{ok}\right]$$

The radial coordinate at which this particle would exit the end of the cylinder is

$$R_U = (S + Z)\tan\theta_{ok}$$

Consequently, the uncollided contribution of the kth particle is recorded in the appropriate range $(R_i - R_{i-1})$ which contains R_U. The uncollided number current and flux for the kth particle is given by

$$J_{oki} = \frac{W_o P_{ok}}{\Delta A_i} \left(\frac{\text{particles}}{\text{cm}^2 - \text{sec}}\right)$$

$$F_{oki} = \frac{W_o P_{ok}}{\cos \theta_{ok} \Delta A_i} \left(\frac{\text{particles}}{\text{cm}^2 - \text{sec}}\right)$$

where ΔA_i is the differential area ($\Delta A = \pi R^2/10$) and the index i connotes the radial range ($R_i - R_{i-1}$).

Case 2: The probability of escaping the side without a collision is given by

$$P_{ok} = \exp\left\{ - \Sigma (E_o) \left[\frac{R}{\sin \theta_{ok}} - \frac{S}{\cos \theta_{ok}} \right] \right\}.$$

The Z-coordinate at which this particle would exit the side of the cylinder is given by

$$Z_U = R \cot \theta_{ok} - S .$$

Consequently, the uncollided contribution of the kth particle is recorded in the appropriate range ($Z_j - Z_{j-1}$) which contains Z_U . The uncollided number current and flux for the kth particle is given by

$$J_{okj} = \frac{W_o P_{ok}}{\Delta S_j} \left(\frac{\text{particles}}{\text{cm}^2 - \text{sec}}\right)$$

$$F_{okj} = \frac{W_o P_{ok}}{\sin \theta_{ok} \cdot \Delta S_j} \left(\frac{\text{particles}}{\text{cm}^2 - \text{sec}}\right) ,$$

where ΔSj is the differential surface area ($\Delta S_j = 2\pi R\ Z_T/10$). After the uncollided transmission is estimated for the kth particle, the distance, d , to the first scattering point is found as follows:

$$d = - \frac{1}{\Sigma(E_o)} \ln \xi$$

where ξ is a random number between 0 and 1. The rectangular coordinates at this first collision point are given by

$$X_{1k} = X_{ok} + d \sin \theta_{ok} \cos \phi_{ok},$$

$$Y_{1k} = Y_{ok} + d \sin \theta_{ok} \sin \phi_{ok},$$

$$Z_{1k} = Z_{ok} + d \cos \theta_{ok} ,$$

and

$$r_{1k}^2 = X_{1k}^2 + Y_{1k}^2 .$$

If either $r_{1k}^2 \geq R^2$, $Z_{1k} \geq Z_T$, or $Z_{1k} \leq 0$, the particle has escaped the cylinder and the history is terminated. If the particle does not escape, the direction of scattering and change in energy is found in the same manner as described in Section I. The spherical coordinates of the new direction vector $\vec{\Omega}_{1k}$ are given by

$$\upsilon_{1k} = \cos\theta_{1k} = \upsilon_{ok}\mu + \sqrt{1-\mu^2}\sqrt{1-\upsilon_{ok}^2}\cos\psi$$

$$\sin\theta_{1k} = \sqrt{1-\upsilon_{1k}^2}$$

$$\cos\phi_{1k} = \cos\phi_{ok}\cos\Delta\phi - \sin\phi_{ok}\sin\Delta\phi$$

$$\sin\phi_{1k} = \sin\phi_{ok}\cos\Delta\phi + \cos\phi_{ok}\sin\Delta\phi .$$

At the coordinates (X_{1k}, Y_{1k}, Z_{1k}), and for the new direction $\vec{\Omega}$ $(\upsilon_{1k}, \phi_{1k})$ of the particle, the probability of escape is again determined. The symmetry of starting from the Z-axis is now destroyed and the calculation proceeds as follows. If the value of $\cos\theta_{1k} > 0$ the distance from the point (X_{1k}, Y_{1k}, Z_{1k}) to the plane defined by $Z = Z_T$ is given by

$$D = \frac{Z_T - Z_{1k}}{\cos\theta_{1k}} , \quad \cos\theta_{1k} > 0 .$$

If $\cos\theta_{1k} < 0$, the distance to the plane $Z = 0$ is given by

$$D = \frac{Z_{1k}}{|\cos\theta_{1k}|} , \quad \cos\theta_{1k} < 0 .$$

Next, the coordinates of the intersection of the vector $\vec{\Omega}_{1k}$ with either the plane $Z = Z_T$ or $Z = 0$ are found:

$$X_D = X_{1k} + D\sin\theta_{1k}\cos\phi_{1k}$$

$$Y_D = Y_{1k} + D\sin\theta_{1k}\sin\phi_{1k}$$

and

$$R_D^2 = X_D^2 + Y_D^2$$

If $R_D^2 \leq R^2$, the direction $\vec{\Omega}_{1k}$ will intercept one end of the cylinder and the probability of escape in the direction $\vec{\Omega}_{1k}$ is

$$P_{1k} = \exp\left[-\Sigma(E_1)\,D\right] .$$

Then, according to whether $\cos\theta_{1k}$ is positive or negative, the transmitted or reflected number current is recorded in the radial range $(R_i - R_{i-1})$ which contains R_D. Thus,

$$J_{1ki} = \frac{W_o P_{1k}}{\Delta A_i} \left(\frac{\text{particles}}{\text{cm}^2 - \text{sec}}\right)$$

$$F_{1ki} = \frac{W_o P_{1k}}{\cos\theta_{1k} \Delta A_i} \left(\frac{\text{particles}}{\text{cm}^2 - \text{sec}}\right)$$

If the particle escapes the side of the cylinder $(R_D^2 > R^2)$, the following procedure is used. The value of D is recalculated and becomes the distance from the point (X_{1k}, Y_{1k}, Z_{1k}) to the surface $X^2 + Y^2 = R^2$ in the direction defined by $\vec{\Omega}_{1k}$. In order to find D, it is expedient to define the direction cosines of the vector $\vec{\Omega}_{1k}$.

Thus,

$$\cos\alpha = \sin\theta_{1k} \cos\phi_{1k}$$

$$\cos\beta = \sin\theta_{1k} \sin\phi_{1k}$$

$$\cos\gamma = \cos\theta_{1k} \quad .$$

Now the distance D to the surface $X^2 + Y^2 = R^2$ can be found by solving the following system of four equations for D:

$$\cos\alpha = \frac{X_D - X_{1k}}{D}$$

$$\cos\beta = \frac{Y_D - Y_{1k}}{D}$$

$$\cos\gamma = \frac{Z_D - Z_{1k}}{D}$$

$$R^2 = X_D^2 + Y_D^2 \ ,$$

where X_D, Y_D, Z_D, and D are variables. The solution of this system of equations gives

$$D = \frac{-A + \sqrt{A^2 + R^2 - r^2_{1k}}}{\sin\theta_{1k}}$$

where

$$A = X_{1k} \cos \phi_{1k} + Y_{1k} \sin \phi_{1k}$$

and

$$r^2_{1k} = X^2_{1k} + Y^2_{1k} .$$

Also,

$$Z_D = Z_{1k} + D \cos \theta_{1k} ;$$

$$X_D = X_{1k} + D \sin \theta_{1k} \cos \phi_{1k}$$

and

$$Y_D = Y_{1k} + D \sin \theta_{1k} \sin \phi_{1k} ,$$

where $X_D^2 + Y_D^2 = R^2$. From the foregoing, it follows that the first scatter contribution to the number current of the kth particle is given by

$$J_{1kj} = \frac{W_o \exp\left[-\Sigma\ (E_1)D\right]}{\Delta S_j} \quad \frac{\text{particles}}{\text{cm}^2\text{-sec}} .$$

This quantity is tabulated in the appropriate interval $(Z_j - Z_{j-1})$ given by Z_D above. In order to calculate the number flux, it is necessary to find the angle, θ_N, that the unit vector $\vec{\Omega}_{1k}$ makes with the surface normal at (X_D, Y_D, Z_D). The cosine of the angle θ_N is given by the vector equation

$$\frac{\vec{\Omega}_{1k} \cdot \vec{R}}{|\vec{R}|} = \cos \theta_N .$$

The $\vec{R}$ is the vector of the surface normal and its direction is defined by the points $(0, 0, Z_D)$ on the axis and (X_D, Y_D, Z_D) on the surface of the cylinder. The direction cosines of $\vec{R}$ are given by

$$\cos \alpha_R = \frac{X_D}{R}$$

$$\cos \beta_R = \frac{Y_D}{R}$$

$$\cos \gamma_R = 0$$

consequently

$$\cos \alpha \ \cos \alpha_R + \cos \beta \ \cos \beta_R + \cos \gamma \ \cos \gamma_R = \cos \theta_N$$

Substituting the values of the direction cosines in the above equations, the following value of $\cos \theta_N$ is found:

$$\cos\theta_N = \frac{\sin\theta_{1k}}{R}\ (X_D \cos\phi_{1k} + Y_D \sin\phi_{1k}).$$

The scattered number flux contribution from the first scatter of the kth particle is now given as

$$F_{1kj} = \frac{W_o \exp\left[-\Sigma(E_1)\ \bar{D}\right]}{\cos\theta_N \cdot \Delta S_j}$$

This quantity is tabulated in the appropriate interval $(Z_j - Z_{j-1})$ given by Z_D above.

The next step is to determine the distance to the second scattering point, $d = -\ln \xi/\Sigma(E_1)$, and continue as before, using the same steps as given for the first scattering event. This procedure is repeated until the particle either escapes the cylinder or else is degraded in energy below a cutoff energy E_n . The final estimates of the number current and flux are the sum of the contributions from all the N histories and their individual scattering events. For example, letting s connote the sequence of scattering of the kth particle,

$$\langle F_i \rangle = \sum_{k=1}^{N} \sum_{s} F_{ski}$$

or

$$\langle F_j \rangle = \sum_{k=1}^{N} \sum_{s} F_{skj} \quad ,$$

gives the final estimate of the number flux transmission for either the ith radial interval at the ends of the cylinders or the jth surface interval on the sides. The value F_{ski} is zero unless the sth scatter of the kth history is directed toward the area defined by i . A similar statement applies to the F_{skj} .

The energy deposition rates are calculated in a manner similar to that for slab geometry. Thus, the total energy deposition rate from n collisions in a differential volume ΔV_{ij} is given by

$$Q_{ij} = \sum_n (W_o \cdot \Delta E_n)/\Delta V_{ij} \left[\mathrm{MEV/cm^3\ -sec}\right].$$

In the foregoing discussion, the transmitted energy current and the energy flux are calculated in the same manner as described in the section on slab geometry (i.e., multiplying the differential number current or flux term by the energy E_{ski} or E_{skj}).

In the present computer code, options are available for path length biasing similar to those described for the plane geometry. However, the likelihood of premature escapes are much greater than in the slab geometry and a study of the biasing effects should be made before extensive calculations are performed. All production runs have been made with at least 10,000 particle histories. The running time for the cylindrical geometry calculations on the IBM 7090 is about 1.3 minutes per thousand histories. Some results of these calculations are given in parts B and C. Because of the intricate details available from the cylindrical Monte Carlo calculations there are presented only thirteen calculated cases for both neutrons and gammas. A larger set of combinations of cases is needed but can be better chosen at a later date when a more definitive application arises. Also, it is intended that the geometry be modified so that cylinders with elliptical ends may be considered.

B. RESULTS OF NEUTRON TRANSPORT

A summary of energy data for neutrons incident on liquid hydrogen cylinders is given in Table XXV. An interesting point is that 94 to 97% of the incident energy is absorbed in the hydrogen cylinder for all six cases examined. Figure 17 illustrates the heat deposition from 3 Mev neutrons in a liquid hydrogen cylinder as a function of both depth and radial distance from the axis of the cylinder. These data are taken from one of the computer printouts described below.

Computer Printouts: The first twelve pages of the computer printout present six cases for neutron transport in hydrogen cylinders. All six cases are for cylinders of five mean free paths length (Fig. 16). The description of the computer data is given in the "Key to IBM Printouts" which follow Fig. 18.

C. RESULTS OF GAMMA RAY TRANSPORT

Table XXVI presents a summary of gamma energy data taken from the last 14 pages of the IBM printouts. Figure 18 illustrates typical results obtained for gamma ray heating in hydrogen cylinders. This figure creates a question about the shape of the heating rate curves at the greater depth ($Z > 20$ feet). It is not certain whether the convexity is due to deep penetration effects or to insufficient statistics at these depths. This trend appears to be energy dependent (i.e., the more energetic initial photons are likely to show this convexity at deep penetrations). The explanation for this may be that since the scattering of a high-energy photon results in a greater energy loss, it subsequently possesses a comparatively larger mean free path.

Computer Printouts: There are fourteen pages representing seven cases of gamma ray transport in cylinders. The description of the output is the same as that described for the neutron transport except for the transmitted gamma angular distribution. Also, the case for the 2.23-Mev gammas is different in two respects from all the other calculations:

(1) the source is taken essentially on the cylinders end (depicting a point source at a surface); and

(2) the layer thicknesses ($\triangle$ Z) are chosen to be exactly three feet, resulting in a total length of 5.30$\frac{1}{2}$ mean free paths for the cylinder.

The table giving the "Transmitted Gamma Angular Distribution" (Mev/cm^2-sec-ster) in the gamma ray printouts is essentially the same quantity discussed in Section I, part C, for slab geometry under "Angular Distributions." The only difference is that in the cylindrical geometry the uncollided and scattered transmissions are added together rather than differentiated as in the slab geometry. Note that the cos θ intervals on the printouts are indicated by the upper limit only; thus, 1.0 represents the interval from 1.0 to 0.9.

TABLE XXV

Neutron Energy Disposition in a 30-Foot Diameter Liquid Hydrogen Cylinder of 5 Mean Free Paths Length; For a Point Isotropic Source on Axis of Cylinder and With Cut Off Energy of 10^{-6} Mev

E_o (Mev)	Separation of Source From Cylinder (Feet)	Solid Angle Fraction of Cylinder	Fraction of Incident Energy Absorbed In H_2 Cylinder	Fraction of Incident Energy Escaping Sides of Cylinder	Fraction of Incident Energy Escaping Far End of Cylinder	Fraction of Incident Energy Reflected at Near End of Cylinder	Total Fractions *
1	11.25	0.2	0.970	0.014	0.011	0.007	1.002
3	11.25	0.2	0.958	0.026	0.010	0.006	1.000
7	11.25	0.2	0.939	0.048	0.009	0.005	1.001
1	20	0.1	0.966	0.015	0.016	0.002	.999
3	20	0.1	0.953	0.028	0.015	0.002	.998
7	20	0.1	0.937	0.050	0.011	0.002	1.000

* Difference From 1.000 indicates error due to statistical estimation.

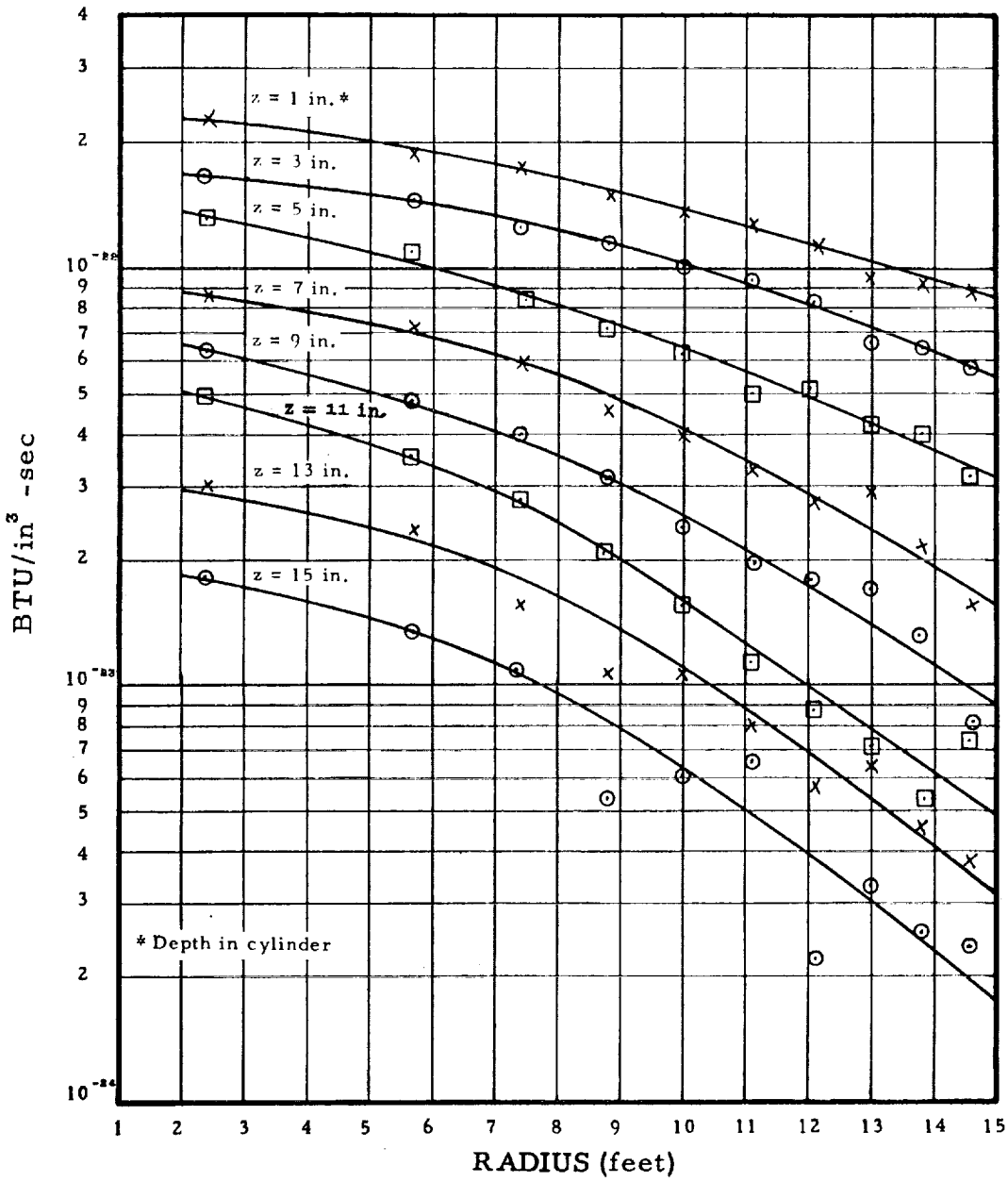

FIGURE 17. NEUTRON HEATING RATE (BTU/IN^3 - SEC) IN A LIQUID HYDROGEN CYLINDER FROM A POINT ISOTROPIC SOURCE (1 NEUTRON/SEC) OF 3 MEV NEUTRONS AT A DISTANCE OF 11.25 FEET FROM THE 30-FOOT DIAMETER CYLINDER

TABLE XXVI

Gamma Ray Energy Disposition in a 30-Foot Diameter Liquid Hydrogen Cylinder of 5 Mean Free Paths Length; For a Point Isotropic Source on Axis of Cylinder

E_o (Mev)	Separation of Source From Cylinder (Feet)	Solid Angle Fraction of Cylinder	Fraction of Incident Energy Adsorbed In H_2 Cylinder	Fraction of Incident Energy Escaping Sides of Cylinder	Fraction of Incident Energy Escaping Far End of Cylinder	Fraction of Incident Energy Reflected at Near End of Cylinder	Total Fraction *	Cutoff Energy (Mev)
1	11.25	0.2	0.658	0.283	.008	.047	0.996	.025
3	11.25	0.2	0.600	0.382	.002	.010	0.994	.075
6	11.25	0.2	0.509	0.477	.001	.003	0.990	.100
1	20	0.1	0.668	0.278	.010	.041	0.997	.025
3	20	0.1	0.613	0.372	.004	.008	0.997	.075
6	20	0.1	0.537	0.450	.002	.002	0.991	.100
2.23	0.03	0.499	0.828	0.102	.002	.060	0.992	.050

* Difference from 1.000 indicates error due to statistical estimation and cutoff energy.

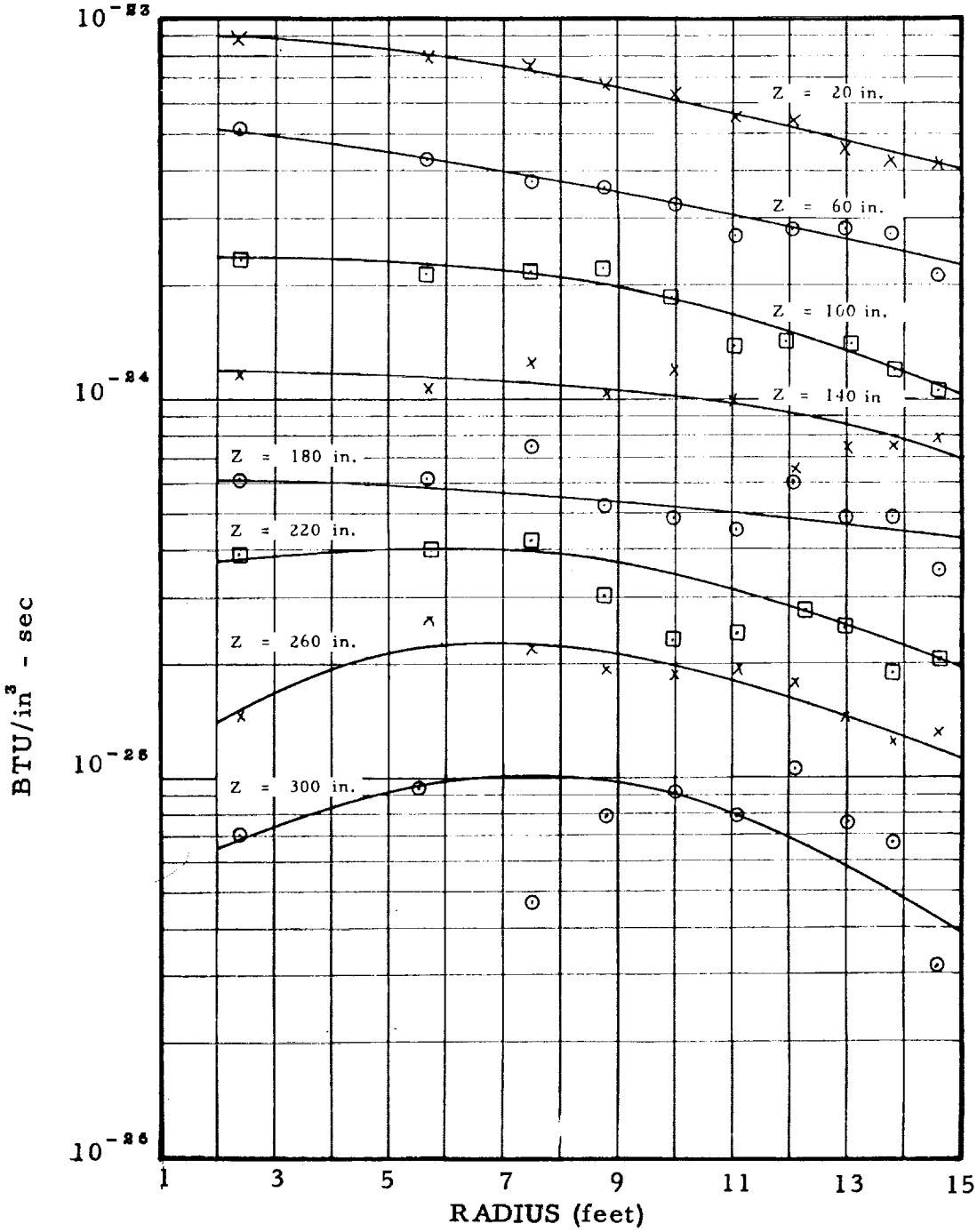

FIGURE 18. GAMMA RAY HEATING RATE (BTU/IN^3-SEC) IN A LIQUID HYDROGEN CYLINDER FROM A POINT ISOTROPIC SOURCE (1 PHOTON/SEC) OF 3 MEV GAMMAS AT A DISTANCE OF 11.25 FEET FROM THE 30-FOOT DIAMETER CYLINDER

D. KEY TO IBM PRINTOUTS

First Sheet

1. Incident energy of neutrons in Mev
2. Cut off energy of neutrons in Mev
3. Length of cylinder in cm
4. Radius of cylinder in cm
5. Distance of source from cylinder in cm
6. Density of hydrogen in gm/cm^3
7. Sample size
8. Special computer instructions
9. Conversion factor for Mev/cm^3 to BTU/in^3
10. Differential volume, $(\pi R^2 Z_T/100)$ cm^3
11. Mean free paths of cylinder's length
12. Differential area on ends of cylinder $(\pi R^2/10)\,cm^2$
13. Differential area in sides of cylinder $(2\pi R Z_T/10)\,cm^2$
14. Solid angle fraction subtended at source by cylinder; also the number of neutrons incident on cylinder's end
15. Number of neutrons/cm^2 incident at center of cylinder $(1/4\pi S^2)$
16. Average current density incident on cylinder's end $(1 - \cos\theta_o)/2\pi R^2$
17. Number of neutrons/cm^2 incident at the edge of the cylinder $(\cos^2\theta_o/4\pi S^2)$
18. Upper limit of radial intervals (cm); the distance from Z-axis of cylinder
19. Row designation for number current, flux and energy current respectively
20. Current, flux and energy current of neutrons transmitted to far end of cylinder in indicated radial interval
21. Same as 20 except for neutrons reflected at incident end of cylinder
22. Total number of neutrons escaping ends or cylinder (neutrons/sec) of (Mev/sec); transmitted or reflected as designated
23. Depth intervals $(Z_T/10)$ cm measured along Z-axis in equal increments
24. Same as 20, 21, and 22, except for neutrons escaping, sides of cylinder as designated by row and column headings

Second Sheet

25. Same as 23
26. Heat rate deposition (BTU/in^3-sec); average for the volume element designated by row and column headings
27. Heat rate deposition (BTU/in^3-sec) averaged over the column intervals and divided by the average incident current density (16). This quantity is comparable to heat rate deposition in slab geometry as a function of depth.
28. Total heat (BTU/sec) deposited in the hydrogen cylinder.
29. Slow neutron (0.5 ev) volume distribution (neutrons/cm^3-sec); average for the volume element and designated by the row and column headings
30. Slow neutron volume distribution (neutron/cm^2-sec) averaged over the column intervals and divided by the average incident current density (16). This quantity is comparable to the slow neutron volumn distribution in slab geometry as a function of depth.
31. The total number of neutrons terminated inside the cylinder (neutrons/sec)

The data are written in the form y.yyE zz and y.yyE-zz. They are to be read as $y.yy \times 10^{zz}$ and $y.yy \times 10^{-zz}$

First Sheet

CYLINDRICAL GEOMETRY - NEUTRONS IN HYDROGEN
POINT ISOTROPIC SOURCE OF 1 NEUTRON/SEC ON AXIS

EO(1)(EV)	EN(2)(EV)	ZT(3)(CM)	R(4)(CM)	S(5)(CM)	RHO(6)(GM/CM3)	7	MI	8	C
3.00E 00	10.00E-07	5.1[illegible]E 01	4.57E 02	3.[illegible]E 02	7.00E-02	10.00	0.	0.	0.
9	10	11	12	13	14	15	16	17	
2.48E-15	[illegible]	[illegible]	CA[illegible]	[illegible]	[illegible]	[illegible]	[illegible]	[illegible]	2.45E-07

NEUTRONS ESCAPING ENDS OF CYLINDER PER CM2-SEC

	1.45E 02	2.04E 02	2.50E 02	2.89E 02	3.23E 02	18	3.83E 02	4.09E 02	4.34E 02	4.57E 02	NO/SEC
	FORE - THETA LESS THAN 90 DEG										
C	2.56E-08	1.52E-08	1.13E-08	8.44E-09	6.88E-09	20	2.66E-09	3.15E-09	1.83E-09	2.99E-09	5.42E-03
FLUX	4.72E-08	2.15E-08	1.89E-08	1.46E-08	9.60E-09	[illegible]	3.64E-09	5.06E-09	2.54E-09	4.35E-09	[illegible]
E*C	2.95E-08	1.96E-08	1.15E-08	9.44E-09	7.48E-09	3.50E-09	2.73E-09	3.18E-09	1.38E-09	3.34E-09	[illegible]
	AFT - THETA GREATER THAN 90 DEG										
C	4.37E-08	3.56E-08	3.02E-08	3.63E-08	3.95E-08	21	3.56E-08	3.08E-08	2.84E-08	2.87E-08	2.33E-02
FLUX	9.19E-08	6.82E-08	6.88E-08	7.11E-08	8.25E-08	[illegible]	7.60E-08	7.01E-08	5.66E-08	6.07E-08	4.91E-02
E*C	1.96E-09	2.85E-09	3.73E-09	4.83E-09	5.17E-09	[illegible]	6.64E-09	6.84E-09	5.01E-09	6.29E-09	3.30E-03

NEUTRONS ESCAPING SIDES OF CYLINDER PER CM2-SEC

	1	2	3	4	5	23	7	8	9	10	NO/SEC
	DEPTH(LAYER NUMBER)										
	FORE - THETA LESS THAN 90 DEG										
C	1.78E-07	1.19E-07	6.37E-08	2.84E-08	2.01E-08	1.11E-08	5.85E-09	5.53E-09	1.04E-09	2.06E-09	6.42E-03
FLUX	2.35E-07	1.42E-07	9.98E-08	4.32E-08	2.99E-08	2.37E-08	9.01E-09	8.65E-09	1.61E-09	8.48E-09	9.18E-03
E*C	4.75E-07	2.55E-07	1.38E-07	6.24E-08	3.48E-08	[illegible]	9.88E-09	1.01E-08	1.90E-09	3.44E-09	1.49E-02
	AFT - THETA GREATER THAN 90 DEG										
C	2.64E-08	2.51E-08	1.17E-08	4.21E-09	5.12E-09	6.37E-09	3.63E-09	2.86E-10	1.29E-09	7.27E-11	1.24E-03
FLUX	3.78E-08	3.25E-08	2.59E-08	8.14E-09	8.72E-09	8.24E-09	4.51E-09	2.95E-10	1.87E-09	1.24E-10	1.89E-03
E*C	1.48E-08	1.01E-08	4.89E-09	3.97E-09	6.28E-10	1.96E-09	4.87E-11	3.71E-10	1.05E-12	2.91E-11	5.45E-04

Second Sheet

NEUTRON HEAT DEPOSITION(BTU/IN3-SEC)

LAYER	1.45E 02	2.04E 02	2.50E 02	2.89E 02	[illegible]23E 02	18	3.83E 02	4.09E 02	4.34E 02	4.57E 02	AVG/J+
1	7.65E-23	7.03E-23	6.91E-23	[illegible]45E-23	6.18E-23	6.27E-23	5.64E-23	5.47E-23	5.57E-23	4.91E-23	4.03E-16
2	6.12E-23	5.47E-23	5.18E-23	5.28E-23	5.00E-23	4.71E-23	4.42E-23	3.87E-23	3.69E-23	3.71E-23	3.12E-16
3	4.52E-23	4.22E-23	3.70E-23	3.09E-23	3.38E-23	3.16E-23	2.92E-23	2.95E-23	2.40E-23	2.48E-23	2.16E-16
4	2.83E-23	2.91E-23	2.79E-23	2.83E-23	2.47E-23	2.16E-23	1.82E-23	2.19E-23	1.65E-23	1.55E-23	[illegible]
5	2.43E-23	2.26E-23	2.07E-23	2.07E-23	1.76E-23	[illegible]	1.28E-23	1.45E-23	1.29E-23	1.26E-23	[illegible]
6	1.47E-23	1.77E-23	1.12E-23	1.17E-23	9.86E-24	[illegible]	9.81E-24	7.94E-24	9.46E-24	6.84E-24	[illegible]
7	1.04E-23	1.11E-23	7.86E-24	7.77E-24	6.02E-24	[illegible]	6.53E-24	6.14E-24	6.01E-24	3.99E-24	[illegible]
8	8.72E-24	6.88E-24	6.49E-24	3.98E-24	4.85E-24	2.44E-24	4.90E-24	3.35E-24	1.94E-24	2.39E-24	3.02E-17
9	4.75E-24	4.36E-24	5.09E-24	3.07E-24	2.86E-24	3.05E-24	2.64E-24	2.00E-24	2.68E-24	9.53E-25	2.07E-17
10	3.95E-24	2.79E-24	3.94E-24	1.98E-24	1.91E-24	1.82E-24	8.03E-25	1.53E-24	1.36E-24	9.34E-25	1.37E-17
										TOTAL BTU/SEC	28 7.11E-16

VOLUME DISTRIBUTION OF THERMALIZED NEUTRONS(NEUTRONS/CM3)

LAYER	1.45E 02	2.04E 02	2.50E 02	2.89E 02	3.23E 02	18	3.83E 02	4.09E 02	4.34E 02	4.57E 02	AVG/J+
1	5.31E-09	5.34E-09	5.05E-09	2.99E-09	3.20E-09	2.72E-09	2.37E-09	2.16E-09	2.25E-09	1.86E-09	1.74E-02
2	5.56E-09	4.71E-09	5.48E-09	4.17E-09	4.88E-09	4.20E-09	4.62E-09	3.34E-09	3.76E-09	3.05E-09	[illegible]
3	5.71E-09	5.51E-09	5.12E-09	5.03E-09	4.29E-09	5.06E-09	3.85E-09	4.11E-09	3.49E-09	2.55E-09	[illegible]
4	4.91E-09	4.82E-09	3.70E-09	4.5[illegible]E-09	3.43E-09	[illegible]0E-09	3.61E-09	3.70E-09	2.90E-09	2.40E-09	[illegible]
5	3.91E-09	4.11E-09	3.97E-09	3.76E-09	3.20E-09	[illegible]E-09	2.72E-09	2.43E-09	2.19E-09	2.25E-09	[illegible]
6	2.90E-09	3.70E-09	2.52E-09	2.81E-09	1.92E-09	[illegible]E-09	1.95E-09	1.98E-09	1.84E-09	1.51E-09	[illegible]
7	2.66E-09	2.22E-09	1.75E-09	1.45E-09	1.63E-09	1.39E-09	1.33E-09	1.51E-09	1.07E-09	7.70E-10	[illegible]
8	1.75E-09	1.48E-09	1.39E-09	1.35E-09	8.77E-10	1.01E-09	7.99E-10	6.81E-10	7.70E-10	4.74E-10	6.58E-03
9	1.18E-09	1.15E-09	1.18E-09	7.10E-10	5.92E-10	7.10E-10	5.62E-10	5.03E-10	3.33E-10	2.94E-10	4.88E-03
10	7.70E-10	4.14E-10	4.74E-10	4.74E-10	2.66E-10	3.55E-10	3.55E-10	7.10E-10	3.55E-10	3.55E-10	2.97E-03
										TOTAL NEUTRONS/SEC	31 5.30E-02

CYLINDRICAL GEOMETRY - NEUTRONS IN HYDROGEN
POINT ISOTROPIC SOURCE OF 1 NEUTRON/SEC ON AXIS

EO(MEV)	EN(MEV)	ZT(CM)	R(CM)	S(CM)	RHO(GM/CM3)	N	M1	M2	U
1.000E 00	10.000E-07	2.787E 01	4.572E 02	3.429E 02	7.000E-02	10000	0.	0.	0.

G	CV(CM3)	XC	CA(CM2)	DS(CM2)	NO. IN	MAX J+	AVG J+	MIN J+
2.486E-15	1.830E 05	5.000E 00	6.567E 04	8.005E 03	2.000E-01	6.768E-07	3.046E-07	2.436E-07

NEUTRONS ESCAPING ENDS OF CYLINDER PER CM2-SEC

	RADIUS 1.45E 02	2.04E 02	2.50E 02	2.89E 02	3.23E 02	3.54E 02	3.83E 02	4.09E 02	4.34E 02	4.57E 02	NO/SEC
	FORE - THETA LESS THAN 90 DEG										
C	3.59E-08	2.39E-08	1.40E-08	1.55E-08	8.51E-09	6.05E-09	6.49E-09	3.81E-09	2.64E-09	1.74E-09	7.79E-03
FLUX	5.24E-08	4.08E-08	2.00E-08	2.32E-08	1.29E-08	9.63E-09	1.38E-08	5.80E-09	5.76E-09	2.53E-09	1.23E-02
E*C	1.14E-08	8.12E-09	3.92E-09	4.15E-09	1.98E-09	1.22E-09	1.18E-09	7.61E-10	6.14E-10	6.24E-10	2.23E-03
	AFT - THETA GREATER THAN 90 DEG										
C	7.37E-08	6.28E-08	6.32E-08	5.57E-08	5.50E-08	4.50E-08	4.61E-08	4.58E-08	4.17E-08	4.13E-08	3.48E-02
FLUX	1.32E-07	1.26E-07	1.23E-07	1.43E-07	1.45E-07	9.51E-08	9.93E-08	1.33E-07	6.87E-06	1.01E-07	7.79E-02
E*C	1.02E-09	8.47E-10	1.42E-09	1.95E-09	2.72E-09	2.10E-09	2.24E-09	2.54E-09	2.50E-09	2.86E-09	1.33E-03

NEUTRONS ESCAPING SIDES OF CYLINDER PER CM2-SEC

	DEPTH(LAYER NUMBER) 1	2	3	4	5	6	7	8	9	10	NO/SEC
	FORE - THETA LESS THAN 90 DEG										
C	1.79E-07	1.11E-07	6.11E-08	4.28E-08	1.83E-08	1.04E-08	1.73E-09	8.59E-09	2.53E-09	1.92E-09	3.51E-03
FLUX	2.34E-07	1.69E-07	9.35E-08	6.33E-08	3.90E-08	1.67E-08	2.36E-09	1.47E-08	3.01E-09	2.77E-09	5.11E-03
E*C	1.60E-07	8.17E-08	3.95E-08	2.46E-08	1.13E-08	7.87E-09	1.37E-09	2.81E-09	6.85E-10	1.65E-09	2.65E-03
	AFT - THETA GREATER THAN 90 DEG										
C	3.32E-08	3.21E-08	1.76E-08	8.07E-09	2.59E-09	4.17E-10	2.05E-10	5.17E-09	5.66E-10	1.45E-09	8.11E-04
FLUX	4.98E-08	5.17E-08	2.32E-08	1.08E-08	2.90E-09	6.10E-10	4.01E-10	7.97E-09	8.72E-10	2.07E-09	1.20E-03
E*C	7.80E-09	3.43E-09	2.31E-09	5.18E-10	1.01E-10	7.36E-12	4.71E-11	2.89E-10	4.87E-13	2.86E-13	1.16E-04

CYLINDRICAL GEOMETRY - NEUTRONS IN HYDROGEN
POINT ISOTROPIC SOURCE OF 1 NEUTRON/SEC ON AXIS

EO(MEV)	EN(MEV)	ZT(CM)	R(CM)	S(CM)	RHO(GM/CM3)	N	M1	M2	U
1.000E 00	10.000E-07	2.787E 01	4.572E 02	3.429E 02	7.000E-02	10000	0.	0.	0.

G	CV(CM3)	XC	DA(CM2)	DS(CM2)	NO. IN	MAX J+	AVG J+	MIN J+
2.486E-15	1.830E 05	5.000E 00	6.567E 04	8.005E 03	2.000E-01	6.768E-07	3.046E-07	2.436E-07

NEUTRON HEAT DEPOSITION(BTU/IN3-SEC)

LAYER	RADIUS 1.45E 02	2.04E 02	2.50E 02	2.89E 02	3.23E 02	3.54E 02	3.83E 02	4.09E 02	4.34E 02	4.57E 02	AVG/J+
1	1.33E-22	1.16E-22	1.02E-22	9.10E-23	8.23E-23	7.42E-23	6.69E-23	6.73E-23	5.93E-23	5.28E-23	2.77E-16
2	1.10E-22	8.53E-23	7.81E-23	6.99E-23	5.69E-23	5.18E-23	4.42E-23	4.49E-23	3.68E-23	3.44E-23	2.01E-16
3	8.15E-23	6.69E-23	5.43E-23	4.58E-23	3.80E-23	3.60E-23	2.62E-23	2.23E-23	2.41E-23	1.82E-23	1.36E-16
4	5.63E-23	4.89E-23	3.64E-23	3.28E-23	2.61E-23	2.13E-23	1.96E-23	1.31E-23	1.34E-23	1.21E-23	9.19E-17
5	4.61E-23	3.33E-23	2.62E-23	1.98E-23	1.68E-23	1.27E-23	1.48E-23	8.85E-24	7.76E-24	6.99E-24	6.35E-17
6	3.00E-23	2.28E-23	1.66E-23	1.24E-23	9.10E-24	9.96E-24	7.85E-24	6.24E-24	3.74E-24	3.10E-24	4.00E-17
7	2.08E-23	1.34E-23	1.12E-23	9.39E-24	5.10E-24	5.08E-24	3.88E-24	3.31E-24	2.10E-24	2.69E-24	2.53E-17
8	1.39E-23	9.27E-24	6.23E-24	5.46E-24	1.89E-24	2.55E-24	1.77E-24	1.78E-24	1.01E-24	1.68E-24	1.50E-17
9	8.43E-24	5.32E-24	3.67E-24	3.15E-24	1.19E-24	2.24E-24	1.87E-24	1.31E-24	4.05E-25	7.88E-25	9.32E-18
10	4.53E-24	4.01E-24	1.75E-24	2.26E-24	1.35E-24	5.62E-25	7.17E-25	3.57E-25	4.29E-25	2.35E-25	5.32E-18
									TOTAL BTU/SEC		2.94 E-17

VOLUME DISTRIBUTION OF THERMALIZED NEUTRONS(NEUTRONS/CM3)

LAYER	RADIUS 1.45E 02	2.04E 02	2.50E 02	2.89E 02	3.23E 02	3.54E 02	3.83E 02	4.09E 02	4.34E 02	4.57E 02	AVG/J+
1	1.34E-08	1.25E-08	1.10E-08	1.19E-08	7.87E-09	6.89E-09	7.32E-09	6.23E-09	5.25E-09	3.83E-09	2.83E-02
2	2.31E-08	1.79E-08	1.75E-08	1.40E-08	1.39E-08	1.08E-08	9.07E-09	1.03E-08	8.52E-09	5.90E-09	4.30E-02
3	2.45E-08	2.33E-08	1.62E-08	1.61E-08	1.28E-08	1.27E-08	9.73E-09	8.63E-09	7.10E-09	7.32E-09	4.54E-02
4	2.56E-08	1.97E-08	1.79E-08	1.49E-08	1.13E-08	9.95E-09	8.42E-09	7.10E-09	8.09E-09	5.03E-09	4.20E-02
5	2.35E-08	1.86E-08	1.48E-08	1.15E-08	9.95E-09	1.06E-08	6.78E-09	6.99E-09	6.23E-09	4.70E-09	3.73E-02
6	1.80E-08	1.53E-08	1.04E-08	8.85E-09	7.32E-09	5.90E-09	7.21E-09	4.59E-09	3.83E-09	2.73E-09	2.76E-02
7	1.44E-08	1.08E-08	9.84E-09	6.34E-09	7.10E-09	4.59E-09	4.70E-09	3.83E-09	2.62E-09	2.19E-09	2.18E-02
8	1.08E-08	7.76E-09	5.25E-09	4.04E-09	3.39E-09	3.50E-09	2.84E-09	3.06E-09	1.86E-09	1.75E-09	1.45E-02
9	7.10E-09	4.92E-09	4.81E-09	3.17E-09	2.30E-09	1.75E-09	1.09E-09	9.84E-10	1.20E-09	1.20E-09	9.37E-03
10	3.50E-09	2.84E-09	1.64E-09	2.30E-09	1.09E-09	1.97E-09	1.09E-10	6.56E-10	3.28E-10	2.19E-10	4.81E-03
									TOTAL NEUTRONS/SEC		1.53E-01

CYLINDRICAL GEOMETRY - NEUTRONS IN HYDROGEN
POINT ISOTROPIC SOURCE OF 1 NEUTRON/SEC ON AXIS

EO(MEV)	EN(MEV)	ZT(CM)	R(CM)	S(CM)	RHO(GM/CM3)	N	M1	M2	U
3.000E 00	10.000E-07	5.145E 01	4.572E 02	3.429E 02	7.000E-02	10000	0.	0.	0.

G	CV(CM3)	XC	DA(CM2)	DS(CM2)	NO. IN	MAX J+	AVG J+	MIN J+
2.486E-15	3.379E 05	5.000E 00	6.567E 04	1.478E 04	2.000E-01	6.768E-07	3.046E-07	2.436E-07

NEUTRONS ESCAPING ENDS OF CYLINDER PER CM2-SEC

	RADIUS										
	1.45E 02	2.04E 02	2.50E 02	2.89E 02	3.23E 02	3.54E 02	3.83E 02	4.09E 02	4.34E 02	4.57E 02	NO/SEC
	FORE - THETA LESS THAN 90 DEG										
C	2.56E-08	1.52E-08	1.13E-08	8.40E-09	6.66E-09	4.45E-09	2.66E-09	3.15E-09	1.83E-09	2.99E-09	5.40E-03
FLUX	4.72E-08	2.15E-08	1.89E-08	1.46E-08	9.60E-09	5.91E-09	3.64E-09	5.06E-09	2.54E-09	4.35E-09	8.76E-03
E*C	2.95E-08	1.96E-08	1.15E-08	9.44E-09	7.48E-09	5.50E-09	2.73E-09	3.18E-09	1.38E-09	3.34E-09	6.15E-03
	AFT - THETA GREATER THAN 90 DEG										
C	4.37E-08	3.58E-08	3.62E-08	3.63E-08	3.95E-08	3.98E-08	3.56E-08	3.08E-08	2.84E-08	2.87E-08	2.33E-02
FLUX	9.19E-08	6.83E-08	6.88E-08	7.11E-08	8.25E-08	1.01E-07	7.60E-08	7.01E-08	5.66E-08	6.07E-08	4.91E-02
E*C	1.96E-09	2.85E-09	3.73E-09	4.83E-09	5.17E-09	6.87E-09	6.64E-09	6.86E-09	5.01E-09	6.29E-09	3.30E-03

NEUTRONS ESCAPING SIDES OF CYLINDER PER CM2-SEC

	DEPTH(LAYER NUMBER)										
	1	2	3	4	5	6	7	8	9	10	NO/SEC
	FORE - THETA LESS THAN 90 DEG										
C	1.78E-07	1.19E-07	6.37E-08	2.84E-08	2.01E-08	1.11E-08	5.85E-09	5.53E-09	1.06E-09	2.06E-09	6.42E-03
FLUX	2.35E-07	1.62E-07	9.98E-08	4.32E-08	2.99E-08	2.37E-08	9.01E-09	8.65E-09	1.61E-09	8.48E-09	9.18E-03
E*C	4.75E-07	2.55E-07	1.38E-07	6.24E-08	3.48E-08	1.82E-08	9.88E-09	1.01E-08	1.90E-09	3.64E-09	1.49E-02
	AFT - THETA GREATER THAN 90 DEG										
C	2.64E-08	2.31E-08	1.17E-08	6.21E-09	5.12E-09	6.37E-09	3.63E-09	2.86E-10	1.29E-09	7.27E-11	1.24E-03
FLUX	3.78E-08	3.25E-08	2.59E-08	8.14E-09	8.72E-09	8.24E-09	4.51E-09	2.95E-10	1.87E-09	1.24E-10	1.89E-03
E*C	1.48E-08	1.01E-08	4.89E-09	3.97E-09	6.28E-10	1.96E-09	4.87E-11	3.71E-10	1.05E-12	2.91E-11	5.45E-04

CYLINDRICAL GEOMETRY - NEUTRONS IN HYDROGEN
POINT ISOTROPIC SOURCE OF 1 NEUTRON/SEC ON AXIS

EO(MEV)	EN(MEV)	ZT(CM)	R(CM)	S(CM)	RHO(GM/CM3)	N	M1	M2	U
3.000E 00	10.000E-07	5.145E 01	4.572E 02	3.429E 02	7.000E-02	10000	0.	0.	0.

G	CV(CM3)	XC	DA(CM2)	DS(CM2)	NO. IN	MAX J+	AVG J+	MIN J+
2.486E-15	3.379E 05	5.000E 00	6.567E 04	1.478E 04	2.000E-01	6.768E-07	3.046E-07	2.436E-07

NEUTRON HEAT DEPOSITION(BTU/IN3-SEC)

	RADIUS										
	1.45E 02	2.04E 02	2.50E 02	2.89E 02	3.23E 02	3.54E 02	3.83E 02	4.09E 02	4.34E 02	4.57E 02	AVG/J+
LAYER											
1	2.25E-22	1.87E-22	1.73E-22	1.49E-22	1.34E-22	1.27E-22	1.13E-22	9.36E-23	9.03E-23	8.66E-23	4.53E-16
2	1.64E-22	1.46E-22	1.25E-22	1.15E-22	9.86E-23	9.28E-23	8.25E-23	6.61E-23	6.43E-23	5.67E-23	3.32E-16
3	1.31E-22	1.09E-22	8.49E-23	7.16E-23	6.18E-23	4.93E-23	5.07E-23	4.15E-23	3.95E-23	3.17E-23	2.20E-16
4	8.37E-23	7.15E-23	5.94E-23	4.50E-23	3.97E-23	3.29E-23	2.72E-23	2.86E-23	2.19E-23	1.54E-23	1.40E-16
5	6.35E-23	4.77E-23	4.02E-23	3.15E-23	2.41E-23	1.95E-23	1.79E-23	1.70E-23	1.31E-23	8.06E-24	9.28E-17
6	4.96E-23	3.52E-23	2.81E-23	2.11E-23	1.56E-23	1.14E-23	8.71E-24	7.39E-24	5.49E-24	7.43E-24	6.24E-17
7	3.04E-23	2.36E-23	1.58E-23	1.07E-23	1.07E-23	8.03E-24	5.82E-24	6.46E-24	4.62E-24	3.80E-24	3.94E-17
8	1.80E-23	1.36E-23	1.09E-23	5.35E-24	6.13E-24	6.53E-24	2.21E-24	3.36E-24	2.54E-24	2.37E-24	2.33E-17
9	1.38E-23	8.91E-24	5.97E-24	5.07E-24	4.23E-24	3.12E-24	1.46E-24	1.41E-24	1.35E-24	1.02E-24	1.52E-17
10	9.11E-24	6.58E-24	4.53E-24	3.46E-24	1.78E-24	1.40E-24	1.27E-24	7.40E-25	1.46E-25	1.38E-24	9.98E-18

TOTAL BTU/SEC 8.73E-17

VOLUME DISTRIBUTION OF THERMALIZED NEUTRONS(NEUTRONS/CM3)

	RADIUS										
	1.45E 02	2.04E 02	2.50E 02	2.89E 02	3.23E 02	3.54E 02	3.83E 02	4.09E 02	4.34E 02	4.57E 02	AVG/J+
LAYER											
1	9.59E-09	7.99E-09	6.27E-09	6.63E-09	4.97E-09	5.09E-09	5.86E-09	3.79E-09	3.91E-09	3.37E-09	1.89E-02
2	1.41E-08	1.37E-08	1.24E-08	1.05E-08	9.65E-09	8.05E-09	7.10E-09	5.62E-09	5.33E-09	4.44E-09	2.99E-02
3	1.74E-08	1.31E-08	1.21E-08	9.77E-09	8.11E-09	6.93E-09	7.75E-09	6.16E-09	5.03E-09	4.20E-09	2.98E-02
4	1.50E-08	1.21E-08	1.03E-08	7.28E-09	7.22E-09	6.39E-09	4.26E-09	5.27E-09	4.03E-09	3.55E-09	2.48E-02
5	1.08E-08	9.12E-09	9.00E-09	5.98E-09	4.68E-09	4.56E-09	4.50E-09	3.91E-09	3.14E-09	2.01E-09	1.90E-02
6	9.23E-09	7.93E-09	5.15E-09	4.26E-09	3.97E-09	3.08E-09	2.78E-09	2.49E-09	2.43E-09	1.54E-09	1.41E-02
7	6.39E-09	6.22E-09	4.26E-09	3.85E-09	2.49E-09	2.19E-09	1.60E-09	1.95E-09	1.18E-09	8.88E-10	1.02E-02
8	4.50E-09	2.90E-09	2.90E-09	2.19E-09	1.78E-09	1.24E-09	8.29E-10	8.29E-10	7.10E-10	7.10E-10	6.10E-03
9	3.14E-09	1.78E-09	1.54E-09	1.36E-09	1.42E-09	9.47E-10	4.74E-10	4.14E-10	5.33E-10	4.14E-10	3.95E-03
10	1.84E-09	1.07E-09	1.36E-09	7.10E-10	7.10E-10	5.33E-10	2.37E-10	2.96E-10	1.18E-10	1.78E-10	2.31E-03

TOTAL NEUTRONS/SEC 1.63E-01

CYLINDRICAL GEOMETRY - NEUTRONS IN HYDROGEN
POINT ISOTROPIC SOURCE OF 1 NEUTRON/SEC ON AXIS

EO(MEV)	EN(MEV)	ZT(CM)	R(CM)	S(CM)	RHO(GM/CM3)	N	M1	M2	U
7.0000 00	10.0000E-07	9.561E 01	4.572E 02	3.429E 02	7.000E-02	10000	0.	0.	0.

G	DV(CM3)	XC	DA(CM2)	DS(CM2)	NO. IN	MAX J+	AVG J+	MIN J+
2.486E-15	6.279E 05	5.0000E 00	6.567E 04	2.747E 04	2.000E-01	6.768E-07	3.046E-07	2.436E-07

NEUTRONS ESCAPING ENDS OF CYLINDER PER CM2-SEC

	RADIUS 1.45E 02	2.04E 02	2.50E 02	2.89E 02	3.23E 02	3.54E 02	3.83E 02	4.09E 02	4.34E 02	4.57E 02	NO/SEC
	FORE - THETA LESS THAN 90 DEG										
C	1.49E-08	1.09E-08	7.81E-09	4.37E-09	4.05E-09	3.19E-09	3.78E-09	1.30E-09	1.13E-09	1.62E-09	3.48E-03
FLUX	2.06E-08	1.49E-08	1.06E-08	5.80E-09	5.02E-09	4.31E-09	4.64E-09	2.20E-09	1.70E-09	2.56E-09	4.75E-03
E*C	5.36E-08	3.29E-08	2.57E-08	1.58E-08	1.62E-08	1.08E-08	1.31E-08	5.75E-09	4.69E-09	4.92E-09	1.20E-02
	AFT - THETA GREATER THAN 90 DEG										
C	2.35E-08	2.39E-08	2.60E-08	2.27E-08	2.19E-08	2.28E-08	1.77E-08	2.18E-08	1.90E-08	2.01E-08	1.44E-02
FLUX	4.24E-08	5.05E-08	6.13E-08	4.22E-08	4.44E-08	5.57E-08	3.95E-08	4.73E-08	5.06E-08	5.02E-08	3.18E-02
E*C	3.05E-09	5.46E-09	6.88E-09	7.16E-09	9.76E-09	1.02E-08	9.75E-09	1.38E-08	1.69E-08	1.44E-08	6.40E-03

NEUTRONS ESCAPING SIDES OF CYLINDER PER CM2-SEC

	DEPTH(LAYER NUMBER) 1	2	3	4	5	6	7	8	9	10	NO/SEC
	FORE - THETA LESS THAN 90 DEG										
C	1.72E-07	1.05E-07	5.85E-08	3.20E-08	1.92E-08	1.12E-08	5.85E-09	5.49E-09	3.31E-09	7.85E-10	1.14E-02
FLUX	2.24E-07	1.47E-07	9.41E-08	5.54E-08	3.06E-08	1.58E-08	1.68E-08	9.11E-09	5.12E-09	1.50E-09	1.65E-02
E*C	1.07E-06	5.66E-07	3.12E-07	1.63E-07	9.60E-08	5.03E-08	2.62E-08	2.09E-08	9.64E-09	2.51E-09	6.37E-02
	AFT - THETA GREATER THAN 90 DEG										
C	2.98E-08	2.06E-08	4.84E-09	5.55E-09	2.48E-09	2.11E-09	1.38E-09	2.03E-10	1.62E-09	2.28E-22	1.88E-03
FLUX	4.33E-08	2.94E-08	6.85E-09	8.00E-09	4.07E-09	2.66E-09	1.78E-09	3.65E-10	2.71E-09	2.63E-22	2.72E-03
E*C	5.00E-08	3.12E-08	5.66E-09	7.41E-09	1.38E-09	2.57E-09	2.36E-09	5.44E-10	1.31E-09	2.29E-25	2.81E-03

CYLINDRICAL GEOMETRY - NEUTRONS IN HYDROGEN
POINT ISOTROPIC SOURCE OF 1 NEUTRON/SEC ON AXIS

EO(MEV)	EN(MEV)	ZT(CM)	R(CM)	S(CM)	RHO(GM/CM3)	N	M1	M2	U
7.000E 00	10.000E-07	9.561E 01	4.572E 02	3.429E 02	7.000E-02	10000	0.	0.	0.

G	CV(CM3)	XC	DA(CM2)	DS(CM2)	NO. IN	MAX J+	AVG J+	MIN J+
2.486E-15	6.279E 05	5.000E 00	6.567E 04	2.747E 04	2.000E-01	6.768E-07	3.046E-07	2.436E-07

NEUTRON HEAT DEPOSITION(BTU/IN3-SEC)

LAYER	RADIUS 1.45E 02	2.04E 02	2.50E 02	2.89E 02	3.23E 02	3.54E 02	3.83E 02	4.09E 02	4.34E 02	4.57E 02	AVG/J+
1	2.71E-22	2.26E-22	2.00E-22	1.92E-22	1.65E-22	1.53E-22	1.30E-22	1.26E-22	1.14E-22	1.10E-22	5.54E-16
2	2.17E-22	1.84E-22	1.52E-22	1.40E-22	1.20E-22	1.06E-22	1.14E-22	8.84E-23	7.86E-23	6.83E-23	4.16E-16
3	1.65E-22	1.35E-22	1.08E-22	9.76E-23	8.36E-23	7.19E-23	5.47E-23	4.70E-23	4.66E-23	4.55E-23	2.81E-16
4	9.84E-23	9.04E-23	7.44E-23	5.93E-23	4.96E-23	4.22E-23	3.45E-23	3.32E-23	3.01E-23	2.21E-23	1.75E-16
5	8.42E-23	5.77E-23	5.15E-23	3.73E-23	3.21E-23	2.35E-23	2.27E-23	1.63E-23	1.68E-23	1.33E-23	1.17E-16
6	4.60E-23	3.76E-23	2.52E-23	2.56E-23	1.90E-23	1.54E-23	1.25E-23	9.20E-24	7.98E-24	8.27E-24	6.79E-17
7	3.17E-23	2.45E-23	2.00E-23	1.78E-23	1.02E-23	1.06E-23	6.64E-24	4.82E-24	4.59E-24	5.09E-24	4.46E-17
8	1.54E-23	1.69E-23	9.84E-24	8.97E-24	1.01E-23	4.54E-24	3.29E-24	6.02E-24	4.27E-24	3.14E-24	2.71E-17
9	1.12E-23	9.15E-24	7.22E-24	6.17E-24	2.67E-24	3.13E-24	2.99E-24	2.26E-24	2.86E-24	1.69E-24	1.62E-17
10	7.94E-24	6.16E-24	4.32E-24	2.23E-24	1.67E-24	1.84E-24	1.36E-24	7.66E-25	1.19E-24	9.37E-25	9.33E-18

TOTAL BTU/SEC 2.00E-16

VOLUME DISTRIBUTION OF THERMALIZED NEUTRONS(NEUTRONS/CM3)

LAYER	RADIUS 1.45E 02	2.04E 02	2.50E 02	2.89E 02	3.23E 02	3.54E 02	3.83E 02	4.09E 02	4.34E 02	4.57E 02	AVG/J+
1	6.12E-09	5.06E-09	5.38E-09	4.52E-09	4.11E-09	3.89E-09	3.19E-09	2.96E-09	3.03E-09	2.33E-09	1.33E-02
2	9.62E-09	7.96E-09	6.85E-09	7.20E-09	5.77E-09	5.54E-09	4.75E-09	4.68E-09	3.19E-09	2.90E-09	1.92E-02
3	9.49E-09	8.79E-09	6.53E-09	5.96E-09	4.62E-09	4.59E-09	3.73E-09	3.25E-09	3.57E-09	2.52E-09	1.74E-02
4	7.26E-09	5.77E-09	5.54E-09	4.78E-09	4.30E-09	3.54E-09	2.96E-09	2.29E-09	2.29E-09	1.94E-09	1.34E-02
5	6.02E-09	4.52E-09	3.63E-09	3.12E-09	2.48E-09	2.33E-09	1.88E-09	1.40E-09	1.34E-09	1.11E-09	9.14E-03
6	4.62E-09	3.54E-09	2.52E-09	2.17E-09	2.10E-09	1.27E-09	1.40E-09	1.11E-09	7.64E-10	6.05E-10	6.60E-03
7	2.74E-09	2.33E-09	1.66E-09	1.56E-09	1.08E-09	8.60E-10	6.69E-10	5.10E-10	3.82E-10	5.10E-10	4.04E-03
8	1.37E-09	1.62E-09	1.15E-09	7.64E-10	7.01E-10	4.46E-10	3.19E-10	5.10E-10	5.10E-10	1.91E-10	2.49E-03
9	1.21E-09	1.05E-09	7.01E-10	5.73E-10	4.78E-10	4.46E-10	2.87E-10	3.82E-10	2.23E-10	2.55E-10	1.84E-03
10	4.46E-10	3.82E-10	4.14E-10	2.23E-10	1.91E-10	1.27E-10	1.59E-10	6.37E-11	6.37E-11	6.37E-11	7.01E-04

TOTAL NEUTRONS/SEC 1.68E-01

CYLINDRICAL GEOMETRY - NEUTRONS IN HYDROGEN
POINT ISOTROPIC SOURCE OF 1 NEUTRON/SEC ON AXIS

EO(MEV)	EN(MEV)	ZT(CM)	R(CM)	S(CM)	RHO(GM/CM3)	N	M1	M2	U
1.000E 00	10.000E-07	2.787E 01	4.572E 02	6.096E 02	7.000E-02	10000	0.	0.	0.

G	CV(CM3)	XC	DA(CM2)	DS(CM2)	NO. IN	MAX J+	AVG J+	MIN J+
2.486E-15	1.830E 05	5.000E 00	6.567E 04	8.005E 03	10.000E-02	2.141E-07	1.523E-07	1.371E-07

NEUTRONS ESCAPING ENDS OF CYLINDER PER CM2-SEC

	RADIUS										
	1.45E 02	2.04E 02	2.50E 02	2.89E 02	3.23E 02	3.54E 02	3.83E 02	4.09E 02	4.34E 02	4.57E 02	NO/SEC
	FORE - THETA LESS THAN 90 DEG										
C	1.38E-08	1.15E-08	1.01E-08	1.13E-08	6.12E-09	8.43E-09	6.33E-09	6.27E-09	4.93E-09	5.57E-09	5.54E-03
FLUX	1.91E-08	1.89E-08	1.72E-08	1.85E-08	9.96E-09	1.35E-08	9.57E-09	8.68E-09	7.15E-09	7.95E-09	8.58E-03
E*C	4.53E-09	3.60E-09	3.22E-09	2.70E-09	2.17E-09	2.12E-09	1.75E-09	1.62E-09	1.07E-09	1.31E-09	1.58E-03
	AFT - THETA GREATER THAN 90 DEG										
C	2.50E-08	2.36E-08	2.09E-08	2.06E-08	2.07E-08	1.72E-08	2.10E-08	2.23E-08	1.73E-08	1.66E-08	1.35E-02
FLUX	4.39E-08	4.36E-08	3.63E-08	4.00E-08	4.15E-08	3.03E-08	3.98E-08	4.26E-08	3.14E-08	3.29E-08	2.51E-02
E*C	2.46E-10	1.74E-10	2.68E-10	2.78E-10	4.07E-10	3.20E-10	4.53E-10	4.75E-10	4.78E-10	3.94E-10	2.29E-04

NEUTRONS ESCAPING SIDES OF CYLINDER PER CM2-SEC

	DEPTH(LAYER NUMBER)										
	1	2	3	4	5	6	7	8	9	10	NO/SEC
	FORE - THETA LESS THAN 90 DEG										
C	9.74E-08	5.40E-08	4.82E-08	3.33E-08	1.98E-08	1.20E-08	1.03E-08	7.24E-09	2.76E-09	2.08E-09	2.30E-03
FLUX	2.03E-07	9.88E-08	8.18E-08	5.33E-08	3.26E-08	1.94E-08	1.64E-08	1.08E-08	5.29E-09	3.52E-09	4.20E-03
E*C	7.53E-08	4.06E-08	2.96E-08	1.84E-08	9.93E-09	5.95E-09	4.30E-09	2.63E-09	7.65E-10	4.68E-10	1.50E-03
	AFT - THETA GREATER THAN 90 DEG										
C	1.50E-08	6.61E-09	1.46E-08	7.92E-09	6.60E-09	2.33E-09	5.47E-09	1.97E-09	1.68E-09	9.08E-14	4.98E-04
FLUX	2.30E-08	1.07E-08	1.99E-08	1.05E-08	9.33E-09	3.42E-09	7.51E-09	2.87E-09	1.82E-09	9.15E-14	7.13E-04
E*C	8.66E-10	8.19E-10	5.09E-10	2.91E-10	1.02E-11	1.26E-10	1.98E-10	2.97E-11	3.61E-12	1.24E-14	2.28E-05

CYLINDRICAL GEOMETRY - NEUTRONS IN HYDROGEN
POINT ISOTROPIC SOURCE OF 1 NEUTRON/SEC ON AXIS

EO(MEV)	EN(MEV)	ZT(CM)	R(CM)	S(CM)	RHO(GM/CM3)	N	M1	M2	U
1.000E 00	10.000E-07	2.787E 01	4.572E 02	6.096E 02	7.000E-02	10000	0.	0.	0.

G	CV(CM3)	XC	DA(CM2)	DS(CM2)	NO. IN	MAX J+	AVG J+	MIN J+
2.486E-15	1.830E 05	5.000E 00	6.567E 04	8.005E 03	10.000E-02	2.141E-07	1.523E-07	1.371E-07

NEUTRON HEAT DEPOSITION(BTU/IN3-SEC)

LAYER	RADIUS 1.45E 02	2.04E 02	2.50E 02	2.89E 02	3.23E 02	3.54E 02	3.83E 02	4.09E 02	4.34E 02	4.57E 02	AVG/J+
1	4.48E-23	4.13E-23	3.98E-23	3.71E-23	3.69E-23	3.45E-23	3.29E-23	3.36E-23	3.04E-23	3.12E-23	2.38E-16
2	3.67E-23	3.62E-23	3.45E-23	3.58E-23	3.09E-23	2.95E-23	2.66E-23	2.77E-23	2.30E-23	2.10E-23	1.98E-16
3	2.98E-23	2.80E-23	2.48E-23	2.07E-23	1.99E-23	2.01E-23	2.07E-23	1.84E-23	1.72E-23	1.63E-23	1.42E-16
4	2.22E-23	2.12E-23	1.77E-23	1.53E-23	1.56E-23	1.42E-23	1.37E-23	1.23E-23	1.19E-23	1.14E-23	1.02E-16
5	1.37E-23	1.26E-23	1.20E-23	1.14E-23	1.23E-23	9.25E-24	8.82E-24	7.50E-24	6.55E-24	7.62E-24	6.63E-17
6	1.09E-23	9.68E-24	8.94E-24	7.72E-24	7.65E-24	7.07E-24	6.12E-24	4.69E-24	5.09E-24	4.91E-24	4.78E-17
7	7.75E-24	5.60E-24	4.71E-24	5.73E-24	3.42E-24	3.72E-24	3.06E-24	2.99E-24	3.24E-24	3.60E-24	2.88E-17
8	3.76E-24	3.49E-24	3.71E-24	4.19E-24	3.08E-24	2.05E-24	2.55E-24	2.50E-24	8.84E-25	1.71E-24	1.33E-17
9	2.75E-24	2.42E-24	3.19E-24	2.33E-24	1.23E-24	1.59E-24	1.52E-24	1.59E-24	1.36E-24	9.70E-25	1.24E-17
10	1.79E-24	1.53E-24	1.45E-24	1.59E-24	6.90E-25	8.73E-25	5.85E-25	9.12E-25	8.13E-25	8.45E-25	7.27E-18

TOTAL BTU/SEC 1.46E-17

VOLUME DISTRIBUTION OF THERMALIZED NEUTRONS(NEUTRONS/CM3)

LAYER	RADIUS 1.45E 02	2.04E 02	2.50E 02	2.89E 02	3.23E 02	3.54E 02	3.83E 02	4.09E 02	4.34E 02	4.57E 02	AVG/J+
1	4.59E-09	4.26E-09	4.64E-09	6.01E-09	3.93E-09	4.26E-09	2.90E-09	3.44E-09	3.66E-09	2.68E-09	2.65E-02
2	7.38E-09	8.20E-09	7.05E-09	7.10E-09	6.23E-09	6.01E-09	6.12E-09	6.45E-09	3.77E-09	3.88E-09	4.08E-02
3	9.29E-09	8.20E-09	7.60E-09	7.10E-09	8.36E-09	6.99E-09	7.10E-09	5.63E-09	5.46E-09	5.19E-09	4.66E-02
4	9.07E-09	7.98E-09	8.03E-09	6.83E-09	6.67E-09	5.14E-09	5.63E-09	4.86E-09	5.08E-09	4.97E-09	4.22E-02
5	7.92E-09	8.14E-09	6.45E-09	6.45E-09	5.74E-09	5.41E-09	5.30E-09	4.70E-09	4.37E-09	3.55E-09	3.81E-02
6	6.45E-09	6.56E-09	5.14E-09	4.97E-09	4.75E-09	4.97E-09	4.10E-09	3.77E-09	4.04E-09	3.06E-09	3.14E-02
7	5.41E-09	4.64E-09	5.30E-09	3.61E-09	3.55E-09	3.66E-09	2.90E-09	2.68E-09	2.84E-09	2.63E-09	2.45E-02
8	3.66E-09	2.51E-09	2.24E-09	2.68E-09	1.69E-09	1.91E-09	2.13E-09	1.69E-09	1.31E-09	1.53E-09	1.40E-02
9	2.19E-09	2.08E-09	1.97E-09	1.75E-09	1.86E-09	1.09E-09	9.29E-10	1.26E-09	8.74E-10	7.65E-10	9.69E-03
10	1.64E-09	9.29E-10	1.04E-09	9.29E-10	1.15E-09	8.74E-10	8.20E-10	1.15E-09	8.74E-10	3.83E-10	6.42E-03

TOTAL NEUTRONS/SEC 7.81E-02

CYLINDRICAL GEOMETRY - NEUTRONS IN HYDROGEN
POINT ISOTROPIC SOURCE OF 1 NEUTRON/SEC ON AXIS

EO(MEV)	EN(MEV)	ZT(CM)	R(CM)	S(CM)	RHO(GM/CM3)	N	M1	M2	U
3.000E 00	10.000E-07	5.145E 01	4.572E 02	6.096E 02	7.000E-02	10000	0.	0.	0.

G	CV(CM3)	XC	DA(CM2)	DS(CM2)	NC. IN	MAX J+	AVG J+	MIN J+
2.486E-15	3.379E 05	5.000E 00	6.567E 04	1.478E 04	10.000E-02	2.141E-07	1.523E-07	1.371E-07

NEUTRONS ESCAPING ENDS OF CYLINDER PER CM2-SEC

	RADIUS 1.45E 02	2.04E 02	2.50E 02	2.89E 02	3.23E 02	3.54E 02	3.83E 02	4.09E 02	4.34E 02	4.57E 02	NO/SEC
	FORE - THETA LESS THAN 90 DEG										
C	1.03E-08	7.34E-09	9.24E-09	5.28E-09	5.10E-09	5.41E-09	4.29E-09	3.39E-09	3.11E-09	3.02E-09	3.71E-03
FLUX	1.59E-08	1.04E-08	1.44E-08	6.98E-09	7.71E-09	7.92E-09	5.47E-09	4.67E-09	4.22E-09	4.08E-09	5.57E-03
E*C	1.28E-08	8.66E-09	9.90E-09	7.09E-09	6.68E-09	5.75E-09	5.37E-09	4.25E-09	2.95E-09	3.69E-09	4.41E-03
	AFT - THETA GREATER THAN 90 DEG										
C	1.31E-08	1.21E-08	1.26E-08	1.41E-08	1.22E-08	1.42E-08	1.32E-08	1.31E-08	1.39E-08	1.53E-08	8.79E-03
FLUX	2.29E-08	2.21E-08	2.35E-08	2.82E-08	2.39E-08	2.85E-08	2.91E-08	3.04E-08	2.53E-08	3.20E-08	1.75E-02
E*C	3.99E-10	5.83E-10	7.41E-10	9.19E-10	7.17E-10	9.25E-10	1.78E-09	1.44E-09	1.09E-09	2.30E-09	7.15E-04

NEUTRONS ESCAPING SIDES OF CYLINDER PER CM2-SEC

	DEPTH(LAYER NUMBER) 1	2	3	4	5	6	7	8	9	10	NO/SEC
	FORE - THETA LESS THAN 90 DEG										
C	8.11E-08	7.08E-08	4.49E-08	2.59E-08	1.86E-08	1.38E-08	6.68E-09	2.62E-09	1.97E-09	1.52E-09	3.96E-03
FLUX	1.34E-07	1.26E-07	8.18E-08	5.76E-08	3.35E-08	2.71E-08	1.17E-08	4.26E-09	3.29E-09	2.54E-09	7.13E-03
E*C	2.12E-07	1.44E-07	8.23E-08	5.16E-08	3.07E-08	2.00E-08	1.10E-08	4.83E-09	3.20E-09	1.56E-09	8.30E-03
	AFT - THETA GREATER THAN 90 DEG										
C	1.06E-08	1.03E-08	7.91E-09	5.81E-09	5.63E-09	1.43E-09	1.98E-09	1.56E-09	8.75E-11	7.17E-12	6.69E-04
FLUX	1.41E-08	1.52E-08	1.40E-08	9.08E-09	1.07E-08	1.96E-09	3.07E-09	1.90E-09	1.08E-10	2.53E-11	1.04E-03
E*C	3.50E-09	2.48E-09	1.83E-09	2.29E-09	1.58E-09	2.82E-10	5.95E-10	2.20E-10	2.64E-14	8.48E-15	1.89E-04

CYLINDRICAL GEOMETRY - NEUTRONS IN HYDROGEN
POINT ISOTROPIC SOURCE OF 1 NEUTRON/SEC ON AXIS

EO(MEV)	EN(MEV)	ZT(CM)	R(CM)	S(CM)	RHO(GM/CM3)	N	M1	M2	U
3.000E 00	10.000E-07	5.145E 01	4.572E 02	6.096E 02	7.000E-02	10000	0.	0.	0.

G	DV(CM3)	XC	DA(CM2)	DS(CM2)	NO. IN	MAX J+	AVG J+	MIN J+
2.486E-15	3.379E 05	5.000E 00	6.567E 04	1.478E 04	10.000E-02	2.141E-07	1.523E-07	1.371E-07

NEUTRON HEAT DEPOSITION(BTU/IN3-SEC)

	RADIUS										
	1.45E 02	2.04E 02	2.50E 02	2.89E 02	3.23E 02	3.54E 02	3.83E 02	4.09E 02	4.34E 02	4.57E 02	AVG/J+
LAYER											
1	7.65E-23	7.03E-23	6.91E-23	6.45E-23	6.18E-23	6.27E-23	5.64E-23	5.47E-23	5.57E-23	4.91E-23	4.08E-16
2	6.12E-23	5.47E-23	5.18E-23	5.28E-23	5.00E-23	4.71E-23	4.42E-23	3.87E-23	3.69E-23	3.71E-23	3.12E-16
3	4.52E-23	4.23E-23	3.70E-23	3.09E-23	3.38E-23	3.16E-23	2.92E-23	2.95E-23	2.40E-23	2.48E-23	2.16E-16
4	2.81E-23	2.91E-23	2.79E-23	2.83E-23	2.47E-23	2.18E-23	1.82E-23	2.19E-23	1.65E-23	1.58E-23	1.53E-16
5	2.43E-23	2.29E-23	2.07E-23	2.07E-23	1.76E-23	1.23E-23	1.28E-23	1.45E-23	1.29E-23	1.26E-23	1.13E-16
6	1.47E-23	1.77E-23	1.12E-23	1.17E-23	9.86E-24	8.96E-24	9.81E-24	7.94E-24	9.46E-24	6.84E-24	7.10E-17
7	1.04E-23	1.11E-23	7.86E-24	7.77E-24	6.02E-24	6.15E-24	6.53E-24	6.14E-24	6.01E-24	3.99E-24	4.73E-17
8	8.72E-24	6.88E-24	6.49E-24	3.98E-24	4.85E-24	2.44E-24	4.90E-24	3.35E-24	1.94E-24	2.39E-24	3.02E-17
9	4.75E-24	4.36E-24	5.09E-24	3.07E-24	2.86E-24	3.05E-24	2.64E-24	2.00E-24	2.68E-24	9.38E-25	2.07E-17
10	3.95E-24	2.79E-24	3.94E-24	1.98E-24	1.91E-24	1.82E-24	8.03E-25	1.53E-24	1.16E-24	9.34E-25	1.37E-17
										TOTAL BTU/SEC	4.34E-17

VOLUME DISTRIBUTION OF THERMALIZED NEUTRONS(NEUTRONS/CM3)

	RADIUS										
	1.45E 02	2.04E 02	2.50E 02	2.89E 02	3.23E 02	3.54E 02	3.83E 02	4.09E 02	4.34E 02	4.57E 02	AVG/J+
LAYER											
1	3.31E-09	3.34E-09	3.05E-09	2.99E-09	3.26E-09	2.72E-09	2.37E-09	2.16E-09	2.25E-09	1.86E-09	1.79E-02
2	5.56E-09	4.71E-09	5.48E-09	4.17E-09	4.88E-09	4.26E-09	4.62E-09	3.34E-09	3.76E-09	3.05E-09	2.88E-02
3	5.71E-09	5.51E-09	5.12E-09	5.03E-09	4.29E-09	5.06E-09	3.85E-09	4.11E-09	3.49E-09	2.55E-09	2.94E-02
4	4.91E-09	4.82E-09	3.70E-09	4.50E-09	3.43E-09	3.40E-09	3.61E-09	3.70E-09	2.90E-09	2.40E-09	2.45E-02
5	3.91E-09	4.11E-09	3.97E-09	3.76E-09	3.20E-09	2.52E-09	2.72E-09	2.43E-09	2.19E-09	2.25E-09	2.04E-02
6	2.90E-09	3.70E-09	2.52E-09	2.81E-09	1.92E-09	1.95E-09	1.95E-09	1.98E-09	1.84E-09	1.51E-09	1.52E-02
7	2.66E-09	2.22E-09	1.75E-09	1.45E-09	1.63E-09	1.39E-09	1.33E-09	1.51E-09	1.07E-09	7.70E-10	1.04E-02
8	1.75E-09	1.48E-09	1.39E-09	1.15E-09	9.77E-10	1.01E-09	7.99E-10	6.81E-10	7.70E-10	4.74E-10	6.88E-03
9	1.18E-09	1.15E-09	1.18E-09	7.10E-10	5.92E-10	7.10E-10	5.62E-10	5.03E-10	5.33E-10	2.96E-10	4.88E-03
10	7.70E-10	4.14E-10	4.74E-10	4.74E-10	2.66E-10	3.55E-10	3.55E-10	7.10E-10	3.55E-10	3.55E-10	2.97E-03
									TOTAL NEUTRONS/SEC		8.30E-02

CYLINDRICAL GEOMETRY - NEUTRONS IN HYDROGEN
POINT ISOTROPIC SOURCE OF 1 NEUTRON/SEC ON AXIS

EO(MEV)	EN(MEV)	ZT(CM)	R(CM)	S(CM)	RHO(GM/CM3)	N	M1	M2	U
7.000E 00	10.000E-07	9.561E 01	4.572E 02	6.096E 02	7.000E-02	10000	0.	0.	0.

G	DV(CM3)	XC	DA(CM2)	DS(CM2)	NO. IN	MAX J+	AVG J+	MIN J+
2.486E-15	6.279E 05	5.000E 00	6.567E 04	2.747E 04	10.000E-02	2.141E-07	1.523E-07	1.371E-07

NEUTRONS ESCAPING ENDS OF CYLINDER PER CM2-SEC

	RADIUS 1.45E 02	2.04E 02	2.50E 02	2.89E 02	3.23E 02	3.54E 02	3.83E 02	4.09E 02	4.34E 02	4.57E 02	NO/SEC
	FORE - THETA LESS THAN 90 DEG										
C	6.41E-09	4.41E-09	4.20E-09	4.38E-09	3.81E-09	2.11E-09	2.10E-09	1.98E-09	2.10E-09	1.52E-09	2.17E-03
FLUX	9.81E-09	5.80E-09	5.60E-09	5.52E-09	5.68E-09	2.92E-09	2.96E-09	2.61E-09	2.79E-09	2.04E-09	3.00E-03
E*C	2.18E-08	1.67E-08	1.49E-08	1.53E-08	1.29E-08	8.43E-09	7.48E-09	7.77E-09	7.40E-09	5.12E-09	7.74E-03
	AFT - THETA GREATER THAN 90 DEG										
C	7.79E-09	1.26E-08	8.91E-09	8.28E-09	6.73E-09	9.11E-09	1.07E-08	8.45E-09	8.13E-09	9.13E-09	5.90E-03
FLUX	1.36E-08	2.34E-08	1.93E-08	1.54E-08	1.58E-08	1.75E-08	2.12E-08	1.73E-08	3.08E-08	2.18E-08	1.29E-02
E*C	7.00E-10	1.61E-09	1.30E-09	1.62E-09	1.64E-09	1.93E-09	2.32E-09	1.98E-09	1.85E-09	2.98E-09	1.18E-03

NEUTRONS ESCAPING SIDES OF CYLINDER PER CM2-SEC

	DEPTH(LAYER NUMBER) 1	2	3	4	5	6	7	8	9	10	NO/SEC
	FORE - THETA LESS THAN 90 DEG										
C	7.90E-08	6.00E-08	3.79E-08	2.45E-08	1.42E-08	8.57E-09	5.86E-09	2.46E-09	1.39E-09	1.08E-09	6.45E-03
FLUX	1.33E-07	1.04E-07	6.29E-08	4.36E-08	2.71E-08	1.55E-08	1.18E-08	4.17E-09	2.60E-09	1.63E-09	1.12E-02
E*C	4.77E-07	3.10E-07	1.89E-07	1.14E-07	6.28E-08	3.53E-08	2.78E-08	1.10E-08	5.15E-09	4.09E-09	3.40E-02
	AFT - THETA GREATER THAN 90 DEG										
C	1.34E-08	9.88E-09	6.63E-09	4.71E-09	2.86E-09	2.93E-09	2.92E-10	8.38E-10	3.94E-10	2.85E-10	1.16E-03
FLUX	1.97E-08	1.57E-08	9.56E-09	8.78E-09	4.53E-09	4.43E-09	4.44E-10	1.25E-09	5.53E-10	3.15E-10	1.79E-03
E*C	1.20E-08	7.83E-09	3.76E-09	4.05E-09	1.83E-09	1.97E-09	2.00E-10	1.16E-09	1.49E-10	1.69E-10	9.09E-04

CYLINDRICAL GEOMETRY - NEUTRONS IN HYDROGEN
POINT ISOTROPIC SOURCE OF 1 NEUTRON/SEC ON AXIS

EO(MEV)	EN(MEV)	ZT(CM)	R(CM)	S(CM)	RHO(GM/CM3)	N	M1	M2	U
7.000E 00	10.000E-07	9.561E 01	4.572E 02	6.096E 02	7.000E-02	10000	0.	0.	0.

G	CV(CM3)	XC	DA(CM2)	DS(CM2)	NO. IN	MAX J+	AVG J+	MIN J+
2.486E-15	6.279E 05	5.000E 00	6.567E 04	2.747E 04	10.000E-02	2.141E-07	1.523E-07	1.371E-07

NEUTRON HEAT DEPOSITION(BTU/IN3-SEC)

	RADIUS										
	1.45E 02	2.04E 02	2.50E 02	2.89E 02	3.23E 02	3.54E 02	3.83E 02	4.09E 02	4.34E 02	4.57E 02	AVG/J+
LAYER											
1	9.14E-23	9.21E-23	8.52E-23	8.28E-23	7.50E-23	7.13E-23	7.37E-23	6.83E-23	6.83E-23	6.52E-23	5.08E-16
2	6.86E-23	7.29E-23	6.71E-23	6.38E-23	6.86E-23	6.08E-23	5.10E-23	5.27E-23	5.11E-23	4.80E-23	3.97E-16
3	5.88E-23	4.94E-23	4.90E-23	4.41E-23	3.72E-23	4.25E-23	3.81E-23	3.80E-23	3.37E-23	3.11E-23	2.77E-16
4	3.76E-23	3.66E-23	3.95E-23	2.84E-23	2.57E-23	2.99E-23	2.69E-23	2.46E-23	2.16E-23	2.13E-23	1.92E-16
5	2.65E-23	2.72E-23	2.28E-23	2.23E-23	1.98E-23	1.84E-23	1.56E-23	1.61E-23	1.70E-23	1.45E-23	1.31E-16
6	2.43E-23	1.66E-23	1.27E-23	1.56E-23	1.37E-23	1.34E-23	1.05E-23	9.84E-24	7.52E-24	8.64E-24	8.72E-17
7	1.42E-23	1.15E-23	6.02E-24	8.70E-24	7.43E-24	7.02E-24	7.09E-24	6.81E-24	3.83E-24	5.41E-24	5.13E-17
8	7.64E-24	5.46E-24	5.92E-24	5.74E-24	6.05E-24	5.19E-24	3.20E-24	4.49E-24	3.22E-24	2.97E-24	3.28E-17
9	6.86E-24	4.84E-24	4.13E-24	2.94E-24	3.25E-24	1.50E-24	2.38E-24	2.87E-24	2.12E-24	1.49E-24	2.13E-17
10	2.86E-24	2.27E-24	2.45E-24	2.35E-24	2.40E-24	7.67E-25	1.35E-24	1.04E-24	9.48E-25	8.56E-25	1.14E-17
										TOTAL BTU/SEC	9.95 E-17

VOLUME DISTRIBUTION OF THERMALIZED NEUTRONS(NEUTRONS/CM3)

	RADIUS										
	1.45E 02	2.04E 02	2.50E 02	2.89E 02	3.23E 02	3.54E 02	3.83E 02	4.09E 02	4.34E 02	4.57E 02	AVG/J+
LAYER											
1	1.80E-09	2.52E-09	2.17E-09	2.09E-09	1.93E-09	1.61E-09	1.61E-09	1.70E-09	1.58E-09	1.15E-09	1.19E-02
2	2.98E-09	3.07E-09	3.09E-09	2.63E-09	2.84E-09	2.61E-09	2.42E-09	2.17E-09	2.64E-09	1.75E-09	1.72E-02
3	3.55E-09	3.07E-09	2.87E-09	2.52E-09	2.69E-09	2.64E-09	2.21E-09	2.55E-09	2.18E-09	1.80E-09	1.71E-02
4	2.56E-09	2.90E-09	2.52E-09	2.07E-09	2.20E-09	2.05E-09	2.23E-09	1.77E-09	1.62E-09	1.42E-09	1.40E-02
5	2.05E-09	1.88E-09	1.96E-09	1.67E-09	1.27E-09	1.45E-09	1.29E-09	1.50E-09	1.07E-09	9.56E-10	9.92E-03
6	1.69E-09	1.59E-09	1.29E-09	1.31E-09	1.04E-09	1.15E-09	7.33E-10	6.69E-10	7.01E-10	7.80E-10	7.19E-03
7	1.07E-09	1.00E-09	6.37E-10	7.01E-10	7.17E-10	8.28E-10	7.80E-10	5.89E-10	4.46E-10	4.30E-10	4.73E-03
8	9.56E-10	5.57E-10	5.57E-10	6.53E-10	3.03E-10	5.26E-10	3.19E-10	2.71E-10	3.82E-10	1.91E-10	3.10E-03
9	6.69E-10	4.78E-10	2.71E-10	3.03E-10	3.98E-10	2.87E-10	2.39E-10	4.14E-10	1.75E-10	1.11E-10	2.20E-03
10	2.87E-10	1.75E-10	2.07E-10	2.07E-10	1.59E-10	1.27E-10	1.11E-10	1.91E-10	1.11E-10	1.27E-10	1.12E-03
									TOTAL NEUTRONS/SEC		8.46E-02

CYLINDRICAL GEOMETRY - GAMMA RAYS IN HYDROGEN
POINT ISOTROPIC SOURCE OF 1 PHOTON/SEC ON AXIS

EO(MEV)	EN(MEV)	ZT(CM)	R(CM)	S(CM)	RHO(GM/CM3)	N	M1	M2	U
1.000E 00	2.500E-02	5.615E 02	4.572E 02	3.429E 02	7.000E-02	10000	0.	0.	0.

G	DV(CM3)	XO	DA(CM2)	DS(CM2)	NO. IN	MAX J+	AVG J+	MIN J+
2.486E-15	3.688E 06	5.002E 00	6.567E 04	1.613E 05	2.000E-01	6.768E-07	3.046E-07	2.436E-07

GAMMAS ESCAPING ENDS OF CYLINDER PER CM2-SEC

	RADIUS										
	1.45E 02	2.04E 02	2.50E 02	2.89E 02	3.23E 02	3.54E 02	3.83E 02	4.09E 02	4.34E 02	4.57E 02	NO/SEC
	FORE - THETA LESS THAN 90 DEG										
C	1.17E-08	1.02E-08	1.08E-08	1.11E-08	8.49E-09	8.66E-09	6.55E-09	5.85E-09	3.75E-09	4.24E-09	5.34E-03
FLUX	1.83E-08	1.43E-08	1.61E-08	1.69E-08	1.35E-08	1.18E-08	1.12E-08	8.18E-09	4.92E-09	5.57E-09	7.93E-03
E*C	3.60E-09	2.88E-09	2.67E-09	3.31E-09	2.36E-09	2.07E-09	2.24E-09	1.76E-09	1.45E-09	1.55E-09	1.57E-03
E*F	4.76E-09	3.50E-09	3.34E-09	4.30E-09	3.54E-09	2.62E-09	3.21E-09	2.18E-09	1.67E-09	1.96E-09	2.04E-03
	AFT - THETA GREATER THAN 90 DEG										
C	1.41E-07	1.29E-07	1.21E-07	9.92E-08	9.25E-08	9.10E-08	7.16E-08	6.18E-08	5.13E-08	3.34E-08	5.86E-02
FLUX	2.86E-07	2.41E-07	2.33E-07	2.02E-07	1.83E-07	1.79E-07	1.33E-07	1.19E-07	1.06E-07	7.13E-08	1.15E-01
E*C	2.08E-08	1.87E-08	1.84E-08	1.53E-08	1.47E-08	1.48E-08	1.18E-08	1.07E-08	1.01E-08	7.13E-09	9.36E-03
E*F	4.36E-08	3.69E-08	3.75E-08	3.44E-08	3.35E-08	3.27E-08	2.41E-08	2.38E-08	2.65E-08	1.68E-08	2.03E-02

GAMMAS ESCAPING SIDES OF CYLINDER PER CM2-SEC

	DEPTH(LAYER NUMBER)										
	1	2	3	4	5	6	7	8	9	10	NO/SEC
	FORE - THETA LESS THAN 90 DEG										
C	1.67E-07	1.06E-07	6.71E-08	4.40E-08	2.75E-08	1.86E-08	1.07E-08	7.90E-09	4.65E-09	3.38E-09	7.36E-02
FLUX	2.23E-07	1.58E-07	1.09E-07	7.38E-08	4.91E-08	3.46E-08	1.97E-08	1.44E-08	9.65E-09	5.90E-09	1.12E-01
E*C	1.49E-07	7.87E-08	4.33E-08	2.51E-08	1.45E-08	7.77E-09	4.31E-09	2.74E-09	1.72E-09	1.22E-09	5.29E-02
E*F	1.95E-07	1.13E-07	6.74E-08	4.18E-08	2.48E-08	1.54E-08	8.20E-09	5.40E-09	3.83E-09	2.36E-09	7.69E-02
	AFT - THETA GREATER THAN 90 DEG										
C	3.28E-08	2.85E-08	1.90E-08	1.46E-08	1.00E-08	5.94E-09	4.30E-09	3.52E-09	1.90E-09	6.22E-10	1.96E-02
FLUX	5.18E-08	4.93E-08	2.79E-08	2.54E-08	1.90E-08	1.19E-08	6.66E-09	5.45E-09	2.71E-09	1.15E-09	3.25E-02
E*C	8.46E-09	5.58E-09	3.45E-09	2.08E-09	1.38E-09	7.82E-10	5.95E-10	3.68E-10	2.89E-10	6.22E-11	3.72E-03
E*F	1.28E-08	8.89E-09	4.79E-09	3.33E-09	2.55E-09	1.48E-09	8.66E-10	5.63E-10	4.05E-10	1.04E-10	5.77E-03

CYLINDRICAL GEOMETRY - GAMMA RAYS IN HYDROGEN
POINT ISOTROPIC SOURCE OF 1 PHOTON/SEC ON AXIS

EO(MEV)	EN(MEV)	ZT(CM)	R(CM)	S(CM)	RHO(GM/CM3)	N	M1	M2	U
1.000E 00	2.500E-02	5.615E 02	4.572E 02	3.429E 02	7.000E-02	10000	0.	0.	0.

G	DV(CM3)	X0	DA(CM2)	DS(CM2)	NO. IN	MAX J+	AVG J+	MIN J+
2.486E-15	3.688E 06	5.002E 00	6.567E 04	1.613E 05	2.000E-01	6.768E-07	3.046E-07	2.436E-07

GAMMA HEAT DEPOSITION(BTU/IN3-SEC)

LAYER	RADIUS 1.45E 02	2.04E 02	2.50E 02	2.89E 02	3.23E 02	3.54E 02	3.83E 02	4.09E 02	4.34E 02	4.57E 02	AVG/J+
1	5.36E-24	4.79E-24	4.40E-24	3.69E-24	3.37E-24	3.06E-24	2.85E-24	2.55E-24	2.36E-24	2.03E-24	1.13E-17
2	3.25E-24	2.86E-24	2.38E-24	2.23E-24	2.05E-24	1.95E-24	1.61E-24	1.51E-24	1.50E-24	1.21E-24	6.75E-18
3	2.32E-24	1.68E-24	1.62E-24	1.48E-24	1.38E-24	1.08E-24	9.71E-25	1.10E-24	8.44E-25	7.20E-25	4.33E-18
4	1.20E-24	1.10E-24	1.06E-24	1.06E-24	8.95E-25	8.33E-25	5.92E-25	5.21E-25	5.72E-25	4.44E-25	2.72E-18
5	7.71E-25	6.26E-25	6.85E-25	4.99E-25	4.53E-25	5.80E-25	3.80E-25	3.09E-25	3.75E-25	3.01E-25	1.63E-18
6	4.92E-25	3.76E-25	3.17E-25	3.22E-25	2.42E-25	2.91E-25	2.09E-25	2.26E-25	1.79E-25	1.94E-25	9.35E-19
7	2.17E-25	2.65E-25	2.23E-25	1.75E-25	2.03E-25	1.68E-25	2.38E-25	1.14E-25	1.48E-25	1.02E-25	6.09E-19
8	1.76E-25	1.42E-25	1.22E-25	1.38E-25	1.39E-25	1.20E-25	1.22E-25	1.15E-25	9.36E-26	4.35E-26	3.98E-19
9	1.14E-25	1.03E-25	6.66E-26	8.89E-26	6.26E-26	8.96E-26	8.53E-26	5.61E-26	3.91E-26	4.00E-26	2.44E-19
10	7.38E-26	7.27E-26	6.66E-26	5.11E-26	4.16E-26	4.58E-26	4.33E-26	4.80E-26	5.11E-26	3.04E-26	1.72E-19
									TOTAL BTU/SEC		2.00 E-17

TRANSMITTED GAMMA ANGULAR DISTRIBUTION(MEV/CM2-SEC-STER)

COS T.	RADIUS 1.45E 02	2.04E 02	2.50E 02	2.89E 02	3.23E 02	3.54E 02	3.83E 02	4.09E 02	4.34E 02	4.57E 02
1.0	3.22E-09	2.77E-09	2.39E-09	2.51E-09	1.92E-09	1.44E-09	1.35E-09	1.44E-09	1.65E-09	9.32E-10
0.9	5.65E-10	7.40E-10	9.58E-10	1.44E-09	5.40E-10	1.04E-09	6.82E-10	5.69E-10	3.77E-10	8.93E-10
0.8	9.40E-10	2.96E-10	3.33E-10	4.21E-10	3.88E-10	3.17E-10	2.38E-10	2.47E-10	1.20E-10	2.65E-10
0.7	3.11E-10	2.61E-10	9.67E-11	4.69E-10	2.33E-10	1.90E-10	6.01E-10	3.32E-10	9.18E-11	1.87E-10
0.6	2.46E-10	3.64E-10	1.77E-10	1.16E-10	1.05E-10	1.25E-10	5.12E-11	9.23E-11	2.00E-11	8.20E-11
0.5	1.22E-10	1.19E-10	2.00E-10	1.91E-10	2.35E-10	4.89E-11	5.81E-10	9.31E-11	1.55E-11	4.82E-11
0.4	1.73E-10	2.82E-11	7.42E-11	4.08E-11	5.64E-11	1.26E-10	1.54E-11	1.22E-11	2.39E-11	8.50E-12
0.3	1.31E-10	4.32E-12	2.33E-11	5.98E-12	1.49E-10	1.01E-11	1.53E-11	8.94E-12	4.56E-12	4.87E-11
0.2	2.70E-11	2.15E-12	2.94E-14	6.78E-11	1.28E-10	1.91E-14	1.37E-11	3.24E-15	4.95E-13	1.06E-12
0.1	1.12E-12	0.	1.62E-12	0.	3.77E-18	1.10E-16	8.82E-12	2.25E-17	0.	0.

CYLINDRICAL GEOMETRY - GAMMA RAYS IN HYDROGEN
POINT ISOTROPIC SOURCE OF 1 PHOTON/SEC ON AXIS

EO(MEV)	EN(MEV)	ZT(CM)	R(CM)	S(CM)	RHO(GM/CM3)	N	M1	M2	U
3.000E 00	7.500E-02	1.030E 03	4.572E 02	3.429E 02	7.000E-02	10000	0.	0.	0.

G	DV(CM3)	XO	DA(CM2)	DS(CM2)	NO. IN	MAX J+	AVG J+	MIN J+
2.486E-15	6.765E 06	5.000E 00	6.567E 04	2.959E 05	2.000E-01	6.768E-07	3.046E-07	2.436E-07

GAMMAS ESCAPING ENDS OF CYLINDER PER CM2-SEC

	RADIUS 1.45E 02	2.04E 02	2.50E 02	2.89E 02	3.23E 02	3.54E 02	3.83E 02	4.09E 02	4.34E 02	4.57E 02	NO/SEC
	FORE - THETA LESS THAN 90 DEG										
C	3.05E-09	1.72E-09	2.15E-09	1.57E-09	1.01E-09	1.25E-09	1.64E-09	1.24E-09	7.88E-10	8.36E-10	1.00E-03
FLUX	3.83E-09	2.18E-09	3.12E-09	1.93E-09	1.36E-09	1.54E-09	1.87E-09	2.62E-09	1.09E-09	9.69E-10	1.35E-03
E*C	2.15E-09	2.49E-09	2.33E-09	2.32E-09	1.94E-09	1.81E-09	2.38E-09	1.58E-09	1.31E-09	1.28E-09	1.29E-03
E*F	2.34E-09	2.64E-09	2.66E-09	2.56E-09	2.21E-09	2.01E-09	2.56E-09	1.97E-09	1.49E-09	1.42E-09	1.43E-03
	AFT - THETA GREATER THAN 90 DEG										
C	4.90E-08	5.75E-08	4.50E-08	4.47E-08	4.26E-08	3.61E-08	3.49E-08	2.53E-08	2.65E-08	1.69E-08	2.49E-02
FLUX	9.83E-08	1.08E-07	8.33E-08	9.30E-08	8.11E-08	8.42E-08	6.75E-08	6.42E-08	8.27E-08	3.97E-08	5.26E-02
E*C	9.90E-09	1.22E-08	9.48E-09	1.01E-08	9.67E-09	8.81E-09	8.46E-09	6.73E-09	6.86E-09	4.69E-09	5.70E-03
E*F	2.17E-08	2.46E-08	1.87E-08	2.41E-08	2.05E-08	2.22E-08	1.65E-08	3.46E-08	1.56E-08	1.12E-08	1.38E-02

GAMMAS ESCAPING SIDES OF CYLINDER PER CM2-SEC

	DEPTH(LAYER NUMBER) 1	2	3	4	5	6	7	8	9	10	NO/SEC
	FORE - THETA LESS THAN 90 DEG										
C	1.50E-07	8.08E-08	4.57E-08	2.51E-08	1.25E-08	7.41E-09	4.59E-09	2.44E-09	1.19E-09	7.64E-10	9.79E-02
FLUX	2.10E-07	1.25E-07	7.93E-08	4.64E-08	2.61E-08	1.55E-08	9.19E-09	5.52E-09	2.69E-09	2.92E-09	1.55E-01
E*C	4.00E-07	1.83E-07	8.81E-08	4.44E-08	2.04E-08	1.06E-08	6.14E-09	2.93E-09	1.56E-09	1.23E-09	2.24E-01
E*F	5.35E-07	2.74E-07	1.48E-07	8.22E-08	4.21E-08	2.30E-08	1.36E-08	7.27E-09	4.06E-09	5.21E-09	3.36E-01
	AFT - THETA GREATER THAN 90 DEG										
C	1.77E-08	1.11E-08	8.00E-09	5.05E-09	3.26E-09	1.69E-09	1.09E-09	6.15E-10	3.27E-10	3.58E-11	1.45E-02
FLUX	2.80E-08	1.82E-08	1.41E-08	9.31E-09	5.22E-09	2.84E-09	1.51E-09	8.22E-10	4.82E-10	4.66E-11	2.38E-02
E*C	7.44E-09	3.85E-09	2.36E-09	1.34E-09	7.35E-10	4.62E-10	2.47E-10	1.61E-10	7.54E-11	6.87E-12	4.93E-03
E*F	1.06E-08	5.80E-09	3.88E-09	2.23E-09	1.12E-09	7.81E-10	3.34E-10	2.04E-10	1.11E-10	8.37E-12	7.42E-03

CYLINDRICAL GEOMETRY - GAMMA RAYS IN HYDROGEN
POINT ISOTROPIC SOURCE OF 1 PHOTON/SEC ON AXIS

EO(MEV)	EN(MEV)	ZT(CM)	R(CM)	S(CM)	RHO(GM/CM3)	N	M1	M2	U
3.000E 00	7.500E-02	1.030E 03	4.572E 02	3.429E 02	7.000E-02	10000	0.	0.	0.

G	DV(CM3)	XO	DA(CM2)	DS(CM2)	NO. IN	MAX J+	AVG J+	MIN J+
2.486E-15	6.765E 06	5.000E 00	6.567E 04	2.959E 05	2.000E-01	6.768E-07	3.046E-07	2.436E-07

GAMMA HEAT DEPOSITION(BTU/IN3-SEC)

LAYER \ RADIUS	1.45E 02	2.04E 02	2.50E 02	2.89E 02	3.23E 02	3.54E 02	3.83E 02	4.09E 02	4.34E 02	4.57E 02	AVG/J+
1	8.79E-24	7.90E-24	7.49E-24	6.65E-24	6.31E-24	5.43E-24	5.37E-24	4.58E-24	4.19E-24	4.13E-24	2.00E-17
2	5.15E-24	4.23E-24	3.71E-24	3.58E-24	3.22E-24	2.67E-24	2.78E-24	2.79E-24	2.71E-24	2.08E-24	1.03E-17
3	2.33E-24	2.12E-24	2.17E-24	2.19E-24	1.88E-24	1.40E-24	1.44E-24	1.42E-24	1.19E-24	1.03E-24	5.64E-18
4	1.16E-24	1.07E-24	1.24E-24	1.02E-24	1.18E-24	9.85E-25	6.48E-25	7.44E-25	7.44E-25	7.81E-25	3.14E-18
5	6.09E-25	6.11E-25	7.39E-25	5.17E-25	4.85E-25	4.54E-25	6.02E-25	4.77E-25	4.85E-25	3.54E-25	1.75E-18
6	3.83E-25	2.75E-25	4.25E-25	3.00E-25	2.30E-25	2.40E-25	2.79E-25	2.50E-25	1.89E-25	2.08E-25	9.12E-19
7	1.45E-25	2.68E-25	2.19E-25	1.91E-25	1.85E-25	1.97E-25	1.79E-25	2.77E-25	1.24E-25	1.33E-25	6.29E-19
8	7.10E-26	9.35E-26	4.67E-26	7.93E-26	9.25E-26	7.94E-26	1.05E-25	7.61E-26	6.81E-26	3.21E-26	2.44E-19
9	3.24E-26	1.03E-25	7.68E-26	7.74E-26	3.60E-26	9.23E-26	4.00E-26	4.64E-26	2.94E-26	2.63E-26	1.84E-19
10	3.96E-26	5.09E-26	4.24E-26	1.79E-26	2.50E-26	1.70E-26	7.44E-27	3.92E-26	2.46E-26	2.58E-26	9.51E-20

TOTAL BTU/SEC 5.46E-17

TRANSMITTED GAMMA ANGULAR DISTRIBUTION(MEV/CM2-SEC-STER)

COS T. \ RADIUS	1.45E 02	2.04E 02	2.50E 02	2.89E 02	3.23E 02	3.54E 02	3.83E 02	4.09E 02	4.34E 02	4.57E 02
1.0	2.93E-09	3.67E-09	3.04E-09	2.94E-09	2.79E-09	2.56E-09	2.95E-09	2.04E-09	1.70E-09	1.39E-09
0.9	2.37E-10	2.06E-10	2.31E-10	2.65E-10	4.70E-11	1.23E-10	7.18E-10	2.09E-10	8.63E-11	3.69E-10
0.8	9.79E-11	3.17E-11	1.63E-10	3.96E-10	1.33E-11	1.06E-11	8.43E-11	4.04E-12	7.51E-11	2.83E-10
0.7	8.14E-11	3.47E-12	1.38E-10	9.09E-11	8.01E-11	1.19E-10	2.35E-11	3.25E-11	2.16E-10	2.99E-13
0.6	3.55E-11	1.92E-11	4.98E-11	9.20E-13	3.10E-14	6.49E-12	1.01E-11	5.95E-11	6.85E-16	5.32E-13
0.5	1.66E-11	0.	1.05E-12	3.79E-14	2.12E-11	3.33E-12	7.71E-14	1.20E-11	9.81E-13	8.21E-14
0.4	2.06E-11	2.36E-11	6.56E-12	1.21E-14	1.33E-10	6.08E-11	0.	8.06E-11	1.18E-11	2.52E-15
0.3	0.	5.11E-12	7.02E-11	5.91E-12	9.01E-13	0.	0.	7.82E-11	0.	5.79E-14
0.2	4.80E-12	0.	8.11E-12	1.54E-13	0.	0.	0.	2.20E-13	1.29E-12	0.
0.1	0.	0.	0.	0.	0.	0.	0.	0.	1.73E-12	0.

CYLINDRICAL GEOMETRY - GAMMA RAYS IN HYDROGEN
POINT ISOTROPIC SOURCE OF 1 PHOTON/SEC ON AXIS

EO(MEV)	EN(MEV)	ZT(CM)	R(CM)	S(CM)	RHO(GM/CM3)	N	M1	M2	U
6.000E 00	10.000E-02	1.619E 03	4.572E 02	3.429E 02	7.000E-02	10000	0.	0.	0.

G	DV(CM3)	XO	DA(CM2)	DS(CM2)	NO. IN	MAX J+	AVG J+	MIN J+
2.486E-15	1.063E 07	5.000E 00	6.567E 04	4.651E 05	2.000E-01	6.768E-07	3.046E-07	2.436E-07

GAMMAS ESCAPING ENDS OF CYLINDER PER CM2-SEC

	RADIUS										
	1.45E 02	2.04E 02	2.50E 02	2.89E 02	3.23E 02	3.54E 02	3.83E 02	4.09E 02	4.34E 02	4.57E 02	NO/SEC
	FORE - THETA LESS THAN 90 DEG										
C	6.74E-10	1.68E-09	4.85E-10	2.09E-10	6.77E-10	6.35E-10	6.05E-10	7.36E-10	8.92E-10	6.32E-10	4.74E-04
FLUX	7.10E-10	1.79E-09	6.15E-10	2.19E-10	7.68E-10	6.75E-10	6.40E-10	1.16E-09	1.62E-09	1.65E-09	6.47E-04
E*C	2.44E-09	4.64E-09	1.60E-09	9.35E-10	1.83E-09	1.78E-09	1.76E-09	2.44E-09	1.98E-09	1.77E-09	1.39E-03
E*F	2.51E-09	4.83E-09	1.76E-09	9.48E-10	1.94E-09	1.84E-09	1.80E-09	2.80E-09	2.69E-09	2.46E-09	1.55E-03
	AFT - THETA GREATER THAN 90 DEG										
C	3.30E-08	2.79E-08	2.33E-08	2.41E-08	1.69E-08	2.12E-08	1.64E-08	1.61E-08	1.47E-08	1.25E-08	1.35E-02
FLUX	6.07E-08	5.84E-08	3.96E-08	4.30E-08	3.25E-08	3.57E-08	3.08E-08	3.27E-08	2.57E-08	2.22E-08	2.50E-02
E*C	7.51E-09	6.46E-09	5.37E-09	5.67E-09	4.17E-09	5.63E-09	4.50E-09	5.22E-09	4.38E-09	4.37E-09	3.50E-03
E*F	1.53E-08	1.36E-08	9.88E-09	1.08E-08	8.59E-09	9.41E-09	9.23E-09	1.24E-08	9.08E-09	8.64E-09	7.01E-03

GAMMAS ESCAPING SIDES OF CYLINDER PER CM2-SEC

	DEPTH(LAYER NUMBER)										
	1	2	3	4	5	6	7	8	9	10	NO/SEC
	FORE - THETA LESS THAN 90 DEG										
C	1.38E-07	6.24E-08	2.80E-08	1.42E-08	6.42E-09	3.33E-09	2.01E-09	8.45E-10	4.35E-10	1.86E-10	1.19E-01
FLUX	1.91E-07	1.03E-07	5.26E-08	3.03E-08	1.52E-08	7.74E-09	4.88E-09	2.08E-09	1.17E-09	5.58E-10	1.90E-01
E*C	7.36E-07	2.79E-07	1.12E-07	5.16E-08	2.22E-08	1.05E-08	5.43E-09	2.42E-09	1.20E-09	5.14E-10	5.68E-01
E*F	9.96E-07	4.54E-07	2.13E-07	1.16E-07	5.71E-08	2.87E-08	1.60E-08	7.64E-09	4.14E-09	1.92E-09	8.81E-01
	AFT - THETA GREATER THAN 90 DEG										
C	1.15E-08	6.24E-09	3.63E-09	2.37E-09	1.20E-09	7.72E-10	3.61E-10	1.97E-10	1.01E-10	1.29E-11	1.23E-02
FLUX	1.98E-08	1.37E-08	6.33E-09	3.53E-09	2.08E-09	1.10E-09	6.71E-10	5.33E-10	1.58E-10	2.35E-11	2.23E-02
E*C	5.31E-09	2.20E-09	1.06E-09	7.02E-10	3.76E-10	2.80E-10	8.93E-11	5.94E-11	2.84E-11	7.41E-12	4.70E-03
E*F	7.82E-09	3.78E-09	1.78E-09	9.99E-10	5.65E-10	3.91E-10	1.37E-10	1.72E-10	4.69E-11	1.39E-11	7.30E-03

CYLINDRICAL GEOMETRY - GAMMA RAYS IN HYDROGEN
POINT ISOTROPIC SOURCE OF 1 PHOTON/SEC ON AXIS

EO(MEV)	EN(MEV)	ZT(CM)	R(CM)	S(CM)	RHO(GM/CM3)	N	M1	M2	U
6.000E 00	10.000E-02	1.619E 03	4.572E 02	3.429E 02	7.000E-02	10000	0.	0.	0.

G	DV(CM3)	XO	DA(CM2)	DS(CM2)	NO. IN	MAX J+	AVG J+	MIN J+
2.486E-15	1.063E 07	5.000E 00	6.567E 04	4.651E 05	2.000E-01	6.768E-07	3.046E-07	2.436E-07

GAMMA HEAT DEPOSITION(BTU/IN3-SEC)

LAYER	RADIUS 1.45E 02	2.04E 02	2.50E 02	2.89E 02	3.23E 02	3.54E 02	3.83E 02	4.09E 02	4.34E 02	4.57E 02	AVG/J+
1	1.20E-23	9.72E-24	8.56E-24	8.25E-24	6.96E-24	6.97E-24	6.55E-24	5.90E-24	5.96E-24	5.82E-24	2.52E-17
2	4.94E-24	4.26E-24	3.90E-24	3.96E-24	3.36E-24	3.47E-24	2.85E-24	2.92E-24	2.42E-24	2.58E-24	1.14E-17
3	1.96E-24	1.66E-24	1.55E-24	1.64E-24	1.58E-24	1.32E-24	1.74E-24	1.68E-24	1.21E-24	1.06E-24	5.06E-18
4	8.44E-25	7.96E-25	7.78E-25	8.46E-25	9.64E-25	8.80E-25	9.71E-25	7.00E-25	6.91E-25	6.44E-25	2.66E-18
5	4.91E-25	3.17E-25	3.53E-25	4.93E-25	5.34E-25	3.79E-25	5.22E-25	4.21E-25	3.95E-25	2.94E-25	1.38E-18
6	1.72E-25	1.58E-25	1.52E-25	1.26E-25	2.99E-25	1.66E-25	1.65E-25	2.11E-25	1.58E-25	2.23E-25	6.01E-19
7	1.21E-25	1.69E-25	1.73E-25	1.57E-25	7.81E-26	1.30E-25	1.17E-25	8.49E-26	1.20E-25	1.31E-25	4.21E-19
8	9.04E-26	4.08E-26	1.89E-26	6.67E-27	7.21E-26	1.36E-25	5.28E-26	8.62E-26	4.12E-26	3.81E-26	1.92E-19
9	6.48E-26	8.17E-27	1.36E-26	1.75E-26	4.09E-26	6.12E-26	3.36E-26	4.68E-26	3.80E-26	4.88E-26	1.23E-19
10	6.61E-27	4.42E-26	8.83E-28	3.05E-26	2.10E-26	7.74E-27	2.57E-27	4.54E-26	4.01E-26	2.81E-28	6.54E-20
									TOTAL BTU/SEC		9.28 E-17

TRANSMITTED GAMMA ANGULAR DISTRIBUTION(MEV/CM2-SEC-STER)

COS T.	RADIUS 1.45E 02	2.04E 02	2.50E 02	2.89E 02	3.23E 02	3.54E 02	3.83E 02	4.09E 02	4.34E 02	4.57E 02
1.0	3.82E-09	6.13E-09	2.17E-09	1.48E-09	2.59E-09	2.71E-09	2.75E-09	3.54E-09	2.28E-09	2.53E-09
0.9	5.22E-11	1.25E-09	3.28E-12	8.92E-12	1.43E-10	4.87E-11	1.90E-11	8.97E-14	7.00E-14	7.43E-11
0.8	1.27E-11	9.44E-13	9.88E-11	4.09E-12	3.65E-16	7.32E-11	2.63E-11	7.96E-11	5.32E-17	3.15E-14
0.7	1.88E-12	0.	2.28E-10	0.	1.74E-10	0.	0.	6.58E-14	1.73E-11	0.
0.6	0.	0.	4.46E-11	1.56E-13	4.17E-18	0.	0.	3.88E-12	4.99E-10	0.
0.5	0.	0.	2.81E-14	0.	0.	0.	0.	0.	0.	0.
0.4	0.	2.55E-12	0.	0.	0.	0.	0.	2.60E-10	3.60E-10	0.
0.3	1.02E-13	0.	0.	0.	0.	2.27E-13	0.	0.	0.	0.
0.2	0.	0.	0.	0.	0.	0.	0.	0.	0.	2.11E-10
0.1	0.	0.	0.	0.	0.	0.	0.	0.	0.	0.

CYLINDRICAL GEOMETRY - GAMMA RAYS IN HYDROGEN
POINT ISOTROPIC SOURCE OF 1 PHOTON/SEC ON AXIS

EO(MEV)	EN(MEV)	ZT(CM)	R(CM)	S(CM)	RHO(GM/CM3)	N	M1	M2	U
1.000E 00	2.500E-02	5.615E 02	4.572E 02	6.096E 02	7.000E-02	10000	0.	0.	0.

G	DV(CM3)	XO	DA(CM2)	DS(CM2)	NO. IN	MAX J+	AVG J+	MIN J+
2.486E-15	3.688E 06	5.002E 00	6.567E 04	1.613E 05	10.000E-02	2.141E-07	1.523E-07	1.371E-07

GAMMAS ESCAPING ENDS OF CYLINDER PER CM2-SEC

	RADIUS										
	1.45E 02	2.04E 02	2.50E 02	2.89E 02	3.23E 02	3.54E 02	3.83E 02	4.09E 02	4.34E 02	4.57E 02	NO/SEC
	FORE - THETA LESS THAN 90 DEG										
C	7.22E-09	8.02E-09	7.40E-09	4.91E-09	5.60E-09	3.59E-09	3.44E-09	3.74E-09	3.36E-09	2.77E-09	3.29E-03
FLUX	1.19E-08	1.15E-08	1.13E-08	7.28E-09	8.05E-09	5.35E-09	4.58E-09	5.81E-09	5.20E-09	3.93E-09	4.92E-03
E*C	1.77E-09	2.14E-09	1.99E-09	1.47E-09	1.77E-09	1.05E-09	1.25E-09	1.01E-09	1.01E-09	9.77E-10	9.49E-04
E*F	2.32E-09	2.58E-09	2.49E-09	1.90E-09	2.17E-09	1.31E-09	1.51E-09	1.43E-09	1.29E-09	1.18E-09	1.20E-03
	AFT - THETA GREATER THAN 90 DEG										
C	5.62E-08	5.44E-08	4.89E-08	4.51E-08	4.20E-08	3.74E-08	3.76E-08	3.05E-08	2.56E-08	2.02E-08	2.61E-02
FLUX	1.09E-07	1.47E-07	9.66E-08	8.89E-08	8.33E-08	7.01E-08	7.04E-08	6.17E-08	5.08E-08	3.90E-08	5.36E-02
E*C	7.33E-09	7.97E-09	7.18E-09	7.13E-09	6.37E-09	5.81E-09	6.25E-09	4.99E-09	4.55E-09	4.11E-09	4.05E-03
E*F	1.57E-08	1.86E-08	1.60E-08	1.57E-08	1.44E-08	1.19E-08	1.28E-08	1.07E-08	9.79E-09	8.92E-09	8.83E-03

GAMMAS ESCAPING SIDES OF CYLINDER PER CM2-SEC

	DEPTH(LAYER NUMBER)										
	1	2	3	4	5	6	7	8	9	10	NO/SEC
	FORE - THETA LESS THAN 90 DEG										
C	7.35E-08	5.38E-08	3.48E-08	2.53E-08	1.78E-08	1.02E-08	8.15E-09	4.90E-09	3.02E-09	1.87E-09	3.76E-02
FLUX	1.27E-07	9.73E-08	6.42E-08	4.82E-08	3.35E-08	2.03E-08	1.72E-08	9.41E-09	6.19E-09	3.95E-09	6.89E-02
E*C	6.55E-08	3.93E-08	2.22E-08	1.37E-08	8.47E-09	4.61E-09	2.98E-09	1.69E-09	1.01E-09	6.13E-10	2.58E-02
E*F	1.13E-07	7.07E-08	4.29E-08	2.75E-08	1.72E-08	1.00E-08	6.67E-09	3.67E-09	2.37E-09	1.48E-09	4.76E-02
	AFT - THETA GREATER THAN 90 DEG										
C	1.64E-08	1.42E-08	1.17E-08	9.25E-09	6.26E-09	4.43E-09	4.09E-09	2.46E-09	8.00E-10	5.61E-10	1.13E-02
FLUX	2.84E-08	2.25E-08	1.87E-08	1.46E-08	9.66E-09	8.06E-09	7.51E-09	3.98E-09	1.24E-09	8.05E-10	1.86E-02
E*C	3.80E-09	2.87E-09	2.00E-09	1.36E-09	9.76E-10	5.04E-10	4.67E-10	2.83E-10	1.04E-10	1.36E-10	2.02E-03
E*F	6.18E-09	4.34E-09	3.09E-09	2.11E-09	1.48E-09	8.61E-10	7.70E-10	4.54E-10	1.61E-10	1.97E-10	3.17E-03

CYLINDRICAL GEOMETRY – GAMMA RAYS IN HYDROGEN
POINT ISOTROPIC SOURCE OF 1 PHOTON/SEC ON AXIS

EO(MEV)	EN(MEV)	ZT(CM)	R(CM)	S(CM)	RHO(GM/CM3)	N	M1	M2	U
1.000E 00	2.500E-02	5.615E 02	4.572E 02	6.096E 02	7.000E-02	10000	0.	0.	0.

G	DV(CM3)	XO	DA(CM2)	DS(CM2)	NO. IN	MAX J+	AVG J+	MIN J+
2.486E-15	3.688E 06	5.002E 00	6.567E 04	1.613E 05	10.000E-02	2.141E-07	1.523E-07	1.371E-07

GAMMA HEAT DEPOSITION(BTU/IN3-SEC)

LAYER	RADIUS 1.45E 02	2.04E 02	2.50E 02	2.89E 02	3.23E 02	3.54E 02	3.83E 02	4.09E 02	4.34E 02	4.57E 02	AVG/J+
1	1.74E-24	1.92E-24	1.83E-24	1.60E-24	1.44E-24	1.52E-24	1.41E-24	1.40E-24	1.23E-24	1.23E-24	1.01E-17
2	1.38E-24	1.45E-24	1.17E-24	1.06E-24	1.11E-24	9.74E-25	9.03E-25	9.93E-25	8.95E-25	8.08E-25	7.05E-18
3	9.50E-25	8.20E-25	7.19E-25	7.58E-25	7.47E-25	7.72E-25	6.76E-25	5.92E-25	5.26E-25	5.02E-25	4.64E-18
4	5.25E-25	5.18E-25	4.43E-25	4.18E-25	4.69E-25	4.51E-25	3.89E-25	4.53E-25	3.75E-25	3.36E-25	2.87E-18
5	3.77E-25	3.14E-25	3.23E-25	3.44E-25	3.10E-25	2.72E-25	2.95E-25	2.47E-25	2.39E-25	2.59E-25	1.96E-18
6	2.19E-25	2.12E-25	1.95E-25	2.41E-25	1.89E-25	1.93E-25	1.38E-25	1.32E-25	1.17E-25	1.09E-25	1.15E-18
7	1.53E-25	1.11E-25	1.53E-25	1.44E-25	1.48E-25	1.27E-25	1.09E-25	8.52E-26	9.82E-26	9.03E-26	8.01E-19
8	1.29E-25	9.81E-26	9.36E-26	6.87E-26	7.09E-26	6.22E-26	7.50E-26	5.71E-26	5.96E-26	4.32E-26	4.97E-19
9	5.09E-26	5.05E-26	7.99E-26	5.57E-26	3.73E-26	6.91E-26	2.36E-26	2.89E-26	2.75E-26	3.39E-26	3.00E-19
10	4.71E-26	2.76E-26	2.13E-26	1.67E-26	2.05E-26	2.32E-26	1.67E-26	2.94E-26	1.78E-26	2.52E-26	1.61E-19
										TOTAL BTU/SEC	1.01E-17

TRANSMITTED GAMMA ANGULAR DISTRIBUTION(MEV/CM2-SEC-STER)

COS T.	RADIUS 1.45E 02	2.04E 02	2.50E 02	2.89E 02	3.23E 02	3.54E 02	3.83E 02	4.09E 02	4.34E 02	4.57E 02
1.0	1.54E-09	2.10E-09	1.75E-09	1.26E-09	1.94E-09	8.90E-10	1.05E-09	9.12E-10	9.27E-10	8.11E-10
0.9	5.77E-10	5.70E-10	6.58E-10	4.71E-10	3.78E-10	3.58E-10	4.36E-10	2.27E-10	2.36E-10	4.05E-10
0.8	2.18E-10	3.34E-10	3.14E-10	1.90E-10	1.78E-10	1.31E-10	2.25E-10	7.20E-11	1.96E-10	1.67E-10
0.7	1.48E-10	1.86E-10	1.40E-10	1.74E-10	1.36E-10	1.15E-10	1.35E-10	9.53E-11	1.38E-10	7.55E-11
0.6	1.09E-10	9.96E-11	2.19E-10	3.08E-11	8.69E-11	5.72E-11	5.06E-11	9.58E-11	4.42E-11	5.87E-11
0.5	1.27E-10	8.35E-11	2.38E-11	1.34E-10	2.93E-11	8.39E-11	4.44E-11	6.20E-11	1.07E-11	2.59E-11
0.4	6.87E-11	1.74E-11	2.92E-11	6.61E-11	3.29E-11	2.50E-11	4.02E-11	4.81E-11	3.91E-11	1.02E-11
0.3	1.26E-11	1.32E-11	3.17E-11	9.86E-13	2.17E-12	4.56E-12	1.79E-13	1.01E-10	1.63E-11	4.71E-13
0.2	1.33E-11	1.03E-11	1.02E-11	1.12E-11	3.31E-11	2.23E-12	8.09E-14	1.06E-14	6.31E-12	2.28E-12
0.1	8.81E-12	1.48E-12	5.52E-13	5.73E-15	3.46E-13	0.	0.	2.37E-17	7.67E-16	2.08E-13

CYLINDRICAL GEOMETRY - GAMMA RAYS IN HYDROGEN
POINT ISOTROPIC SOURCE OF 1 PHOTON/SEC ON AXIS

EO(MEV)	EN(MEV)	ZT(CM)	R(CM)	S(CM)	RHO(GM/CM3)	N	M1	M2	U
3.000E 00	7.500E-02	1.030E 03	4.572E 02	6.096E 02	7.000E-02	10000	0.	0.	0.

G	DV(CM3)	XO	DA(CM2)	DS(CM2)	NO. IN	MAX J+	AVG J+	MIN J+
2.486E-15	6.765E 06	5.000E 00	6.567E 04	2.959E 05	10.000E-02	2.141E-07	1.523E-07	1.371E-07

GAMMAS ESCAPING ENDS OF CYLINDER PER CM2-SEC

	RADIUS										
	1.45E 02	2.04E 02	2.50E 02	2.89E 02	3.23E 02	3.54E 02	3.83E 02	4.09E 02	4.34E 02	4.57E 02	NO/SEC
	FORE - THETA LESS THAN 90 DEG										
C	1.16E-09	1.21E-09	9.55E-10	1.59E-09	1.07E-09	1.29E-09	1.56E-09	1.11E-09	9.67E-10	5.06E-10	7.50E-04
FLUX	1.39E-09	1.59E-09	1.30E-09	2.36E-09	1.30E-09	1.62E-09	2.33E-09	1.26E-09	1.19E-09	6.59E-10	9.86E-04
E*C	1.67E-09	1.50E-09	1.64E-09	2.13E-09	1.66E-09	1.70E-09	2.38E-09	1.90E-09	1.74E-09	1.06E-09	1.14E-03
E*F	1.81E-09	1.67E-09	1.83E-09	2.59E-09	1.84E-09	1.98E-09	2.97E-09	2.09E-09	1.94E-09	1.20E-09	1.31E-03
	AFT - THETA GREATER THAN 90 DEG										
C	2.01E-08	2.10E-08	2.09E-08	2.27E-08	2.09E-08	1.61E-08	1.35E-08	1.48E-08	1.12E-08	8.93E-09	1.12E-02
FLUX	4.01E-08	4.26E-08	4.34E-08	4.54E-08	4.24E-08	3.06E-08	2.84E-08	2.84E-08	2.56E-08	1.71E-08	2.26E-02
E*C	4.10E-09	4.33E-09	4.55E-09	4.65E-09	4.36E-09	3.72E-09	3.07E-09	3.54E-09	2.80E-09	2.53E-09	2.47E-03
E*F	8.83E-09	9.92E-09	1.08E-08	9.61E-09	9.00E-09	7.63E-09	6.97E-09	7.22E-09	8.20E-09	5.36E-09	5.49E-03

GAMMAS ESCAPING SIDES OF CYLINDER PER CM2-SEC

	DEPTH(LAYER NUMBER)										
	1	2	3	4	5	6	7	8	9	10	NO/SEC
	FORE - THETA LESS THAN 90 DEG										
C	6.80E-08	4.07E-08	2.41E-08	1.37E-08	7.80E-09	4.19E-09	2.36E-09	1.51E-09	6.49E-10	5.77E-10	4.84E-02
FLUX	1.18E-07	7.63E-08	4.97E-08	2.81E-08	1.65E-08	9.75E-09	5.18E-09	3.30E-09	1.53E-09	1.29E-09	9.17E-02
E*C	1.79E-07	9.10E-08	4.65E-08	2.44E-08	1.26E-08	6.11E-09	3.30E-09	2.17E-09	8.43E-10	4.99E-10	1.09E-01
E*F	3.12E-07	1.75E-07	9.88E-08	5.43E-08	2.98E-08	1.66E-08	8.76E-09	5.56E-09	2.61E-09	1.48E-09	2.09E-01
	AFT - THETA GREATER THAN 90 DEG										
C	9.19E-09	6.13E-09	4.53E-09	2.50E-09	1.95E-09	1.20E-09	6.23E-10	2.93E-10	2.29E-10	1.37E-10	7.93E-03
FLUX	1.54E-08	1.04E-08	7.50E-09	3.77E-09	3.86E-09	1.99E-09	9.59E-10	5.58E-10	3.56E-10	2.37E-10	1.33E-02
E*C	3.22E-09	1.86E-09	1.30E-09	6.94E-10	5.25E-10	3.24E-10	1.57E-10	8.72E-11	5.48E-11	2.55E-11	2.44E-03
E*F	5.01E-09	2.91E-09	2.06E-09	1.02E-09	9.87E-10	4.96E-10	2.21E-10	1.22E-10	8.30E-11	3.99E-11	3.83E-03

CYLINDRICAL GEOMETRY - GAMMA RAYS IN HYDROGEN
POINT ISOTROPIC SOURCE OF 1 PHOTON/SEC ON AXIS

EO(MEV)	EN(MEV)	ZT(CM)	R(CM)	S(CM)	RHO(GM/CM3)	N	M1	M2	U
3.000E 00	7.500E-02	1.030E 03	4.572E 02	6.096E 02	7.000E-02	10000	0.	0.	0.

G	DV(CM3)	X0	DA(CM2)	DS(CM2)	NO. IN	MAX J+	AVG J+	MIN J+
2.486E-15	6.765E 06	5.000E 00	6.567E 04	2.959E 05	10.000E-02	2.141E-07	1.523E-07	1.371E-07

GAMMA HEAT DEPOSITION(BTU/IN3-SEC)

LAYER	RADIUS 1.45E 02	2.04E 02	2.50E 02	2.89E 02	3.23E 02	3.54E 02	3.83E 02	4.09E 02	4.34E 02	4.57E 02	AVG/J+
1	3.52E-24	3.27E-24	3.32E-24	2.93E-24	3.19E-24	2.52E-24	2.71E-24	2.60E-24	2.51E-24	2.26E-24	1.89E-17
2	1.93E-24	1.80E-24	1.84E-24	1.81E-24	1.59E-24	1.50E-24	1.56E-24	1.50E-24	1.30E-24	1.37E-24	1.06E-17
3	1.12E-24	1.12E-24	1.02E-24	1.08E-24	9.53E-25	9.93E-25	1.03E-24	8.73E-25	7.56E-25	9.23E-25	6.49E-18
4	6.46E-25	7.52E-25	5.92E-25	5.61E-25	5.50E-25	4.66E-25	4.97E-25	4.15E-25	5.21E-25	3.96E-25	3.54E-18
5	4.01E-25	4.21E-25	4.28E-25	3.19E-25	2.74E-25	2.56E-25	2.31E-25	2.57E-25	2.27E-25	2.92E-25	2.04E-18
6	1.76E-25	2.07E-25	2.25E-25	2.23E-25	1.46E-25	2.09E-25	1.90E-25	1.68E-25	2.17E-25	1.28E-25	1.24E-18
7	1.55E-25	9.53E-26	9.35E-26	1.14E-25	1.17E-25	1.02E-25	1.05E-25	5.97E-26	7.60E-26	7.54E-26	6.51E-19
8	6.59E-26	5.64E-26	3.93E-26	1.17E-25	4.88E-26	7.09E-26	9.34E-26	4.85E-26	6.49E-26	6.15E-26	4.38E-19
9	2.12E-26	3.13E-26	1.76E-26	3.64E-26	3.67E-26	7.73E-26	5.27E-26	1.61E-26	1.90E-26	1.31E-26	2.11E-19
10	1.67E-26	2.10E-26	1.32E-26	1.88E-26	2.21E-26	4.16E-26	1.61E-26	2.48E-26	1.26E-26	2.38E-26	1.38E-19
										TOTAL BTU/SEC	2.79E-17

TRANSMITTED GAMMA ANGULAR DISTRIBUTION(MEV/CM2-SEC-STER)

COS T.	RADIUS 1.45E 02	2.04E 02	2.50E 02	2.89E 02	3.23E 02	3.54E 02	3.83E 02	4.09E 02	4.34E 02	4.57E 02
1.0	1.98E-09	1.93E-09	2.21E-09	2.50E-09	1.85E-09	1.82E-09	2.51E-09	1.81E-09	1.73E-09	1.41E-09
0.9	3.59E-10	2.66E-10	3.20E-10	2.05E-10	5.03E-10	2.54E-10	6.55E-10	9.98E-10	9.70E-10	8.51E-11
0.8	2.81E-10	1.40E-10	4.63E-12	1.96E-10	1.34E-10	2.65E-10	2.56E-10	6.95E-11	1.43E-11	9.13E-11
0.7	2.11E-11	3.20E-11	4.68E-11	1.80E-10	6.24E-11	3.13E-10	7.66E-11	1.47E-10	9.36E-13	5.63E-11
0.6	1.45E-12	2.55E-12	1.94E-13	8.11E-11	9.25E-11	5.54E-11	4.18E-13	3.66E-13	2.27E-12	1.32E-11
0.5	1.22E-12	3.51E-12	0.	1.46E-10	7.10E-13	6.21E-13	1.66E-12	3.01E-13	1.76E-12	0.
0.4	1.42E-11	7.74E-12	8.03E-16	1.37E-11	0.	0.	2.90E-10	1.10E-12	5.24E-11	6.05E-15
0.3	1.48E-12	4.54E-13	2.78E-15	7.14E-11	0.	0.	0.	0.	4.03E-15	3.82E-11
0.2	0.	1.28E-11	2.96E-11	4.94E-13	0.	1.46E-14	0.	3.01E-14	5.89E-14	0.
0.1	7.22E-13	0.	0.	0.	0.	0.	0.	0.	0.	0.

CYLINDRICAL GEOMETRY - GAMMA RAYS IN HYDROGEN
POINT ISOTROPIC SOURCE OF 1 PHOTON/SEC ON AXIS

EO(MEV)	EN(MEV)	ZT(CM)	R(CM)	S(CM)	RHO(GM/CM3)	N	M1	M2	U
6.000E 00	10.000E-02	1.619E 03	4.572E 02	6.096E 02	7.000E-02	10000	0.	0.	0.

G	DV(CM3)	XO	DA(CM2)	DS(CM2)	NO. IN	MAX J+	AVG J+	MIN J+
2.486E-15	1.063E 07	5.000E 00	6.567E 04	4.651E 05	10.000E-02	2.141E-07	1.523E-07	1.371E-07

GAMMAS ESCAPING ENDS OF CYLINDER PER CM2-SEC

	RADIUS										
	1.45E 02	2.04E 02	2.50E 02	2.89E 02	3.23E 02	3.54E 02	3.83E 02	4.09E 02	4.34E 02	4.57E 02	NO/SEC
	FORE - THETA LESS THAN 90 DEG										
C	8.60E-10	5.23E-10	3.76E-10	5.78E-10	2.87E-10	5.43E-10	3.21E-10	2.98E-10	2.33E-10	2.70E-10	2.82E-04
FLUX	9.31E-10	5.74E-10	3.88E-10	2.97E-09	3.14E-10	7.43E-10	3.32E-10	3.12E-10	2.50E-10	3.33E-10	4.69E-04
E*C	2.58E-09	1.71E-09	1.83E-09	1.28E-09	1.15E-09	1.61E-09	1.54E-09	1.34E-09	1.07E-09	9.40E-10	9.89E-04
E*F	2.64E-09	1.80E-09	1.85E-09	2.69E-09	1.18E-09	1.93E-09	1.58E-09	1.39E-09	1.11E-09	1.04E-09	1.13E-03
	AFT - THETA GREATER THAN 90 DEG										
C	1.26E-08	1.21E-08	1.07E-08	1.08E-08	1.11E-08	8.08E-09	8.37E-09	7.97E-09	6.10E-09	4.26E-09	6.05E-03
FLUX	2.29E-08	2.56E-08	1.88E-08	2.12E-08	2.19E-08	1.57E-08	1.68E-08	1.39E-08	1.10E-08	9.63E-09	1.17E-02
E*C	2.79E-09	2.78E-09	2.30E-09	2.74E-09	2.38E-09	2.11E-09	2.26E-09	1.90E-09	1.70E-09	1.28E-09	1.46E-03
E*F	5.35E-09	5.92E-09	4.38E-09	5.78E-09	4.99E-09	4.42E-09	5.24E-09	3.62E-09	3.30E-09	3.33E-09	3.04E-03

GAMMAS ESCAPING SIDES OF CYLINDER PER CM2-SEC

	DEPTH(LAYER NUMBER)										
	1	2	3	4	5	6	7	8	9	10	NO/SEC
	FORE - THETA LESS THAN 90 DEG										
C	6.20E-08	3.05E-08	1.52E-08	7.44E-09	3.98E-09	1.84E-09	1.08E-09	4.25E-10	2.99E-10	1.22E-10	5.72E-02
FLUX	1.11E-07	6.16E-08	3.61E-08	1.80E-08	1.02E-08	4.92E-09	3.18E-09	1.23E-09	1.25E-09	3.69E-10	1.16E-01
E*C	3.27E-07	1.36E-07	5.96E-08	2.69E-08	1.38E-08	6.25E-09	3.26E-09	1.27E-09	8.80E-10	3.41E-10	2.68E-01
E*F	5.87E-07	2.85E-07	1.48E-07	7.25E-08	4.03E-08	2.03E-08	1.15E-08	4.77E-09	4.83E-09	1.36E-09	5.46E-01
	AFT - THETA GREATER THAN 90 DEG										
C	4.87E-09	3.50E-09	1.87E-09	1.06E-09	6.95E-10	2.08E-10	1.52E-10	8.69E-11	5.10E-11	3.56E-11	5.83E-03
FLUX	8.11E-09	6.05E-09	3.18E-09	1.80E-09	9.84E-10	2.76E-10	2.10E-10	1.88E-10	7.63E-11	3.73E-11	9.73E-03
E*C	1.91E-09	1.17E-09	5.70E-10	3.09E-10	2.35E-10	5.92E-11	3.76E-11	2.51E-11	2.26E-11	1.38E-11	2.02E-03
E*F	2.91E-09	1.85E-09	9.13E-10	4.93E-10	3.23E-10	7.58E-11	5.22E-11	4.85E-11	3.30E-11	1.44E-11	3.12E-03

CYLINDRICAL GEOMETRY - GAMMA RAYS IN HYDROGEN
POINT ISOTROPIC SOURCE OF 1 PHOTON/SEC ON AXIS

EO(MEV)	EN(MEV)	ZT(CM)	R(CM)	S(CM)	RHO(GM/CM3)	N	M1	M2	U
6.000E 00	10.000E-02	1.619E 03	4.572E 02	6.096E 02	7.000E-02	10000	0.	0.	0.

G	DV(CM3)	XO	DA(CM2)	DS(CM2)	NO. IN	MAX J+	AVG J+	MIN J+
2.486E-15	1.063E 07	5.000E 00	6.567E 04	4.651E 05	10.000E-02	2.141E-07	1.523E-07	1.371E-07

GAMMA HEAT DEPOSITION(BTU/IN3-SEC)

LAYER \ RADIUS	1.45E 02	2.04E 02	2.50E 02	2.89E 02	3.23E 02	3.54E 02	3.83E 02	4.09E 02	4.34E 02	4.57E 02	AVG/J+
1	4.61E-24	4.39E-24	4.18E-24	4.05E-24	3.77E-24	3.59E-24	3.34E-24	3.44E-24	3.22E-24	2.95E-24	2.47E-17
2	2.15E-24	2.06E-24	2.12E-24	1.80E-24	1.69E-24	1.76E-24	1.76E-24	1.83E-24	1.76E-24	1.46E-24	1.21E-17
3	1.14E-24	9.85E-25	9.40E-25	1.07E-24	9.74E-25	9.30E-25	8.12E-25	7.76E-25	9.30E-25	6.58E-25	6.05E-18
4	4.93E-25	6.40E-25	4.60E-25	5.35E-25	4.89E-25	3.69E-25	4.08E-25	4.26E-25	3.98E-25	4.31E-25	3.05E-18
5	3.22E-25	2.53E-25	2.65E-25	2.36E-25	2.45E-25	2.33E-25	2.79E-25	2.65E-25	2.17E-25	2.59E-25	1.69E-18
6	2.06E-25	1.73E-25	1.71E-25	1.27E-25	1.64E-25	1.50E-25	1.50E-25	1.37E-25	8.86E-26	1.14E-25	9.73E-19
7	1.03E-25	5.39E-26	9.91E-26	8.84E-26	7.95E-26	8.19E-26	7.73E-26	2.74E-26	7.53E-26	4.55E-26	4.80E-19
8	1.02E-25	5.85E-26	5.49E-26	4.51E-26	4.20E-26	2.20E-26	2.15E-26	2.96E-26	5.35E-26	1.00E-26	2.88E-19
9	2.04E-26	5.24E-26	1.86E-26	9.47E-27	3.33E-26	9.27E-27	2.79E-26	2.61E-26	1.73E-26	3.50E-26	1.64E-19
10	7.14E-28	3.64E-26	2.56E-26	3.38E-27	1.05E-26	1.48E-26	8.23E-29	3.86E-28	6.10E-27	1.06E-26	7.13E-20
									TOTAL BTU/SEC		4.89E-17

TRANSMITTED GAMMA ANGULAR DISTRIBUTION(MEV/CM2-SEC-STER)

COS T. \ RADIUS	1.45E 02	2.04E 02	2.50E 02	2.89E 02	3.23E 02	3.54E 02	3.83E 02	4.09E 02	4.34E 02	4.57E 02
1.0	3.88E-09	2.33E-09	2.87E-09	1.71E-09	1.77E-09	1.62E-09	2.44E-09	1.81E-09	1.59E-09	1.23E-09
0.9	1.92E-10	2.00E-10	2.09E-12	4.37E-11	4.49E-11	5.88E-10	8.47E-13	3.25E-10	8.83E-11	1.54E-11
0.8	3.41E-11	1.80E-10	2.66E-11	8.16E-11	5.18E-12	1.76E-11	2.25E-14	3.15E-16	7.47E-13	3.01E-16
0.7	4.12E-12	1.59E-11	3.75E-16	0.	1.09E-15	9.32E-13	2.14E-14	1.09E-13	2.30E-11	2.50E-10
0.6	0.	0.	4.33E-12	1.72E-17	1.23E-11	2.27E-11	1.71E-16	0.	0.	0.
0.5	0.	9.08E-16	0.	2.32E-14	0.	3.22E-10	0.	0.	0.	3.53E-14
0.4	0.	0.	1.33E-15	0.	0.	0.	0.	0.	0.	0.
0.3	0.	0.	0.	1.05E-10	0.	0.	0.	0.	0.	0.
0.2	0.	0.	0.	0.	0.	0.	0.	0.	0.	0.
0.1	0.	0.	0.	1.02E-10	0.	0.	0.	0.	0.	0.

CYLINDRICAL GEOMETRY - GAMMA RAYS IN HYDROGEN
POINT ISOTROPIC SOURCE OF 1 PHOTON/SEC ON AXIS

EO(MEV)	EN(MEV)	ZT(CM)	R(CM)	S(CM)	RHO(GM/CM3)	N	M1	M2	U
2.230E 00	5.000E-02	9.144E 02	4.572E 02	9.144E-01	7.000E-02	20000	0.	0.	0.

G	DV(CM3)	XO	DA(CM2)	DS(CM2)	NO. IN	MAX J+	AVG J+	MIN J+
2.486E-15	6.005E 06	5.301E 00	6.567E 04	2.627E 05	4.990E-01	9.517E-02	7.599E-07	3.807E-07

GAMMAS ESCAPING ENDS OF CYLINDER PER CM2-SEC

	RADIUS										
	1.45E 02	2.04E 02	2.50E 02	2.89E 02	3.23E 02	3.54E 02	3.83E 02	4.09E 02	4.34E 02	4.57E 02	NO/SEC
	FORE - THETA LESS THAN 90 DEG										
C	2.94E-09	4.07E-09	4.19E-09	4.17E-09	2.35E-09	3.14E-09	2.26E-09	3.06E-09	1.94E-09	8.44E-10	1.90E-03
FLUX	4.11E-09	5.21E-09	5.35E-09	4.97E-09	3.44E-09	5.13E-09	2.82E-09	3.98E-09	2.52E-09	1.03E-09	2.53E-03
E*C	2.93E-09	3.40E-09	3.99E-09	4.10E-09	1.91E-09	2.36E-09	1.62E-09	1.96E-09	1.68E-09	1.28E-09	1.66E-03
E*F	3.27E-09	3.74E-09	4.48E-09	4.56E-09	2.18E-09	2.95E-09	1.84E-09	2.24E-09	2.01E-09	1.49E-09	1.89E-03
	AFT - THETA GREATER THAN 90 DEG										
C	1.48E-06	4.35E-07	2.47E-07	1.68E-07	1.26E-07	9.15E-08	7.02E-08	5.80E-08	4.35E-08	2.72E-08	1.81E-01
FLUX	3.81E-06	1.06E-06	5.85E-07	3.96E-07	2.91E-07	2.01E-07	1.50E-07	1.46E-07	9.86E-08	7.71E-08	4.47E-01
E*C	5.67E-07	1.55E-07	8.85E-08	6.29E-08	4.24E-08	3.16E-08	2.35E-08	2.37E-08	1.57E-08	1.21E-08	6.71E-02
E*F	2.21E-06	6.92E-07	3.22E-07	2.68E-07	1.82E-07	1.15E-07	6.82E-08	8.68E-08	4.88E-08	5.79E-08	2.66E-01

GAMMAS ESCAPING SIDES OF CYLINDER PER CM2-SEC

	DEPTH(LAYER NUMBER)										
	1	2	3	4	5	6	7	8	9	10	NO/SEC
	FORE - THETA LESS THAN 90 DEG										
C	6.26E-08	7.66E-08	6.53E-08	4.34E-08	2.66E-08	1.55E-08	8.65E-09	4.73E-09	2.46E-09	1.25E-09	8.07E-02
FLUX	7.16E-08	9.77E-08	9.07E-08	6.44E-08	4.15E-08	2.69E-08	1.55E-08	8.13E-09	4.69E-09	2.51E-09	1.11E-01
E*C	1.03E-07	1.02E-07	7.51E-08	4.72E-08	2.70E-08	1.51E-08	7.85E-09	4.33E-09	2.17E-09	1.38E-09	1.01E-01
E*F	1.07E-07	1.13E-07	9.10E-08	6.22E-08	3.83E-08	2.45E-08	1.34E-08	7.68E-09	4.33E-09	2.99E-09	1.22E-01
	AFT - THETA GREATER THAN 90 DEG										
C	3.69E-08	3.18E-08	2.17E-08	1.46E-08	8.32E-09	4.12E-09	1.71E-09	1.57E-09	7.24E-10	2.17E-10	3.19E-02
FLUX	5.47E-08	4.88E-08	3.21E-08	2.30E-08	1.34E-08	7.31E-09	2.42E-09	2.38E-09	9.70E-10	2.88E-10	4.87E-02
E*C	2.33E-08	1.22E-08	6.12E-09	3.73E-09	2.11E-09	8.05E-10	3.08E-10	2.86E-10	1.80E-10	4.83E-11	1.29E-02
E*F	2.90E-08	1.66E-08	8.19E-09	5.29E-09	3.14E-09	1.44E-09	4.27E-10	3.95E-10	2.52E-10	6.02E-11	1.70E-02

CYLINDRICAL GEOMETRY - GAMMA RAYS IN HYDROGEN
POINT ISOTROPIC SOURCE OF 1 PHOTON/SEC ON AXIS

EO(MEV)	EN(MEV)	ZT(CM)	R(CM)	S(CM)	RHO(GM/CM3)	N	M1	M2	U
2.230E 00	5.000E-02	9.144E 02	4.572E 02	9.144E-01	7.000E-02	20000	0.	0.	0.

G	DV(CM3)	XO	DA(CM2)	DS(CM2)	NO. IN	MAX J+	AVG J+	MIN J+
2.486E-15	6.005E 06	5.301E 00	6.567E 04	2.627E 05	4.990E-01	9.517E-02	7.599E-07	3.807E-07

GAMMA HEAT DEPOSITION(BTU/IN3-SEC)

	RADIUS										
	1.45E 02	2.04E 02	2.50E 02	2.89E 02	3.23E 02	3.54E 02	3.83E 02	4.09E 02	4.34E 02	4.57E 02	AVG/J+
LAYER											
1	1.62E-22	2.49E-23	1.21E-23	7.62E-24	4.76E-24	3.76E-24	2.58E-24	2.28E-24	2.05E-24	1.28E-24	2.93E-17
2	3.51E-23	1.51E-23	9.07E-24	5.95E-24	4.18E-24	3.17E-24	2.31E-24	2.00E-24	1.48E-24	1.26E-24	1.05E-17
3	1.17E-23	7.29E-24	5.43E-24	3.58E-24	2.95E-24	2.47E-24	1.30E-24	1.64E-24	1.44E-24	9.93E-25	5.10E-18
4	4.74E-24	3.31E-24	2.50E-24	2.06E-24	1.64E-24	1.62E-24	9.85E-25	1.08E-24	7.79E-25	6.83E-25	2.55E-18
5	1.99E-24	1.76E-24	1.25E-24	1.30E-24	9.42E-25	7.11E-25	5.09E-25	5.08E-25	4.31E-25	3.43E-25	1.28E-18
6	9.09E-25	7.43E-25	7.73E-25	5.59E-25	6.01E-25	4.20E-25	4.05E-25	2.45E-25	3.21E-25	3.61E-25	7.02E-19
7	5.65E-25	6.36E-25	4.98E-25	3.38E-25	2.77E-25	1.70E-25	2.36E-25	2.11E-25	1.55E-25	1.20E-25	4.22E-19
8	2.16E-25	2.62E-25	1.42E-25	1.50E-25	1.25E-25	1.20E-25	1.18E-25	1.19E-25	6.35E-26	1.00E-25	1.86E-19
9	9.43E-26	5.47E-26	8.97E-26	8.03E-26	8.77E-26	7.06E-26	5.20E-26	7.01E-26	3.78E-26	4.57E-26	8.99E-20
10	4.12E-26	2.89E-26	4.33E-26	2.02E-26	2.01E-26	3.06E-26	3.72E-26	4.07E-26	1.03E-26	1.05E-26	3.73E-20

TOTAL BTU/SEC 1.40 E-16

TRANSMITTED GAMMA ANGULAR DISTRIBUTION(MEV/CM2-SEC-STER)

	RADIUS									
	1.45E 02	2.04E 02	2.50E 02	2.89E 02	3.23E 02	3.54E 02	3.83E 02	4.09E 02	4.34E 02	4.57E 02
COS T.										
1.0	3.58E-09	4.23E-09	5.01E-09	4.65E-09	2.53E-09	2.33E-09	1.82E-09	2.22E-09	1.47E-09	5.65E-10
0.9	5.35E-10	8.36E-10	6.70E-10	1.09E-09	2.09E-10	5.01E-10	4.76E-10	4.38E-10	4.10E-10	1.35E-09
0.8	8.82E-11	2.15E-10	6.07E-11	7.01E-10	6.17E-11	1.85E-10	1.79E-10	1.22E-10	5.84E-10	1.65E-11
0.7	3.94E-10	1.80E-11	4.58E-12	3.88E-11	4.60E-11	6.07E-10	7.71E-11	2.50E-10	1.85E-10	2.54E-11
0.6	8.10E-12	2.04E-11	5.53E-10	2.23E-11	7.84E-11	1.20E-12	9.85E-12	7.84E-11	3.09E-12	7.65E-11
0.5	4.74E-13	6.72E-11	4.05E-11	2.86E-11	9.19E-11	1.01E-11	1.53E-11	7.93E-12	2.17E-12	5.05E-13
0.4	1.22E-11	4.89E-12	1.80E-12	4.08E-12	1.82E-11	6.63E-11	0.	1.44E-14	1.23E-11	1.15E-14
0.3	4.54E-11	1.70E-11	2.02E-13	0.	1.01E-14	4.51E-11	1.91E-13	0.	2.58E-13	7.10E-13
0.2	1.24E-13	8.70E-13	0.	5.25E-15	1.41E-12	1.62E-11	0.	0.	8.33E-15	0.
0.1	0.	0.	0.	0.	9.22E-16	0.	0.	0.	0.	0.

REFERENCES

1. Whittemore, W. L., et al, "Differential Neutron Thermalization," General Atomic (Div. of Gen. Dynamics), GA-2503, Annual Summary Report, Oct. 1961.

2. Meyer, Herbert A., Ed., Symposium on Monte Carlo Methods, John Wiley and Sons, Inc., 1956.

3. Goldstein, Herbert, Fundamental Aspects of Reactor Shielding, Addison-Wesley, 1959.

4. Aronson, R., "Neutron Penetration in Hydrogen," NDA 15C-39 June 1954.

5. Goldstein, H. and Wilkins, Jr, J.E., "Calculations of the Penetrations of Gamma Rays," NYO-3075, June 1954.

6. Burrell, M.O. and Cribbs, D.L., "A Monte Carlo Calculation of Gamma Ray Penetrations Through Iron Slabs," Lockheed Nuclear Report NR-82, Vol. II, January 1960.

7. Burrell, M.O. and Cribbs, D.L., "A Monte Carlo Calculation of Neutron Penetrations Through Iron Slabs," Lockheed Nuclear Report, NR-82, Vol. III, May 1960.

8. Burrell, M.O., et al, "Nuclear Radiation Doses in Radiologically Shielded Vehicles," Lockheed Nuclear Report, NR-121, May 1961.

NASA-Langley, 1962

NASA TN D-1115
National Aeronautics and Space Administration.
NUCLEAR RADIATION TRANSFER AND HEAT DEPOSITION RATES IN LIQUID HYDROGEN.
M. O. Burrell. August 1962. 96p. OTS price, $2.25. (NASA TECHNICAL NOTE D-1115)

Stochastic methods are used to calculate the radiation transport and energy deposition of neutrons and gamma rays in liquid hydrogen slabs and cylinders. The sources are treated as monoenergetic and either point isotropic for the cylinder or plane parallel rays for the slabs. A description of the methods used and a rather extensive compilation of results are given. The results include heat rate deposition as a function of depth, albedo factors, slow neutron spatial distributions, and transmitted angular distributions of gamma rays.

I. Burrell, M. O.
II. NASA TN D-1115

(Initial NASA distribution: 31, Physics, nuclear and particle; 38, Propulsion systems, air-jet; 42, Propulsion systems, nuclear.)

NASA

NASA TN D-1115
National Aeronautics and Space Administration.
NUCLEAR RADIATION TRANSFER AND HEAT DEPOSITION RATES IN LIQUID HYDROGEN.
M. O. Burrell. August 1962. 96p. OTS price, $2.25. (NASA TECHNICAL NOTE D-1115)

Stochastic methods are used to calculate the radiation transport and energy deposition of neutrons and gamma rays in liquid hydrogen slabs and cylinders. The sources are treated as monoenergetic and either point isotropic for the cylinder or plane parallel rays for the slabs. A description of the methods used and a rather extensive compilation of results are given. The results include heat rate deposition as a function of depth, albedo factors, slow neutron spatial distributions, and transmitted angular distributions of gamma rays.

I. Burrell, M. O.
II. NASA TN D-1115

(Initial NASA distribution: 31, Physics, nuclear and particle; 38, Propulsion systems, air-jet; 42, Propulsion systems, nuclear.)

NASA

NASA TN D-1115
National Aeronautics and Space Administration.
NUCLEAR RADIATION TRANSFER AND HEAT DEPOSITION RATES IN LIQUID HYDROGEN.
M. O. Burrell. August 1962. 96p. OTS price, $2.25. (NASA TECHNICAL NOTE D-1115)

Stochastic methods are used to calculate the radiation transport and energy deposition of neutrons and gamma rays in liquid hydrogen slabs and cylinders. The sources are treated as monoenergetic and either point isotropic for the cylinder or plane parallel rays for the slabs. A description of the methods used and a rather extensive compilation of results are given. The results include heat rate deposition as a function of depth, albedo factors, slow neutron spatial distributions, and transmitted angular distributions of gamma rays.

I. Burrell, M. O.
II. NASA TN D-1115

(Initial NASA distribution: 31, Physics, nuclear and particle; 38, Propulsion systems, air-jet; 42, Propulsion systems, nuclear.)

NASA

NASA TN D-1115
National Aeronautics and Space Administration.
NUCLEAR RADIATION TRANSFER AND HEAT DEPOSITION RATES IN LIQUID HYDROGEN.
M. O. Burrell. August 1962. 96p. OTS price, $2.25. (NASA TECHNICAL NOTE D-1115)

Stochastic methods are used to calculate the radiation transport and energy deposition of neutrons and gamma rays in liquid hydrogen slabs and cylinders. The sources are treated as monoenergetic and either point isotropic for the cylinder or plane parallel rays for the slabs. A description of the methods used and a rather extensive compilation of results are given. The results include heat rate deposition as a function of depth, albedo factors, slow neutron spatial distributions, and transmitted angular distributions of gamma rays.

I. Burrell, M. O.
II. NASA TN D-1115

(Initial NASA distribution: 31, Physics, nuclear and particle; 38, Propulsion systems, air-jet; 42, Propulsion systems, nuclear.)

NASA